RESEARCH TRIANGLE INSTITUTE

NASA CR-132276

INVESTIGATION INTO THE PROPAGATION OF OMEGA VERY LOW FREQUENCY SIGNALS AND TECHNIQUES FOR IMPROVEMENT OF NAVIGATION ACCURACY INCLUDING DIFFERENTIAL AND COMPOSITE OMEGA

Final Report

Prepared Under Contract No. NAS1-11298

For

National Aeronautics and Space Administration
Langley Research Center
Hampton, Virginia 23365

By

Research Triangle Institute
Research Triangle Park
North Carolina 27709

Project No. 43U-718-2

NASA-CR-132276) INVESTIGATION INTO THE PROPAGATION OF OMEGA VERY LOW FREQUENCY SIGNALS AND TECHNIQUES FOR IMPROVEMENT OF NAVIGATION ACCURACY INCLUDING (Research Triangle Inst.)
CSCL 17G
N74-12359
G3/21
Unclas
23387

February 1973

Reproduced by
NATIONAL TECHNICAL
INFORMATION SERVICE
US Department of Commerce
Springfield, VA. 22151

ACKNOWLEDGEMENT

This report was prepared by the Research Triangle Institute, Research Triangle Park, North Carolina, for the National Aeronautics and Space Administration under Contract NAS1-11298. The work is being administered by the Flight Instrumentation Division, Langley Research Center.

This report describes results of studies under the VLF navigation systems task of the aforementioned contract. This task has been closely coordinated with Mr. E. Bracalente and Mr. C. Lytle of the Communications Research Branch under the direction of Mr. J. Schrader. The remaining tasks of the contract are documented in a separate final report entitled, "Study of the Impact of Air Traffic Management Systems on Advanced Aircraft and Avionics Systems."

RTI staff members participating in this study are as follows:

C. L. Britt, Jr., Laboratory Supervisor
E. G. Baxa, Jr., Project Leader
M. M. Wisler, Systems Engineer
J. L. Gatz, Research Assistant
E. D. Clayton, Secretary.

PRECEDING PAGE BLANK NOT FILMED

TABLE OF CONTENTS

PRECEDING PAGE BLANK NOT FILMED

TABLE OF CONTENTS
(Continued)

LIST OF ILLUSTRATIONS

LIST OF ILLUSTRATIONS
(Continued)

LIST OF ILLUSTRATIONS
(Continued)

LIST OF ILLUSTRATIONS
(Continued)

LIST OF ILLUSTRATIONS
(Continued)

LIST OF ILLUSTRATIONS
(Continued)

LIST OF TABLES

ABSTRACT

This report describes results of studies conducted by the Research Triangle Institute under Contract NAS1-11298. An analysis of Very Low Frequency propagation in the atmosphere in the 10-14 kHz range leads to a discussion of some of the more significant causes of phase perturbation. The method of generating sky-wave corrections developed by the Naval Electronics Laboratory Center to predict the Omega phase is discussed. Composite Omega is considered as a means of lane identification and of reducing Omega navigation error. A simple technique for generating trapezoidal model (T-model) phase prediction is presented and compared with the Navy predictions and actual phase measurements made by J. A. Pierce at Harvard University. The T-model prediction analysis illustrates the ability to account for the major phase shift created by the diurnal effects on the lower ionosphere. The T-model predictions exhibit promise as a means of generating phase corrections due to the inherent simplicity of their generation. Finally, an analysis of the Navy sky-wave correction table is used to provide information about spatial and temporal correlation of phase correction relative to the differential mode of operation.

PRECEDING PAGE BLANK NOT FILMED

1.0 INTRODUCTION

The need for simple and precise navigation systems which provide large area coverage is rapidly expanding as the number of aircraft and ships increases. Some presently-used aircraft navigation aids (e.g., DME) are active devices which have limited range and definite saturation limits in today's growing population of aircraft. Passive techniques which cannot be saturated and are potentially low in cost will have an increasingly important role in the future of navigation. The Omega very low frequency (VLF) navigation system developed by the Navy as a means of long-range navigation for ships at sea offers many advantages as an aircraft navigational aid. World-wide coverage can be attained with only eight transmitter stations, and consistent accuracies of less than 2 nautical miles (n. mi.) rms have been demonstrated in the normal operational mode. In a differential mode, consistent daylight accuracies on the order of .5 n. mi. rms are reported for ranges up to 300 n. mi.

A need exists to determine the limiting factors in VLF navigation accuracies and to explore new techniques to use all of the information in the Omega format of transmissions to improve accuracies. To fulfill this need, more knowledge must be obtained about the propagation characteristics of the VLF signals, the factors which contribute to phase perturbations, and the anomalies which affect phase stability. Additionally, simple techniques are needed to apply the necessary corrections to raw phase and phase difference readings so that the system may be available in an inexpensive, simple-to-operate version for use by general aviation aircraft in situations where navigation aids such as VHF Omnirange (VOR) and Distance Measuring Equipment (DME) are not available and Visual Flight Rules (VFR) navigation may not be practical.

This report describes work which has been directed toward an investigation of a very simple technique for providing Omega phase measurement corrections. Additionally, some effort has been applied toward the concept of reducing navigation error by using composite frequency phase measurements. Finally, an initial look at the technique termed Differential Omega is considered, not only to provide a new perspective on analyzing the medium, but as a means of significantly reducing the Omega navigation error.

Chapter 2 discusses the Omega navigation system and provides some background material. A bibliography has been compiled in Appendix A which

includes a large number of publications pertaining to VLF propagation and the Omega navigation system. Chapter 3 provides a summarized analysis of the waveguide model, a description of the known factors contributing to phase perturbations, a summary of the method of prediction of sky-wave corrections (SWC) used and published by the Navy, and an analysis of some aspects of composite frequency phase propagation characteristics.

Chapter 4 describes the trapezoidal model for generating sky-wave corrections, and Chapter 5 provides an analysis of this model, comparing it to the Navy predictions and to some actual phase measurement data obtained from Professor J. A. Pierce of Harvard University*. Finally, Chapter 6 discusses the differential Omega concept and provides some insight, through analysis of sky-wave correction tables, into factors affecting differential Omega accuracy.

*Permission to use the Cambridge data was granted by Professor Pierce.

2.0 THE OMEGA NAVIGATION SYSTEM

2.1 General

The Omega navigation system is a world-wide hyperbolic system which will ultimately employ eight transmitter stations providing a global navigation capability on the earth's surface and in the air. Presently, there are four transmitters in operation at frequencies of 10.2, $11\frac{1}{3}$, and 13.6 kHz. The present stations are located at Aldra, Norway; Trinidad, West Indies; Oahu, Hawaii; and in North Dakota. A station at Shashima, Japan, is currently under construction and plans have been made to provide transmitters at Reunion Island in the Indian Ocean, at Tre-lu, Argentina, and in Australia. Eventually, all stations will have output power of 10 kW and will use atomic frequency standards.

The U. S. Navy has been primarily responsible for the development of the Omega system and through the administration of the Omega Projects Office has designed the specifications for equipment and the format for transmissions. Recently, the U. S. Coast Guard has been designated to administer the Omega system and the Defense Mapping Agency is responsible for publishing the sky-wave correction tables previously published by the Navy.

2.2 How Omega Works

Each transmitter station transmits each frequency for approximately one second (continuous wave) every ten seconds according to a prescribed format. Table 1 is a chart which shows the eight station formats. The entire format is repeated every ten seconds.

The present Omega configuration, consisting of four transmitting stations in the northern hemisphere, provides coverage of one third of the world with a theoretical probable positioning error of $\pm$ 1 n. mi. daytime and $\pm$ 2 n. mi. nighttime. Signals from transmitter stations can be received out to maximum usable ranges of 4000 n. mi. to 8000 n. mi. from the transmitters, depending on the bearing of the receiver from the transmitter. The shorter range can be expected west of the transmitter, the longer range east of the transmitter.

The system is based on the principle that the velocity of propagation of electromagnetic radiation is constant. Thus, the difference in distance from a receiver to each of two synchronized transmitting stations is indicated by

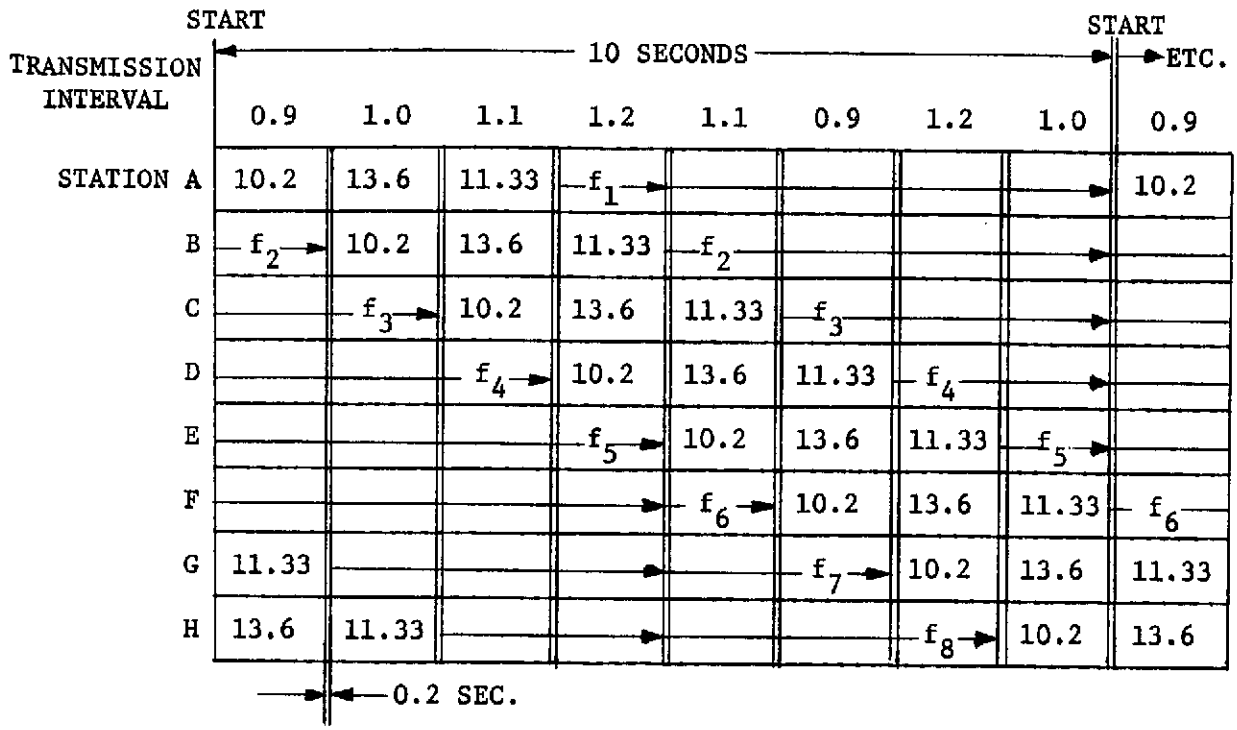

Omega Stations

Station Name	Designator	Latitude	Longitude
Norway	A	66°25'15.00"N	13°09'10.00"E
Trinidad	B	10°42'06.20"N	61°38'20.30"W
Hawaii	C	21°24'20.67"N	157°49'47.75"W
New York	D	43°26'40.92"N	75°05'09.80"W

Table 1. Omega signal format.

the difference in the phase of the signals received. This phase difference may be a fraction of a wavelength or many wavelengths, depending upon the relative distance between the receiver and each transmitter. The locus of points at a constant difference in distance between the receiver and transmitter stations is a hyperbola. At any given constant difference in distance, a hyperbola or line of position (LOP) is described. All LOP's intersect the line joining the transmitter stations (baseline) at right angles. Thus, a receiver measuring the difference in distance between two transmitters can be placed somewhere on a particular LOP between the transmitters.

Using a second pair of transmitters, measurement of phase difference will place the receiver on another LOP. The intersection of the two LOP's then defines a point on the earth's surface which determines the location of the receiver. The navigator will choose Omega LOP's for good accuracy and for large crossing angles.

There are an infinite number of hyperbolic lines of position between any two transmitting stations. With the transmitter sites fixed at precise geographic locations and all transmitting signals accurately phase synchronized, the hyperbolic LOP's formed between each pair of stations are fixed and precisely located. Figure 1 provides a sample of published navigational charts which show a representative quantity of these LOP's. These charts are also provided in tabular form (see ref. 1) so that each LOP is defined in terms of a set of latitudes and longitudes defining points through which each LOP passes. The navigator can then determine from a pair of LOP measurements the latitude and longitude of his receiver position.

Since phase difference measurements are cyclic as the receiver position changes, there is in practical application ambiguity in determining the position of the receiver. Lanes between LOP's corresponding to the same measured phase difference represent the largest regions of unambiguous position determination. These lanes have a ground distance width along the base line corresponding to one-half wavelength at the particular frequency used. (See Appendix B.) For example, the LOP lane width is approximately 8 n. mi. at 10.2 kHz. Thus, in using Omega, the navigator must know his receiver position within 8 n. mi. to obtain an unambiguous position fix from the LOP measurements. At the higher frequencies the lane widths are reduced somewhat, but by using two frequencies, such as 10.2 and 13.6 kHz, the composite frequency 3.4 kHz lane width of unambiguous position determination

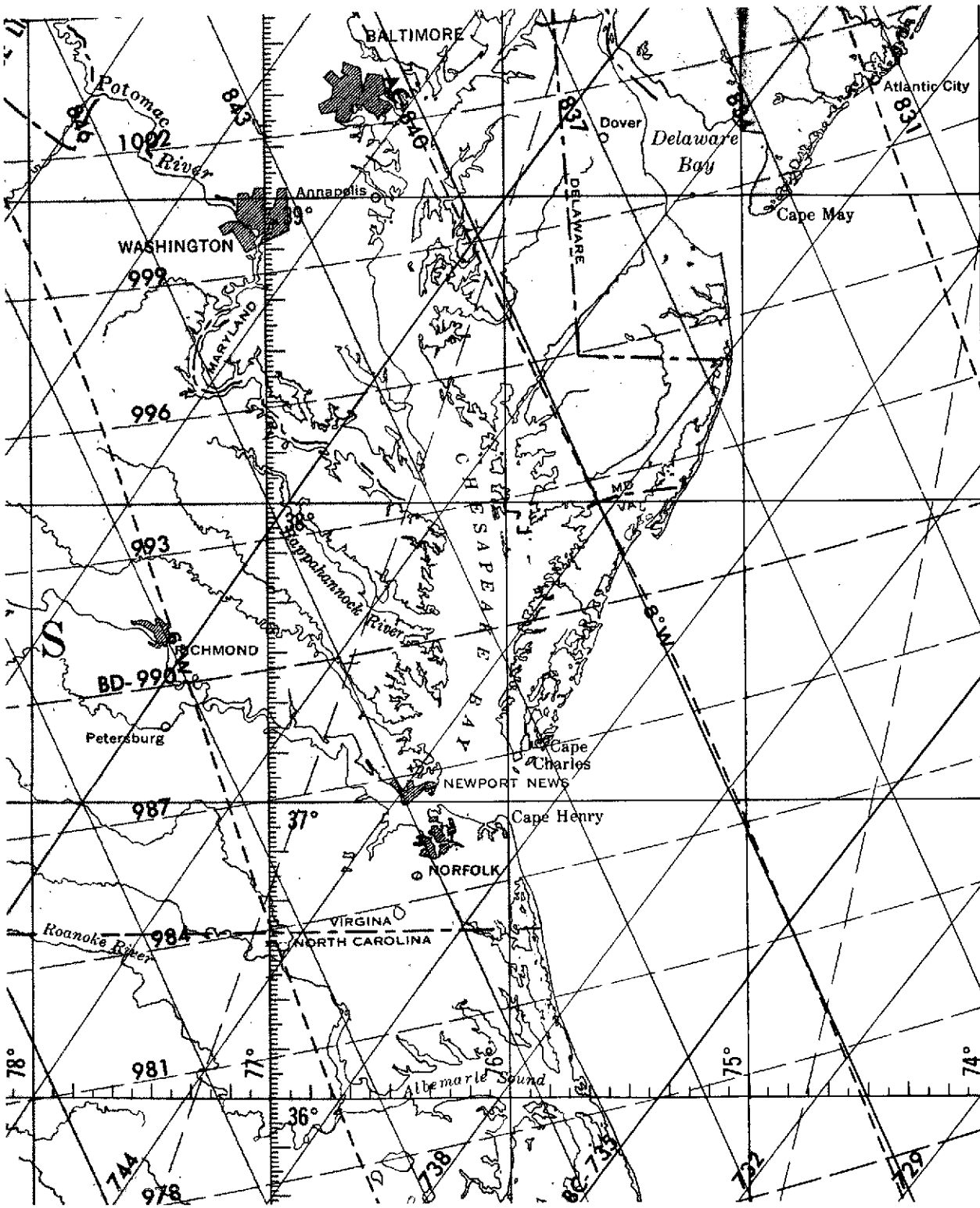

Fig. 1. Omega navigation chart.

is extended to 24 n. mi. Consequently, by using the 1.133 kHz difference between 10.2 and $11\frac{1}{3}$ kHz, it is possible to extend the lane width to 72 n. mi.

2.3 Using Omega to Determine Position

As an example of how Omega phase measurements can be used to determine position, consider the following illustration. A Tracor Omega receiver 599R, located in Building 1299 at Langley Research Center (LRC), Hampton, Va., was used to make measurements. The exercise illustrates how the published sky-wave correction (SWC) tables are used to provide for a position fix.

On May 11, 1972, at 1300 hr, Omega phase measurements with respect to the 599R internally generated reference signal were made at 10.2 kHz. Table 2 summarizes the phase measurement readings.

Table 2. Selected station relative readings.

(centicycles @ 10.2 kHz)

Time/Date	Stations				
	A-R	B-R	C-R	D-R	F-R
1300/5-11-72	84	20	24.5	27.5	87.5

Six phase differences calculated from the data in Table 2 are given in Table 3.

Table 3. Station pair readings.

(centicycles @ 10.2 kHz)

Time/Date	Stations					
	A-B	A-C	A-D	B-C	B-D	C-D
1300/5-11-72	64	59.5	56.5	-4.5 (95.5)	-7.5 (92.5)	-3.0 (97.0)

Using the SWC tables (see ref. 2), the corrections for 1800Z on 11 May 1972 for the stations are repeated in Table 4. The location of the receiver is estimated at 37°5'N, 76°23'W so that the SWC for 36°N, 76°W are used.

Table 4. SWC for 36°N, 76°W.

Time/Date	Stations			
	A	B	C	D
1800Z/5-11-72	-4	5	-1	-7

	Station Pairs					
	A-B	A-C	A-D	B-C	B-D	C-D
	-9	-3	3	6	12	6

The corrected readings for the station pairs are tabulated in Table 5.

Table 5. Corrected readings.

Time/Date	Station Pairs					
	(A-B)*	(A-C)*	(A-D)*	(B-C)*	(B-D)*	(C-D)*
1800Z/5-11-72	55	56.5	59.5	1.5	4.5	3
LOP	1001.55	845.56	1088.59	744.01	987.04	1096.03

Using the Omega chart (see ref. 3), it appears that the receiver at LRC was located in lanes AB 1001, AC 845, AD 1088, BC 744, BD 987 and CD 1096. Using the results presented in Table 5, the corresponding LOP's of the receiver are given in Table 5.

Using the Omega lattice tables, the Omega lines can be plotted on a map. For pair B-C, the corrected reading is 744.01. From the B-C lattice tables (see ref. 1, p. 48),

Lat.	Tabulated Long.	Δ
37°N	76.28.4W	13.3'
38°N	75.32.6W	13.8'

the lane is BC 744. Thus, the corrected reading less the lane count is .01 cycle. To find the interpolated longitude, multiply Δ and the difference

*Corrected.

of 0.01. Then

$(13.3')(.01) = .13'$, and
$(13.8')(.01) = .14'$ } so that the interpolated longitude becomes

76°28.5' @ 37°N , and
75°32.7' @ 38°N .

Table 6 summarizes these results and the interpolated LOP points for pairs BC, BD, AB, and CD.

Table 6. Interpolated LOP's for Omega fix.

Station Pair LOP	BC 744.01	BD 987.04	AB 1001.55	CD 1096.03
Long., Lat. Points of Intersec-tion	76°28.5'W37°N	76°W37°10'N	76°W37°6.7'N	76°W36°41.1'N
	75°32.7'W38°N	77°W37°00.8'N	77°W37°5.8'N	77°W37°3.5'N

Figure 2 is an overlay plot to determine the Omega fix of the receiver. The LOP's BC, BD, and AB intercept at a point 37°6'N 76°23'W. Line of position CD 1096.03 is several miles off. This discrepancy cannot be explained except that the CD pair is not recommended for use in this area.

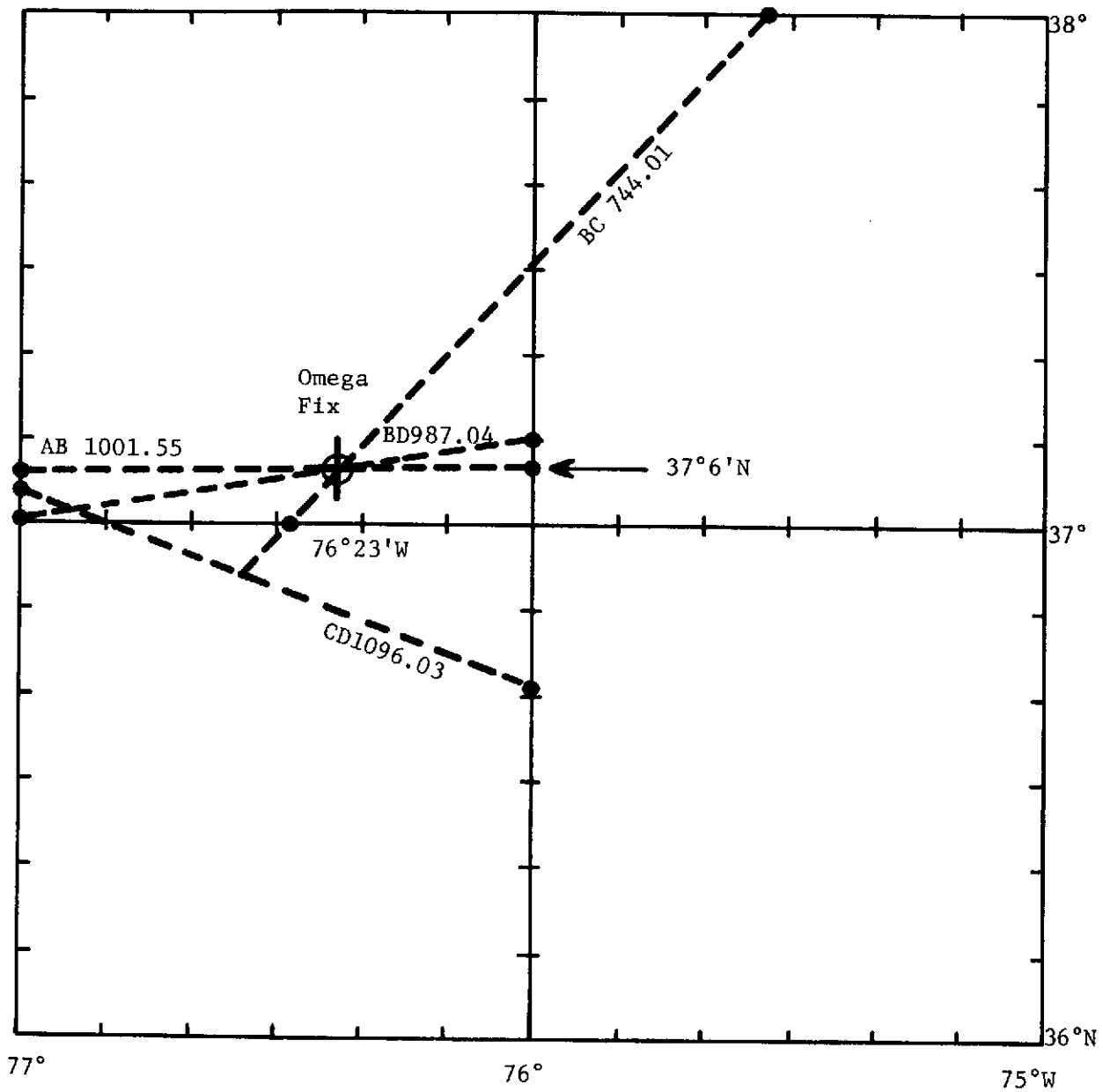

Fig. 2. Plot of the Omega fix.

3.0 ANALYSIS OF VLF PROPAGATION

3.1 Waveguide Model

Determining the electromagnetic field radiated between the earth and the ionosphere by an Omega transmitter is basically a boundary-value problem. The field is expanded in wave equation solution functions which are nearly compatible geometrically with the earth-ionosphere waveguide and then boundary conditions are applied to provide equations which may be solved for the eigenvalues of the solution functions. Unfortunately, the problem is an extremely difficult one because the boundary conditions and shape of the guide vary in such a way as to make a closed form solution impossible. All available solutions, therefore, have simplifying assumptions as cornerstones in their developments. The idea in solving for the fields radiated by the antenna is to determine which assumptions can be made without invalidating the results.

Although the problem of an antenna radiating into the earth-ionosphere waveguide is one of the oldest electromagnetics problems, not until 1959 did Budden (ref. 4) offer a method to obtain a full wave solution to a model which takes into account a curved earth, a ground of finite but constant conductivity, an ionosphere whose properties vary with height above the earth, and an arbitrary but constant orientation of the earth's magnetic field. Budden's model was actually rectangular with the earth's curvature being taken into account by a varying permittivity. A computer program to calculate the fields using this model was developed by Pappert et al. at NELC (ref. 5), reported in 1967. Prior to this, in 1964, Wait and Spies (ref. 6) offered a solution using a spherically-shaped waveguide model and a layered ionosphere which also took into account all the critical parameters. Their method of including the effect of the anisotropy of the ionosphere was less rigorous, however, and although the first order mode calculations are very close between the two methods, there is a significant difference in second order calculations. The work of Wait was directed toward obtaining a closed form mathematical solution for ease of calculation, whereas the Pappert formulation is more dependent on the computer.

Even though the calculations of Pappert take into account the inhomogeneity and anisotropy of the ionosphere, the waveguide model is nevertheless a homogeneous one. This means that the properties do not change along the

direction of propagation in the guide which is not true of the ionosphere; thus it would be inconsistent to attempt a rigorous full wave solution of the entire earth-ionosphere waveguide. Therefore, assumptions are employed in order to use the homogeneous guide results in a practical problem. Consequently, the chief use of the calculations and theory based on a homogeneous waveguide has been to assist in the design of more practical propagation models such as the one due to E. R. Swanson of NELC, which is used to generate the tables of correction values through the U. S. Naval Oceanographic office.

3.2 Factors Which Affect Omega Phase

To "affect" phase means to alter it, and in order to measure the alteration a standard is first needed from which a deviation can be noticed. For reasonable interpretation it is believed that the unaltered standard should be the first order mode of the Omega wave propagated in a spherical earth-ionosphere waveguide with no magnetic field, a nominal ionosphere varying exponentially with height only, and a homogeneous ground. Under these conditions the phase waveguide problem has been solved, and changes in conditions will alter the phase from the predicted value. Practical considerations, of course, dictate the types of changes that can occur and the ones that will affect the phase appreciably.

The propagation path from Omega transmitter to receiver is the region wherein changes in the earth-ionosphere waveguide will affect the received signal. This path is principally the first fresnel zone of the receiver looking back at the transmitter. The central width may be approximated by (see ref. 7)

$$\cos \frac{w}{2a} = \frac{\cos \left(\frac{\lambda}{4a} + \frac{d}{2a}\right)}{\cos \frac{d}{2a}}$$

where a = radius of earth,

d = distance between transmitter and receiver,

and λ = Omega wavelength.

The causes of phase changes can be placed into two categories: one, those caused by higher order mode interference; and two, those caused by changes in the conditions of propagation of the first mode. The higher order mode interference occurs near the transmitter and near boundaries in the propagation path. The higher order modes excited at the transmitter attenuate

quickly so that they are of little consequence at distances over 650 n. mi. from the transmitter (400 n. mi. for all land paths). At boundaries in the propagation path such as a sea-land interface or day-night line, first order mode waves may couple into higher order modes. Fortunately, mode coupling at the lower end of the VLF spectrum, appropriate to Omega, is slight and the higher order modes are attenuated quickly and are only of local consequence.

The first order mode attenuation and phase velocity become the factors of interest to a navigating user of the Omega system. Attenuation rates of VLF are very low and are therefore only a factor during anomalous propagation conditions. Sunspot activity and solar flares can cause absorption of VLF waves at the higher latitudes. An enhancement of solar cosmic rays (SCR event) can cause both auroral absorption (AA) and polar cap absorption (PCA). Auroral absorption occurs between 62.5° and 65° geomagnetic latitude and can last up to two weeks. Propagation from the Norway Omega station at 66°N latitude would be the only station affected by this anomaly for users south of the auroral absorption zone. Polar cap absorption is also caused by SCR's and affects principally LF, and sometimes VLF, waves above 60° geomagnetic latitude. For propagation paths below 60°, attenuation should not be a factor, although reception of the signal may be altered by variables such as precipitation static and interference from noise sources.

The phase velocity is the limiting factor for Omega accuracy. It is affected by variations in ionospheric height which in turn vary seasonally, daily, and with latitude, as well as with propagation anomalies caused by solar flares. Phase velocity is also affected by ionospheric roughness and by the complex reflection occurring at the ionosphere that is a function of the relation between lower ionospheric electron density profile and the geomagnetic dip angle. One more factor which fortunately seems to be independent of the others is ground conductivity. Despite all of these factors the phase of the Omega wave is extremely stable, within 6 centicycles (cec), and predictable to within a phase difference shift of 10 to 20 cec. Ten cec are normally equated to position error of 1 n. mi. when navigating using phase differences (see Appendix B). Changes in phase velocity due to solar activity cause the predictability to be much worse, however. Ionospheric lowering due to sudden ionospheric disturbances (SID) caused by X-radiation from a solar flare can cause errors of up to 30 or 40 cec (3 to 4 n. mi.) for all daylight paths. These disturbances form in a matter of minutes after

the flare begins and last 2 to 3 hours. Extreme flares ("M" type flares) have been recorded that caused errors for 12 hours, the maximum being 20 cec on a Trinidad to Forrestport, N.Y., path. Although rare, they are of significance because of their duration (see ref. 8). PCA events have much the same effect on the phase and are of longer duration, 5 to 15 days, but they are only of consequence for propagation paths that extend into the higher latitudes. For most navigation situations, other lower latitude Omega stations could be selected.

3.3 Naval Electronics Laboratory Center (NELC) Phase Prediction Program

A computer program to predict the phase of the 10.2 kHz Omega signals in selected regions of the earth was generated at NELC in order for Omega navigators to correct their phase readings for propagation conditions. E. R. Swanson described the program as using a single mode parametric model with force-fit statistical smoothing (see ref. 9). Only the principal waveguide mode is considered, and parameters which describe the propagation are directly related to easily defined path characteristics such as orientation, latitude, ground conductivity, and time of day and year.

Electromagnetic waveguide solutions would relate the propagation parameters to physical characteristics of the guide such as ionospheric height, electron density profile, magnetic field, and ground conductivity. The parametric approach was taken because of the uncertainty in these characteristics, although the waveguide solutions were used to provide guidance on the separability of the variables and to suggest functional forms for the variations. The parametric approach amounts to postulating functional forms with unset dummy parameters for the variation of the phase with the path characteristics. These dummy parameters are then chosen by attempting to isolate each one's effect on the phase and picking the one which gives the best fit to measured phase data. Regression analysis techniques are used to determine the generating function parameters.

Parameters based on data collected over 11 years from 300 sites, along with continuous modification of the phase prediction program, have contributed to make the computed position of the navigator using the Omega sky-wave correction tables to be within 1 mile of his actual position (ref. 10).

3.4 Composite Omega

Composite Omega refers to the use of multiple frequencies from the transmitter stations in making phase difference measurements. The ability to take advantage of the available phase information at more than one frequency can serve to enhance navigation accuracies in that the phase perturbations at VLF are to some extent frequency dependent (refs. 11-13). Furthermore, as has been mentioned in Chapter 2, the use of difference frequency phase (between pairs of transmitter Omega frequencies) can serve to increase the physical width of the region of unambiguous phase difference measurements. With lane width increases, the utility of Omega navigation increases, since the navigator does not need to know his approximate position as accurately as in single-frequency Omega. As mentioned in Chapter 2, the lane width of the 3.4 kHz* beat frequency is 24 n. mi. as opposed to the 8 n. mi. lane width of the 10.2 kHz signal (see Appendix B).

The extended lane width accomplished through the use of composite Omega makes it possible to use a difference frequency to identify in which 10.2 kHz lane the receiver is located. For example, the 3.4 kHz signal phase could, in principle, identify one of three possible 10.2 kHz lanes, thus extending the interval between ambiguities to 24 n. mi. As noted in ref. 13, the primary problem in lane identification is the error in prediction of phase.

Since transmission time T_f at a given frequency f is proportional to phase over a given path, the relationship

$$T_{3.4} = 4\,T_{13.6} - 3\,T_{10.2} \tag{1}$$

relates the phase of the 3.4 kHz difference frequency to the phase of the 13.6 kHz and phase of the 10.2 kHz Omega signals (see Appendix C). In (1), all times or phases are in units of centicycles (cec) of 10.2 kHz.

If, as an example, an unexpected variation of 9 cec at 10.2 kHz occurs and a variation of 5 cec in the same direction and in the same units occurs at 13.6 kHz, then from (1),

$$\Delta T_{3.4} = -7 \text{ cec of } 10.2 \text{ kHz} \tag{2}$$

occurs at 3.4 kHz. The difference between the 3.4 kHz and 10.2 kHz signals

---

*3.4 kHz = 13.6 kHz - 10.2 kHz.

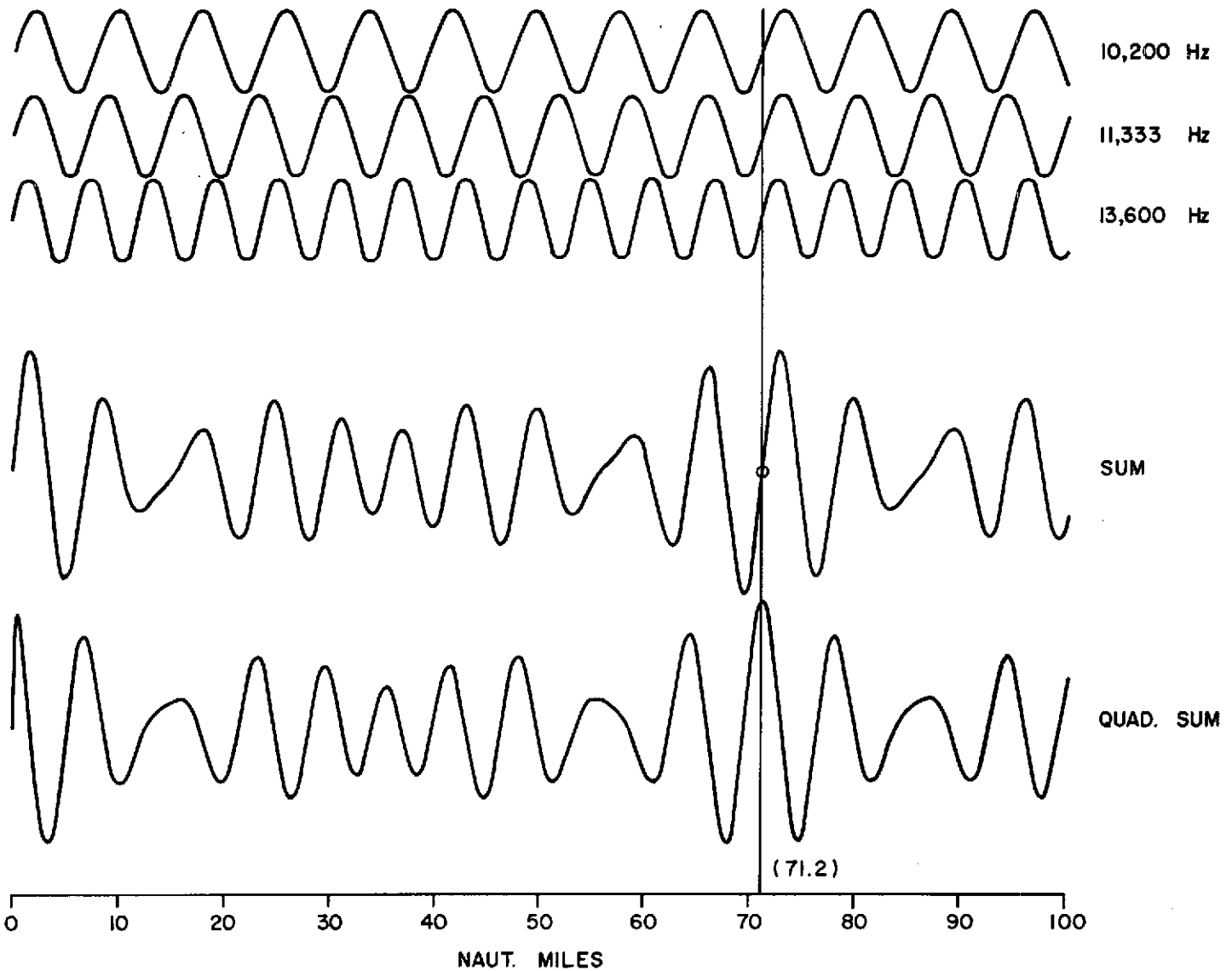

Fig. 3. Omega 10.2 kHz, 11.3 kHz, and 13.6 kHz signals initially in phase and resultant sum and quadrature sum signals.

has changed by 16 cec. Thus, as pointed out in refs. 11 and 13, part of the lane identification problem occurs because propagationally-induced variations in 10.2 kHz and 3.4 kHz usually appear in opposite senses, and the difference is greater than either change alone. For this reason it is particularly critical that predictions be very good in order to obtain reliable lane identification with composite Omega.

Langley Research Center has indicated some interest in a three-frequency composite Omega system where the sum signal of all three frequencies is used and permits resolution of ambiguities over approximately 72 n. mi. on the baseline between stations.

To illustrate the sensitivity of such a technique to phase perturbations of individual Omega frequencies, consider a detector which might track the sum signal using a phase-locked loop. The zero point of the sum signal where the individual component signals are also zero and positive going represents the point where the phase detector is locked on, as illustrated in Fig. 3. This point reoccurs after 9 cycles of the 10.2 kHz signal, 10 cycles of the 11.3 kHz signal, and 12 cycles of the 13.6 kHz signal. The quadrature sum signal is also shown on the figure. The horizontal scale is in nautical miles along a baseline between station pairs, and permits resolution of ambiguities over approximately 72 n. mi. on this baseline.

Figures 4 and 5 show the effect of a phase shift on one or more of the individual phase detector outputs. In Fig. 4 the 11.3 kHz signal has been shifted -45 deg. and, as may be seen, an error of approximately .2 n. mi. appears on the zero point of the sum signal. In Fig. 5, the 13.6 kHz signal has been shifted -90 deg. and the sum signal zero point has changed by almost one complete cycle of the 10.2 kHz phase, or 7.4 n. mi.

While the three-frequency composite Omega system is tolerant of small uncorrected phase variations, larger uncorrected phase variations of the individual signals will cause an automatic phase tracker to, in effect, skip cycles and provide erroneous position data. Thus, as has been pointed out in two-frequency composite Omega, care must be taken in correcting each of the individual frequencies in three-frequency composite Omega.

As indicated in refs. 11 to 13, composite Omega in which the phase data from two separate carriers are linearly combined in a specific manner can exhibit higher phase stability and predictability than that obtainable with either carrier alone. Also, the composite signal offers potentially greater

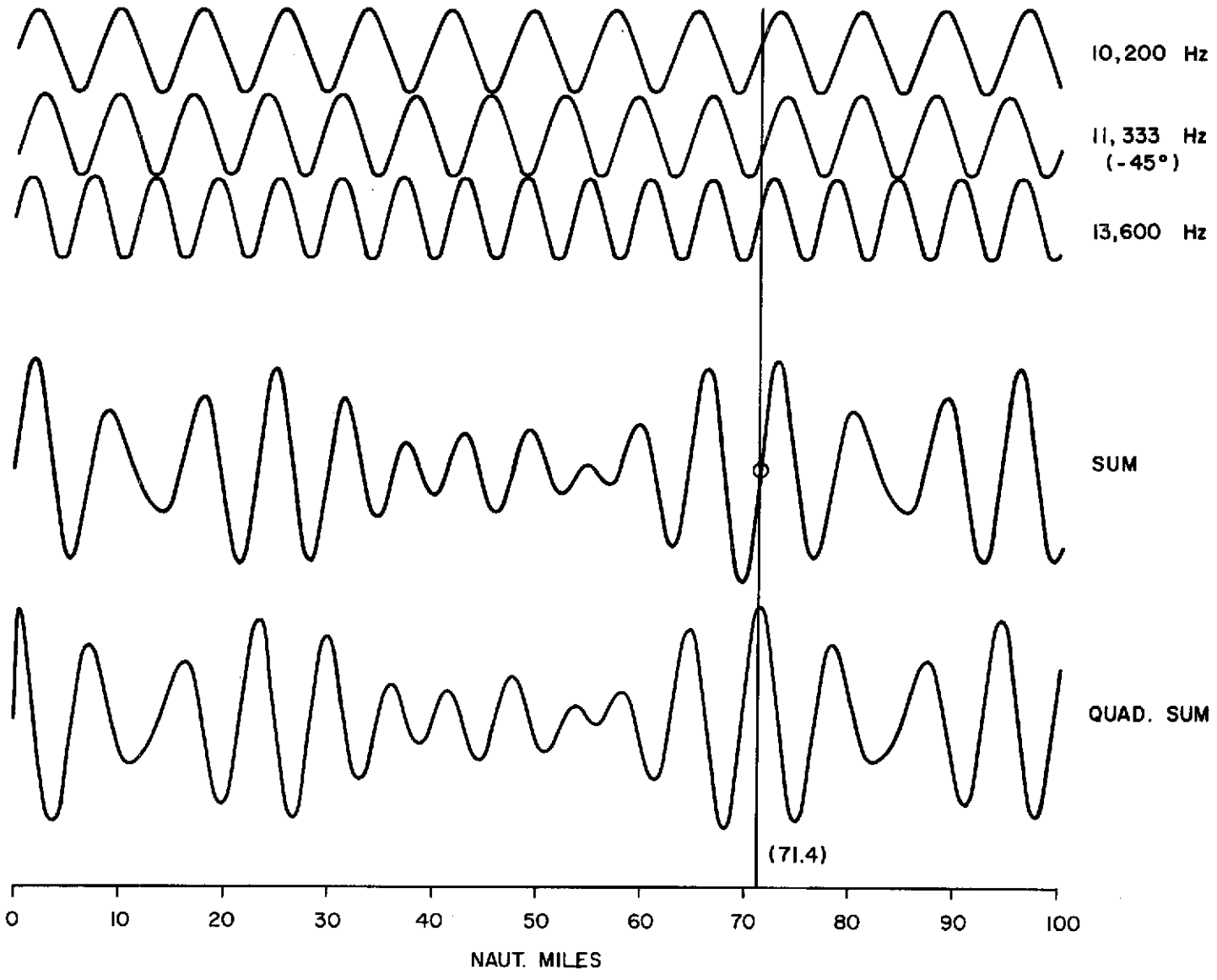

Fig. 4. Omega 10.2 kHz, 11.3 kHz, and 13.6 kHz signals initially in phase except 11.3 kHz 12.5 cec lagging and resultant sum and quadrature sum signals.

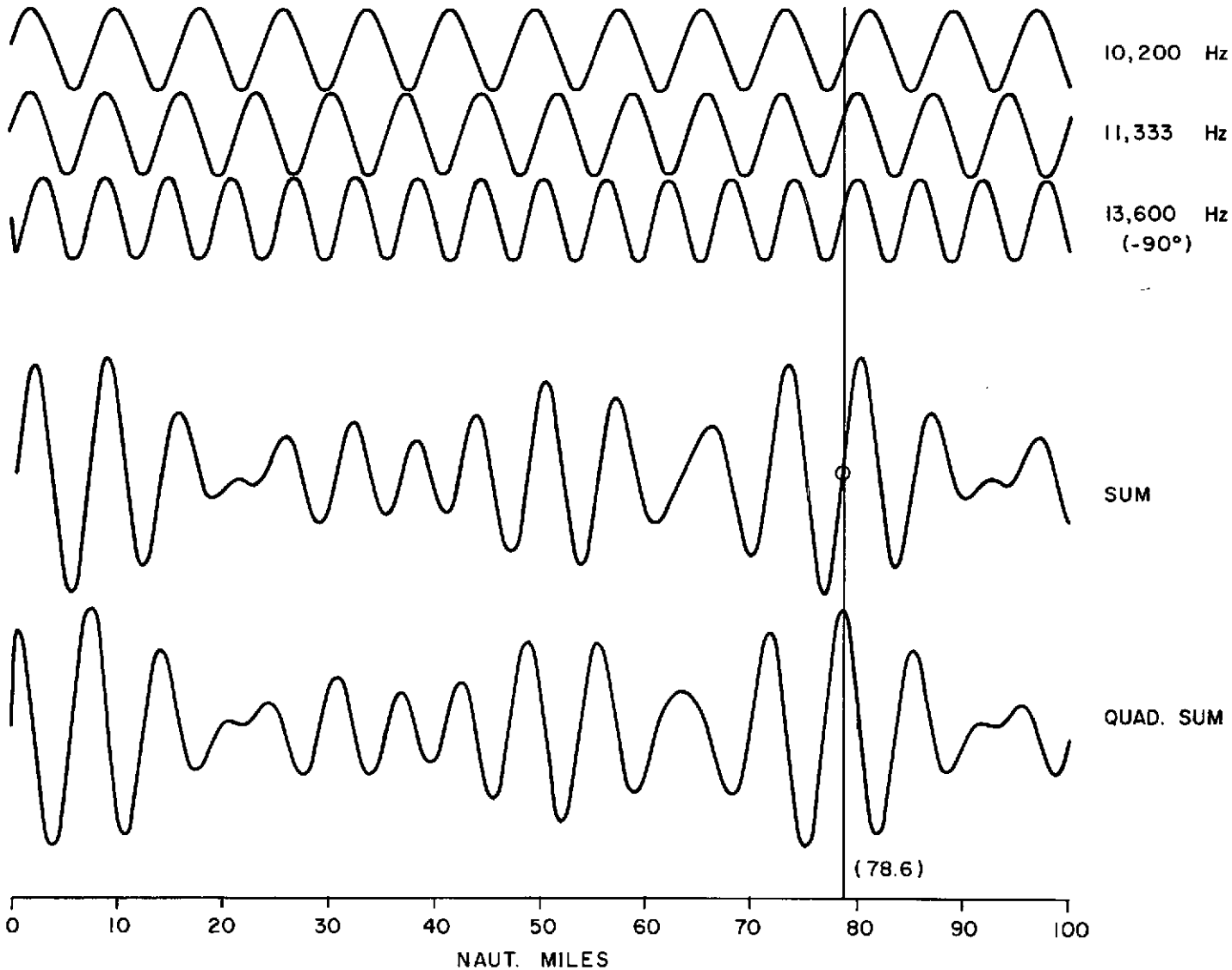

Fig. 5. Omega 10.2 kHz, 11.3 kHz, and 13.6 kHz signals initially in phase except 13.6 kHz 25 cec lagging and resultant sum and quadrature sum signals.

accuracy than the simple 3.4 kHz difference frequency (ref. 11). In ref. 12, conclusions made on the basis of data analysis indicate that use of this composite signal can reduce diurnal variation, propagation anomalies, and may make it possible to obtain sufficient accuracies without the use of sky-wave corrections. This would have a profound effect on the use of Omega in aircraft.

In ref. 11, the idea of using the composite signal to detect the presence and magnitude of propagation anomalies is stated. In a mode when a difference frequency is used to make lane identification, the known magnitude of an unpredictable phase shift could be used to correct both the carrier and difference frequency to nearly the values they would have in the absence of an anomaly. Thus, lane count could be maintained while taking advantage of the increased precision of the composite signal.

4.0 TRAPEZOIDAL CORRECTION MODEL FOR OMEGA (T-MODEL)

4.1 Introduction

The trapezoidal model (T-model) (ref. 14) for determining predicted transmitter phase measurement at a given receiver site is one of the simplest means of providing such information. When compared to the complexity of calculating the Navy sky-wave correction tables (see ref. 9) or to the polynomial generating function (see ref. 15), the T-model offers a great advantage. Fundamentally, the T-model accounts for the diurnal variations by using an all-daylight condition phase prediction, an all-nighttime condition phase prediction and assumes a linear change in phase during transition times. The critical parameters in completely describing the T-model for a given transmitter-receiver path are the sunset and sunrise times at the receiver and transmitter sites, the range between the transmitter and receiver, and the relative phase velocity at night and during the day. The relative phase velocities used are generally long-term averages determined through experimentation.

This chapter describes a simple method for generating the T-model phase prediction and sky-wave corrections. The method presented is based in part on previously documented schemes but has been simplified and generalized. Needed inputs are the latitudes and longitudes of the transmitter and receiver, the sun ephemeris, an "average" earth radius, and the estimates of daytime and nighttime relative phase velocity of the Omega signal at the frequency of interest. Corrections are determined by comparing phase predictions with the nominal or chart-value* of phase. Finally, a discussion of error in T-model predictions as a function of errors in estimating transmitter-receiver path lengths is provided.

4.2 Calculation of Sunset and Sunrise Times

Given the latitude and longitude of any point on the earth, the sunrise and sunset times referenced to Greenwich mean time (GMT) can be calculated. To accomplish this, the given latitude (map latitude), which is a geodetic latitude, must be converted to a geocentric latitude which, geometrically

---

*Chart-value refers to phase computed using $(c/v_{phase}) = .9974$ as in the Navy SWC charts.

speaking, describes the given latitude on the earth's surface as a projected latitude on a spherical approximation to the earth's surface.

The geodetic system describes the latitude of a point on the elliptical earth's surface in terms of an angle measured between the major earth axis and an intersecting line drawn perpendicular to the earth's surface tangent line at the point of interest. In Figure 6, ϕ represents the geodetic latitude of point (x,y) where a cross-section view of the earth is illustrated. From the equation of an ellipse,

$$\frac{x^2}{a_0^2} + \frac{y^2}{b_0^2} = 1.$$

To find the slope of the tangent to the ellipse at point (x_1,y_1), take the derivative such that

$$\frac{2xdx}{a_0^2} + \frac{2ydy}{b_0^2} = 0$$

or

$$\frac{dy}{dx} = -\frac{b_0^2}{a_0^2}\frac{x}{y}\Bigg|_{x_1,y_1} .$$

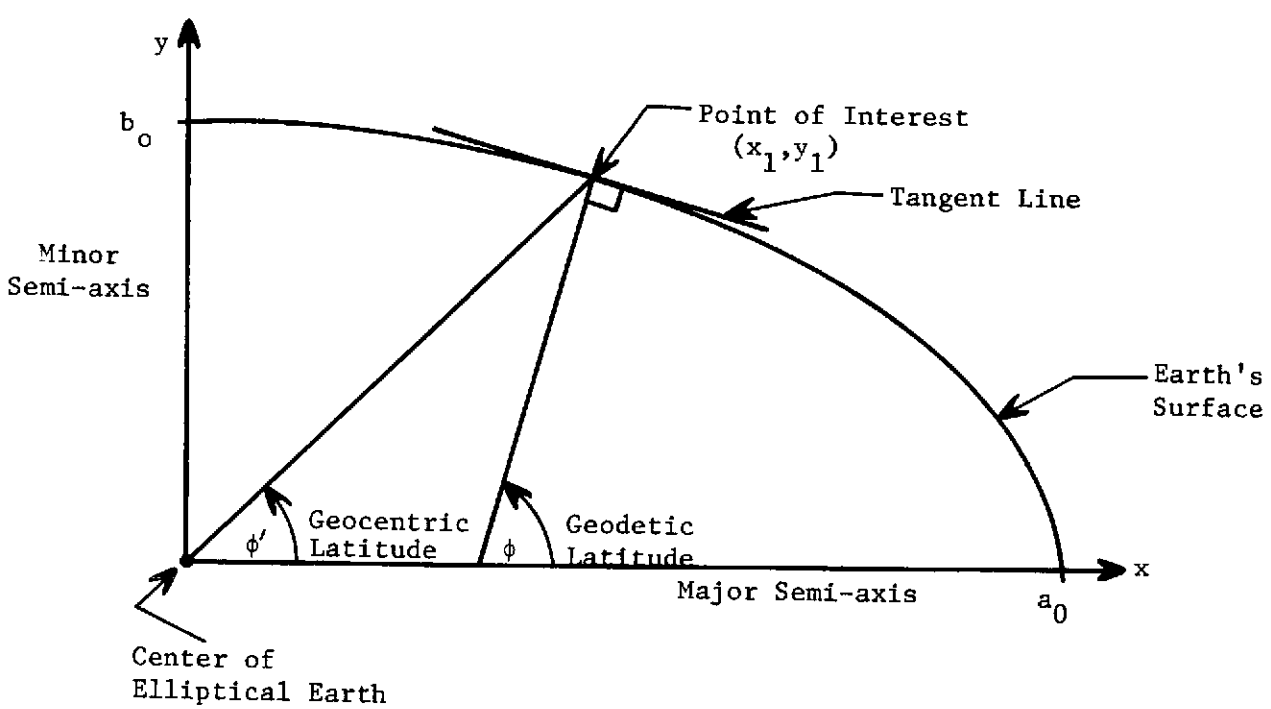

Fig. 6. Cross-section of the earth's surface showing geodetic and geocentric latitudes.

But

$$\frac{dy}{dx} = -\cot \phi \quad \text{and} \quad \frac{x_1}{y_1} = \cot \phi'$$

so that

$$\tan \phi = \frac{a_0^2}{b_0^2} \tan \phi'$$

or

$$\phi' = \tan^{-1}\left[\frac{b_0^2}{a_0^2} \tan \phi\right] \quad . \tag{1}$$

Equation (1) describes the geocentric latitude of point $(x_1,y_1),\phi'$, in terms of the geodetic latitude ϕ and the square of the ratio of minor to major axis of the earth. Using the values of a_0 and b_0 given in ref. 16 which are based on the Clark Spheroid of 1866 (used as the basis for U.S. geographical positions), b_0^2/a_0^2 yields a value 0.9932.

Figure 7 describes the geometry of interest in calculating sunrise and sunset times. The half angle of darkness β at a given latitude can be calculated using Figure 7 as

$$\beta = \cos^{-1}\{\tan \delta' \tan \phi'\} \tag{2}$$

where $\tan \phi' = \frac{d}{r}$ and $\tan \delta' = \frac{a}{d}$. In (2), ϕ' represents the geocentric latitude of the point of interest and δ' represents the geocentric latitude of the sub-solar point for a particular day (declination of the sun). Using ϕ and δ as geodetic latitudes, (1) can be used to rewrite (2) as

$$\beta = \cos^{-1}\{(.9932)^2 \tan \delta \tan \phi\} \quad . \tag{3}$$

The longitude of the sub-solar point λ_S for a given day can be obtained from the ephemeris of the sun (see ref. 17) by using the equation of time tabulations. Thus

$$\lambda_S = -\left[\frac{\text{Time in minutes}}{4 \text{ min/degree of longitude}}\right] .$$

The ephemeris also provides the declination of the sun.

Using Fig. 7, the longitude of the sunrise line is

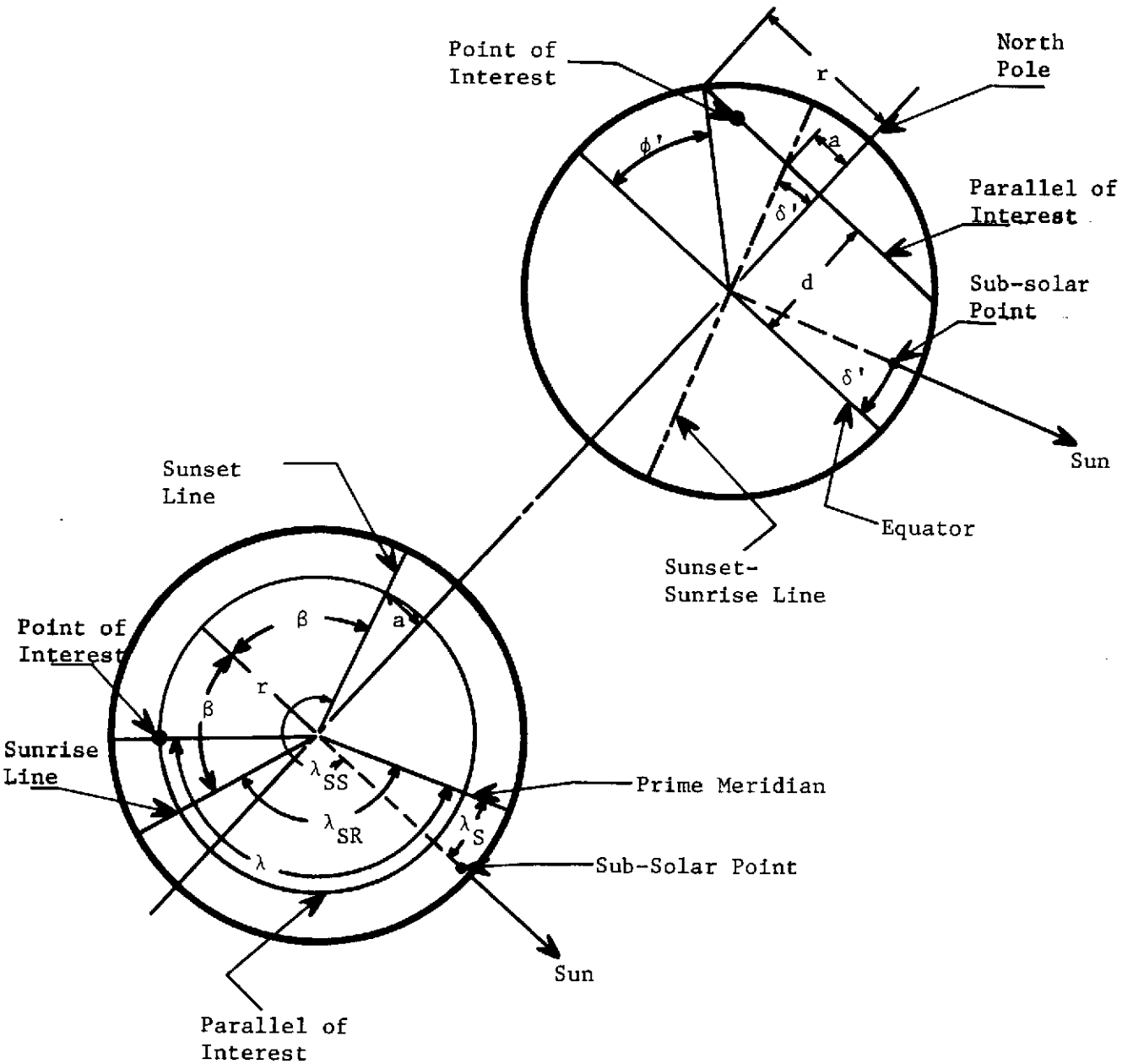

Fig. 7. Geometry of interest for calculating sunrise and sunset times.

$$\lambda_{SR} = \lambda_S + \pi - \beta$$

while the sunset line is

$$\lambda_{SS} = \lambda_S + \pi - \beta \ .$$

Therefore, the GMT of sunrise and sunset can be calculated as

$$GMT_{SR} = \frac{\lambda - \lambda_{SR}}{15} + 12$$

$$GMT_{SS} = \frac{\lambda - \lambda_{SS}}{15} + 12 \qquad (4)$$

where the denominator on the right side of (4), 15, represents degrees per hour of earth rotation and the sub-solar point is defined at 1200 GMT.

As an example to determine the GMT_{SR} and GMT_{SS} at 71°W, 42°N on June 13, use (3) to get

$$\beta = \cos^{-1}[(.9932)^2 \tan(23.16°) \tan(42°)]$$

$$\beta = 67.7° \ .$$

The subsolar time is 0.3 min after 1200 GMT, so that

$$\lambda_S = - \frac{.3}{4} = -0.075° \ .$$

Here $\lambda_{SR} = -0.075 + 180 - 67.7 = 112.2,$

and $\lambda_{SS} = 247.6° \ .$

Therefore, at 71°W, 42°N, (4) yields

$$GMT_{SR} = \frac{71 - 112.2}{15} + 12 = 0915$$

$$GMT_{SS} = \frac{71 - 247.6}{15} + 12 = 0012 \ .$$

4.3 Daytime and Nighttime Phase Levels

With respect to the T-model Omega phase prediction, daytime refers to the period of time when the receiver and selected transmitter and the intervening path are in a daylight condition. Nighttime is that period where the total path is in darkness. Other times are referred to as transition periods which are either sunrise transitions or sunset transitions, depending upon whether the path is changing from nighttime to daytime or vice versa.

The ionosphere level is higher at night than during the day so that the phase velocity of the Omega signal is lower at night than during the day. This diurnal perturbation of phase velocity changes the wavelength of the Omega signal so that at a given receiver position the measured nighttime phase will be greater than the measured daytime phase. The T-model assumes that the nighttime phase is constant and greater than the assumed constant phase during the daytime period. A linear change in phase is assumed during the transition periods. Figure 8 illustrates a typical T-model phase prediction curve. In determining the daytime and nighttime levels, measured estimates of phase velocity relative to the speed of light have been used. In ref. 13, relative phase velocities are estimated as $(c/v_p)_{night} = 1.00040$ and $(c/v_p)_{day} = 0.99730$ at 10.2 kHz. In Figure 8, ϕ_c represents the free space wavelengths from transmitter to receiver, and ϕ_n represents the chart wavelength corresponding to the average phase velocity $v_p = c/.9974$ used by the Navy in published Omega charts.

The nighttime phase prediction is then calculated as

$$\phi_{night} = \left(\frac{c}{v_p}\right)_{night} \cdot \phi_c$$

where

$$\phi_c = \frac{2\pi d}{\lambda_c} = \left(\frac{2\pi f}{c}\right) d.$$

Here, ϕ_c is the free space phase at the receiver separated from the transmitter by a distance d, with c the free space phase velocity (speed of light), and f the frequency of transmission. Similarly, the daytime phase prediction is

$$\phi_{day} = \left(\frac{c}{v_p}\right)_{day} \cdot \phi_c \quad .$$

The sunrise transition phase prediction is given by simply drawing a straight line from the nighttime phase value at the earliest sunrise time (0915 GMT at Cambridge) to the daytime phase prediction at the latest sunrise time (0940 GMT at Trinidad). The sunset transition phase prediction is obtained by extending a straight line from the daytime value at the earliest sunset time (2230 GMT at Trinidad) to the nighttime phase prediction at the latest sunset time (0012 GMT at Cambridge)

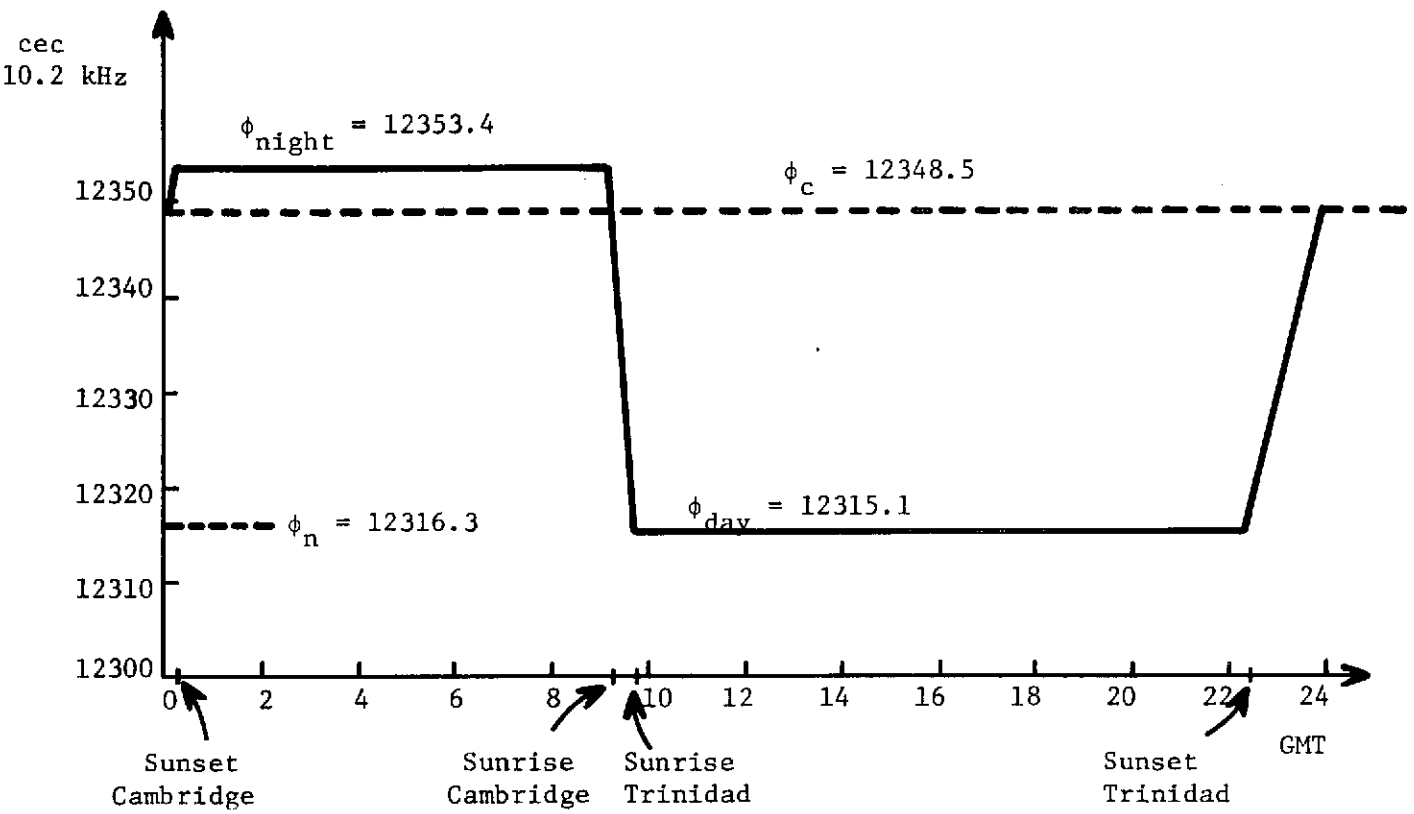

Fig. 8. T-model phase prediction at Cambridge, Mass., for 10.2 kHz Omega signal transmitted from Trinidad transmitter on June 13.

4.4 T-Model Phase Difference Predictions

In predicting the phase difference or LOP type phase measurement, the T-model is used to provide a phase prediction at the receiver from each transmitter. The difference between the two curves is then used as the phase difference prediction at the receiver site. Figure 9 illustrates a typical LOP phase prediction for a receiver located at Cambridge, Massachusetts.

The T-model provides directly a phase prediction at a given receiver site. In order to be of practical use, a phase correction is needed which can be

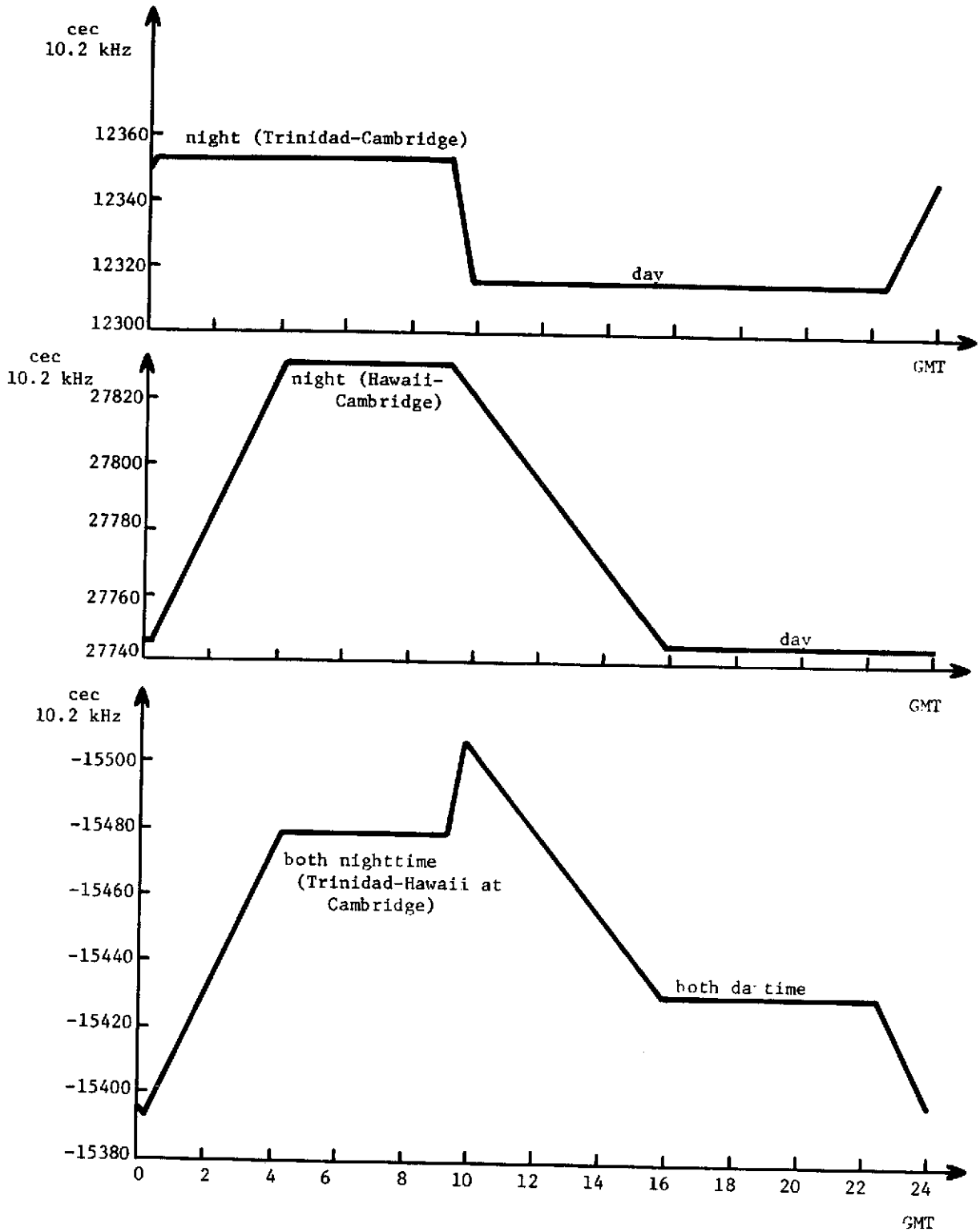

Fig. 9. T-model phase and phase difference prediction at Cambridge, Mass., for 10.2 kHz Omega signal transmitted from Trinidad and from Hawaii on June 13.

applied to an actual received signal to reduce navigation errors. To obtain a sky-wave correction (SWC), the T-model predictions are compared to the chart phase, which is the nominal phase for a particular path based on a nominal value for phase velocity. This value, $v_p = c/.9974$, is the velocity used in navigation charts (see ref. 1) published by the Navy.

Figure 10 illustrates the sky-wave corrections for stations B and C and the correction for (B-C) LOP at Cambridge, based on the predictions illustrated in Figure 9.

4.5 Free Space Wavelength Distance

To calculate the daytime and nighttime phase prediction at a given receiver, it is necessary to determine the distance between the receiver and the transmitter. Distances between points on the earth's surface can be approximated by transforming the geodetic coordinates of the points to geocentric coordinates and then computing the arc length as if it were a geodesic on a sphere.

Figure 11 illustrates two points P and P' on the earth's surface with their geocentric coordinates (α,β) and (α',β') respectively. By constructing two vectors from the earth's center to each of these points, the cosine of the angle between these vectors can be related to their coordinates by their dot product. Define the vector

$$\overline{P} = \hat{i}\, R \cos\alpha \cos\beta + \hat{j}\, R \sin\alpha + \hat{k}\, R \cos\alpha \sin\beta$$

and $$\overline{P}' = \hat{i}\, R \cos\alpha' \cos\beta' + \hat{j}\, R \sin\alpha' + \hat{k}\, R \cos\alpha' \sin\beta' \quad .$$

Then
$$\gamma = \cos^{-1}\left\{\frac{\overline{P}\cdot\overline{P}'}{|P|^2}\right\}$$

$$= \cos^{-1}\{\cos\alpha \cos\alpha' \cos\beta \cos\beta' + \sin\alpha \sin\alpha' + \cos\alpha \cos\alpha' \sin\beta \sin\beta'\} \quad .$$

The distance between the two points P and P', d, can then be found as

$$d = R\gamma$$

where R is the mean earth radius and γ is in radians.

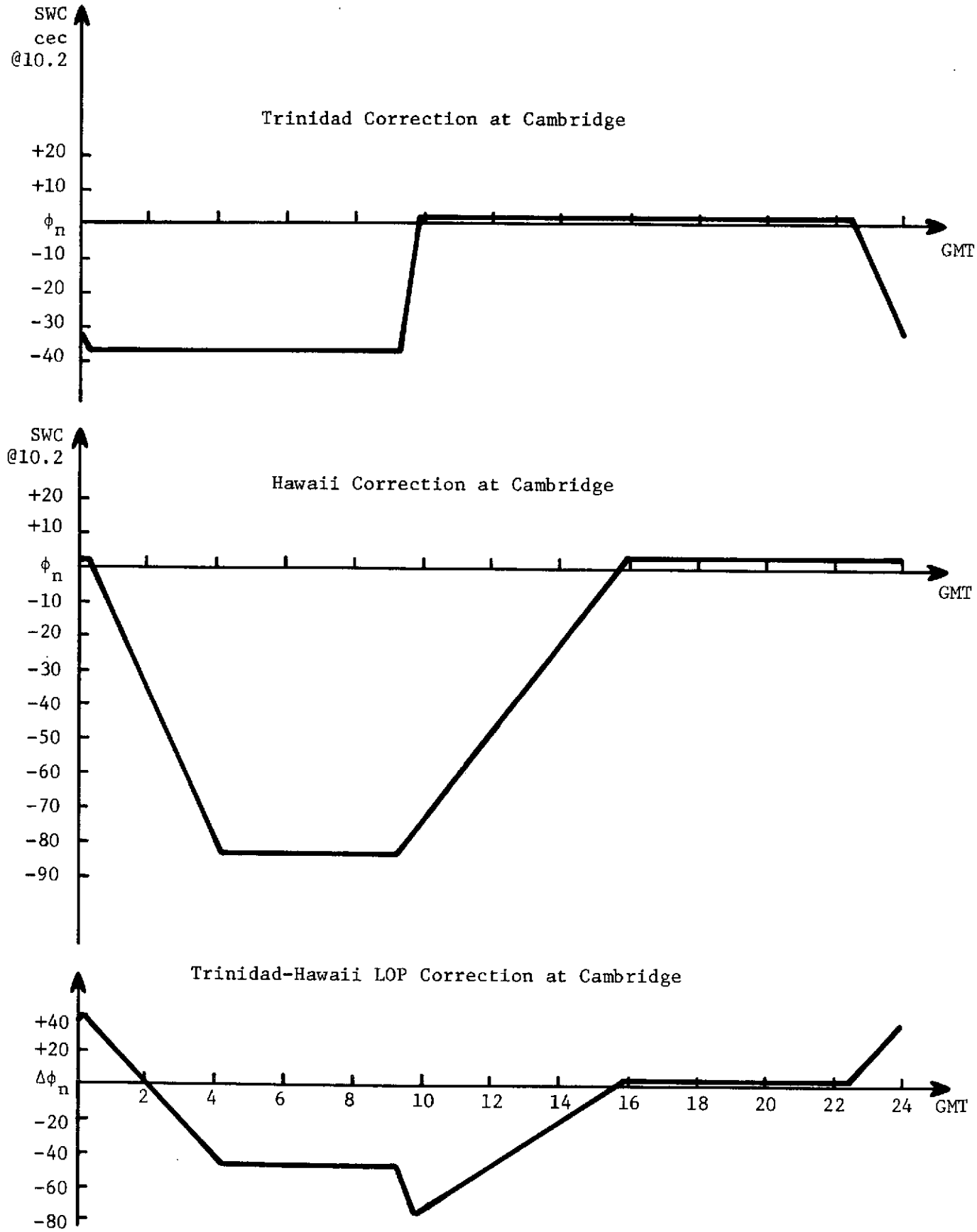

Fig. 10. T-model sky-wave correction predictions at Cambridge, Mass., for 10.2 kHz Omega signal transmitted from Trinidad and from Hawaii on June 13.

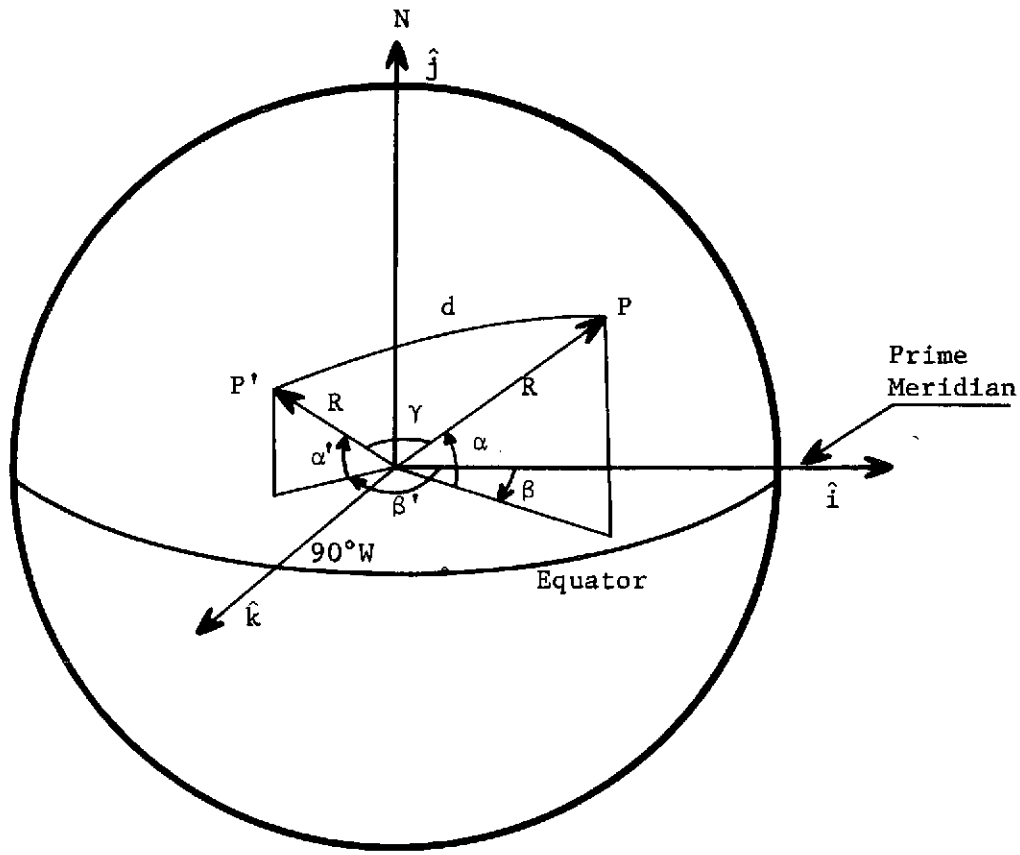

Fig. 11. Calculating distance y on the earth's surface (between two points).

4.6 Effect of Transmitter-Receiver Distance on Phase Corrections

As has been shown, the trapezoidal model prediction of phase measurement can be used to generate sky-wave corrections to be applied to phase measurements made at the receiver. This analysis relates the error in estimating the distance between transmitter and receiver to the error in the sky-wave corrections yielded from the trapezoidal model.

4.6.1 Daytime and nighttime error.— Consider a receiver transmitter path. Let d_1 be the distance between transmitter and receiver, where

$$d_1 = d_{T_1} + \varepsilon_{d_1} ,$$

with d_{T_1} the true transmitter receiver path difference and ε_{d_1} the distance error in estimating d_{T_1}.

The nominal phase reading at the receiver would be

$$\phi_1 = \phi_{T_1} + \phi_{e_1} = \frac{2\pi f}{v_c} (d_{T_1} + \varepsilon_{d_1}) = \frac{2\pi f}{v_c} d_{T_1} + \frac{2\pi f}{v_c} \varepsilon_{d_1}$$

where ϕ_{T_1} represents the nominal phase reading based on the true distance, d_{T_1}, and ϕ_{e_1} represents the phase error introduced by the error in the distance estimate. The quantity v_c represents the nominal phase velocity or the velocity, where $v_c = 0.9974c$, with c representing the velocity of light.

Using the trapezoidal model,

$$\phi_{1_{day}} = \phi_c \left(\frac{c}{v_p}\right)_{day}$$

where ϕ_c is the phase at the receiver based on a free-space wavelength. The nominal phase reading is

$$\phi_1 = \phi_c\left(\frac{c}{v_c}\right) = .9974\ \phi_c \quad .$$

Here $\left(\frac{c}{v_p}\right)_{day}$ is a daytime average relative phase velocity.

Therefore,

$$\phi_{1_{day}} = \frac{\phi_1}{.9974}\left(\frac{c}{v_p}\right)_{day} \quad ,$$

and similarly,

$$\phi_{1_{night}} = \frac{\phi_1}{.9974}\left(\frac{c}{v_p}\right)_{night}$$

where $\left(\frac{c}{v_p}\right)_{day} = 0.99730^*$, and $\left(\frac{c}{v_p}\right)_{night} = 1.00040^*$.

The phase correction or SWC then becomes for daytime

$$\Delta\phi_{1_{day}} = \phi_1 - \phi_{1_{day}} = \phi_1 - \frac{\phi_1}{.9974}\left(\frac{c}{v_p}\right)_{day}$$

$$= \phi_1\left[1 - \frac{\left(\frac{c}{v_p}\right)_{day}}{.9974}\right]$$

$$= \phi_{T_1}\left[1 - \frac{\left(\frac{c}{v_p}\right)_{day}}{.9974}\right] + \phi_{e_1}\left[1 - \frac{\left(\frac{c}{v_p}\right)_{day}}{.9974}\right] \quad .$$

*Nominal based on Pierce's results.

The first term in the expression for $\Delta\phi_{1_{day}}$ is the phase difference based on the true distance between receiver and transmitter, whereas the second term represents the contribution to phase error from the error in the distance estimate. Then

$$\Delta\phi_1 = \Delta\phi_{T_{1_{day}}} + \varepsilon_{\Delta\phi_{1_{day}}}$$

where

$$\varepsilon_{\Delta\phi_{1_{day}}} = \left[1 - \frac{\left(\frac{c}{v_p}\right)_{day}}{.9974}\right]\frac{2\pi f}{v_c}\,\varepsilon_{d_1} \quad . \tag{5}$$

Assume $\varepsilon_{d_1} = \alpha d_{T_1}$ where $0 \leq \alpha \leq 1$. Then

$$\varepsilon_{\Delta\phi_{1_{day}}} = \alpha\left[1 - \frac{\left(\frac{c}{v_p}\right)_{day}}{.9974}\right]\frac{2\pi f}{v_c}\,d_{T_1} \tag{6}$$

or

$$\varepsilon_{\Delta\phi_{1_{day}}} = \alpha\left[1 - \frac{\left(\frac{c}{v_p}\right)_{day}}{.9974}\right]\phi_{T_1}$$

where ϕ_{T_1} is the nominal phase measurement based on the true distance d_{T_1}.

For nighttime,

$$\varepsilon_{\Delta\phi_{1_{night}}} = \alpha\left[\frac{\left(\frac{c}{v_p}\right)_{night}}{.9974} - 1\right]\phi_{T_1} \quad . \tag{7}$$

To convert $\varepsilon_{\Delta\phi_1}$ to n. mi., define distance error incurred at the receiver as

$$\varepsilon_1 = \frac{\lambda_c}{2\pi}\,\varepsilon_{\Delta\phi_1}$$

where λ_c is chart wavelength in n. mi. Therefore,

$$\varepsilon_{1_{day}} = \alpha\left[1 - \frac{\left(\frac{c}{v_p}\right)_{night}}{.9974}\right]\frac{\lambda_c}{2\pi}\left(\frac{2\pi}{\lambda_c}\,d_{T_1}\right)$$

where $\phi_{T_1} = \frac{2\pi f}{v_c}\,d_{T_1} = \frac{2\pi}{\lambda_c}\,d_{T_1}$. Recalling that $\varepsilon_{d_1} = \alpha d_{T_1}$, then

$$\varepsilon_{1_{day}} = \left[1 - \frac{\left(\frac{c}{v_p}\right)_{day}}{.9974}\right] \varepsilon_{d_1}$$

and similarly

$$\varepsilon_{1_{night}} = \left[\frac{\left(\frac{c}{v_p}\right)_{night}}{.9974} - 1\right] \varepsilon_{d_1} \quad .$$

For receiver-transmitter pair 2,

$$\varepsilon_{2_{day}} = \left[1 - \frac{\left(\frac{c}{v_p}\right)_{day}}{.9974}\right] \varepsilon_{d_2}$$

and

$$\varepsilon_{2_{night}} = \left[\frac{\left(\frac{c}{v_p}\right)_{night}}{.9974} - 1\right] \varepsilon_{d_2} \quad .$$

Then the error incurred in the phase difference SWC generated from the trapezoidal model is

$$\Delta\varepsilon^{1,2}_{day} = \varepsilon_{1_{day}} - \varepsilon_{2_{day}} = \left[1 - \frac{\left(\frac{c}{v_p}\right)_{day}}{.9974}\right] (\varepsilon_{d_1} - \varepsilon_{d_2}) \tag{8}$$

and

$$\Delta\varepsilon^{1,2}_{night} = \left[\frac{\left(\frac{c}{v_p}\right)_{night}}{.9974} - 1\right] (\varepsilon_{d_1} - \varepsilon_{d_2}) \quad . \tag{9}$$

The errors ε_{d_1} and ε_{d_2} are independent so that

$$\sigma^2_{1,2} = \sigma^2_{\varepsilon_{d_2}} + \sigma^2_{\varepsilon_{d_2}} \quad \text{or} \quad \sigma_{1,2} = \left[\sigma^2_{\varepsilon_{d_1}} + \sigma^2_{\varepsilon_{d_2}}\right]^{1/2}$$

and the standard deviation of the daytime and nighttime errors becomes

$$\sigma_{\Delta_{1,2_{day}}} = \left[1 - \frac{\left(\frac{c}{v_p}\right)_{day}}{.9974}\right] \left[\sigma^2_{\varepsilon_{d_1}} + \sigma^2_{\varepsilon_{d_2}}\right]^{1/2}$$

$$\sigma_{\Delta_{1,2_{night}}} = \left[\frac{\left(\frac{c}{v_p}\right)_{night}}{.9974} - 1\right] \left[\sigma^2_{\varepsilon_{d_1}} + \sigma^2_{\varepsilon_{d_2}}\right]^{1/2} \quad . \tag{10}$$

These represent the maximum SWC error incurred in navigation due to errors in the estimates of the distances between transmitter and receivers when using the trapezoidal model to generate sky-wave corrections.

4.6.2 Error as a function of time of day.— The section above has described the maximum position error using trapezoidal model SWC as a function of the error in estimating the distance between the receiver and transmitter pair. Next, consider this error as a function of time of day.

Define

$\Delta T_{SR} \triangleq$ difference in time between sunrise at the receiver and transmitter

$\Delta T_{SS} \triangleq$ difference in time between sunset at the receiver and transmitter.

These times are indicated in Fig. 12.

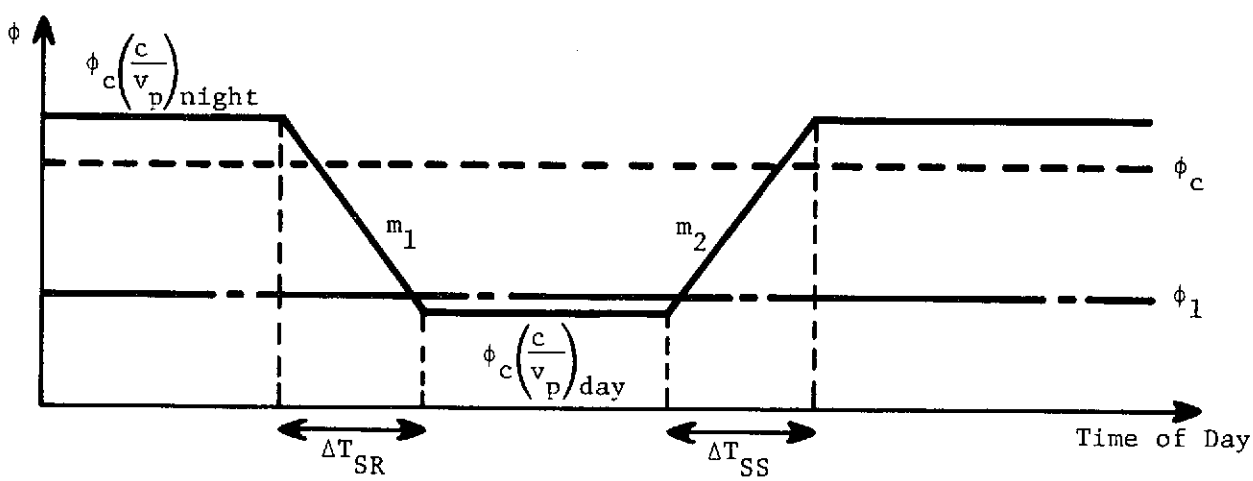

Fig. 12. Trapezoidal phase prediction.

From Fig. 12, slope m_1 is given by

$$m_1 = -\frac{\phi_c\left(\frac{c}{v}\right)_n - \phi_c\left(\frac{c}{v}\right)_d}{\Delta T_{SR}} \qquad T \epsilon \Delta T_{SR}$$

and

$$m_2 = \frac{\phi_c\left(\frac{c}{v}\right)_n - \phi_c\left(\frac{c}{v}\right)_d}{\Delta T_{SS}} \qquad T \epsilon \Delta T_{SS} \quad .$$

For the night-to-day transition during the period ΔT_{SR}

$$\Delta\phi(T) = \left|\phi(T) - \phi_1\right| = \left|\phi_c\left(\frac{c}{v}\right)_n + m_1 T - \phi_1\right| \qquad T\epsilon\Delta T_{SR}$$

$$\Delta\phi(T) = \left|\phi_c\left(\frac{c}{v}\right)_n - \frac{\phi_c\left(\frac{c}{v}\right)_n - \phi_c\left(\frac{c}{v}\right)_d}{\Delta T_{SR}} T - \phi_1\right| \qquad T\epsilon\Delta T_{SR}$$

$$\Delta\phi(T) = \left|\phi_1\left[\frac{\left(\frac{c}{v}\right)_n}{.9974} - 1\right] - \frac{\phi_1}{.9974}\left[\left(\frac{c}{v}\right)_n - \left(\frac{c}{v}\right)_d\right]\frac{T}{\Delta T_{SR}}\right| \qquad T\epsilon\Delta T_{SR}$$

where ϕ_1 is chart phase and $\left(\frac{c}{v}\right)_d = \left(\frac{c}{v}\right)_{p\ day}$ and $\left(\frac{c}{v}\right)_n = \left(\frac{c}{v}\right)_{p\ night}$.

For $T = 0$; $\quad \Delta\phi(T) = \phi_1\left[\frac{\left(\frac{c}{v}\right)_n}{.9974} - 1\right]$

For $T = \Delta T_{SR}$; $\quad \Delta\phi(T) = \phi_1\left[1 - \frac{\left(\frac{c}{v}\right)_d}{.9974}\right]$.

Fig. 13 illustrates $\Delta\phi(T)$ as a function of $T\epsilon\Delta T_{SR}$.

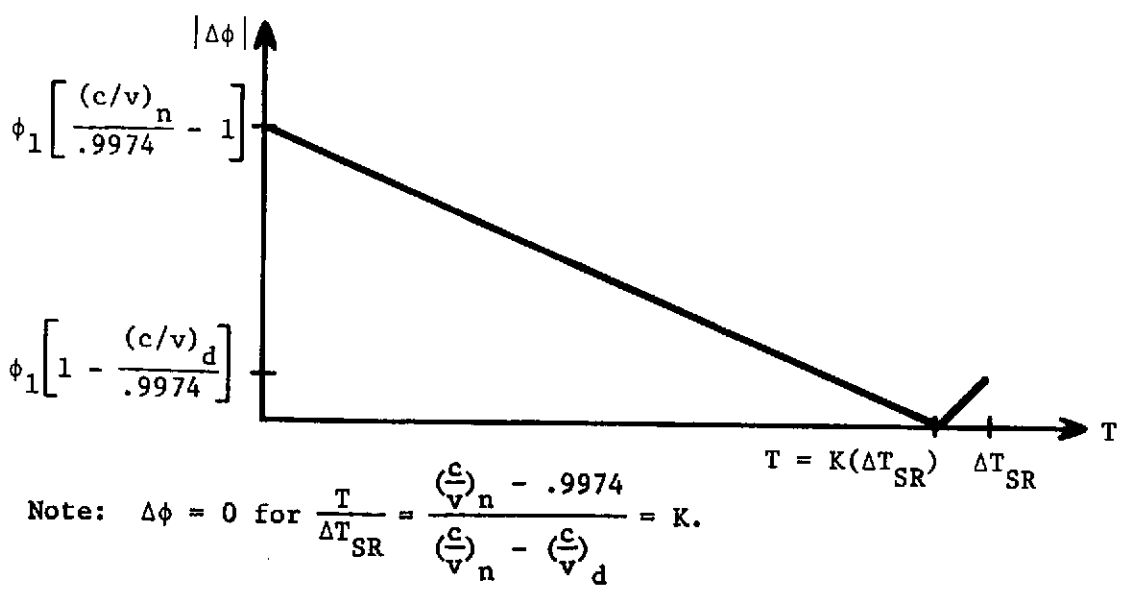

Note: $\Delta\phi = 0$ for $\frac{T}{\Delta T_{SR}} = \frac{\left(\frac{c}{v}\right)_n - .9974}{\left(\frac{c}{v}\right)_n - \left(\frac{c}{v}\right)_d} = K.$

Fig. 13. Phase error in night-to-day transition period.

For the day-to-night transition period in Fig. 14,

$$\Delta\phi'(T) = |\phi(T) - \phi_1| = \left|\phi_c\left(\frac{c}{v}\right)_d + m_2 T - \phi_1\right|$$

$$= \left|-\phi_c\left[1 - \left(\frac{c}{v}\right)_d\right] + \frac{\phi_c\left(\frac{c}{v}\right)_n - \phi_c\left(\frac{c}{v}\right)_d}{\Delta T_{SS}}\, T\right|$$

$$= \left|\frac{\phi_1}{.9974}\left[\left\{\left(\frac{c}{v}\right)_n - \left(\frac{c}{v}\right)_d\right\}\frac{T}{\Delta T_{SS}} - \left\{1 - \frac{\left(\frac{c}{v}\right)_d}{.9974}\right\}\right]\right| \quad T \epsilon \Delta T_{SS} \,.$$

For $T = 0$; $\quad \Delta\phi'(T) = \phi_1\left[1 - \frac{\left(\frac{c}{v}\right)_d}{.9974}\right]$

For $T = \Delta T_{SS}$; $\quad \Delta\phi'(T) = \phi_1\left[\frac{\left(\frac{c}{v}\right)_n}{.9974} - 1\right]$.

Figure 14 illustrates $\Delta\phi'(T)$ as a function of $T \epsilon \Delta T_{SR}$.

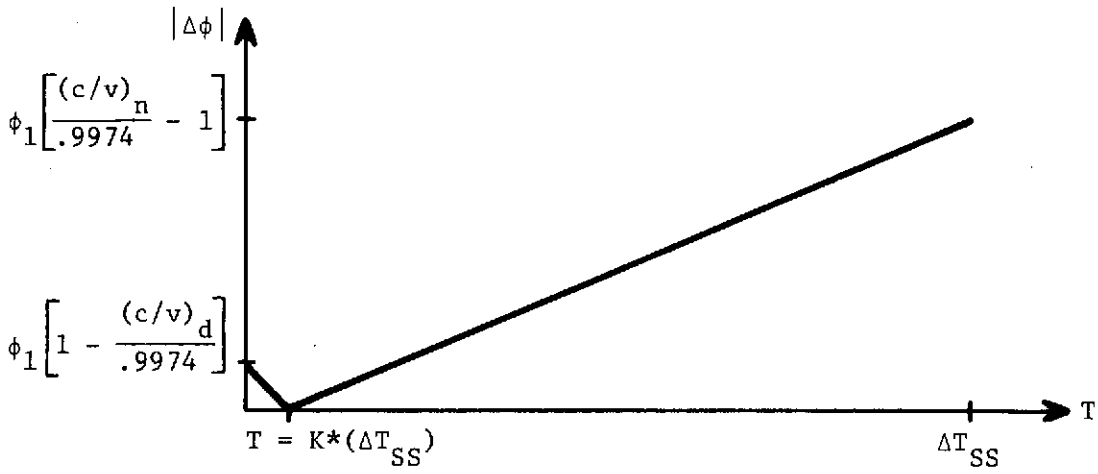

Fig. 14. Phase error in day-to-night transition period.

Figure 15 presents the position error as a function of time-of-day superimposed on the trapezoidal prediction of Fig. 12.

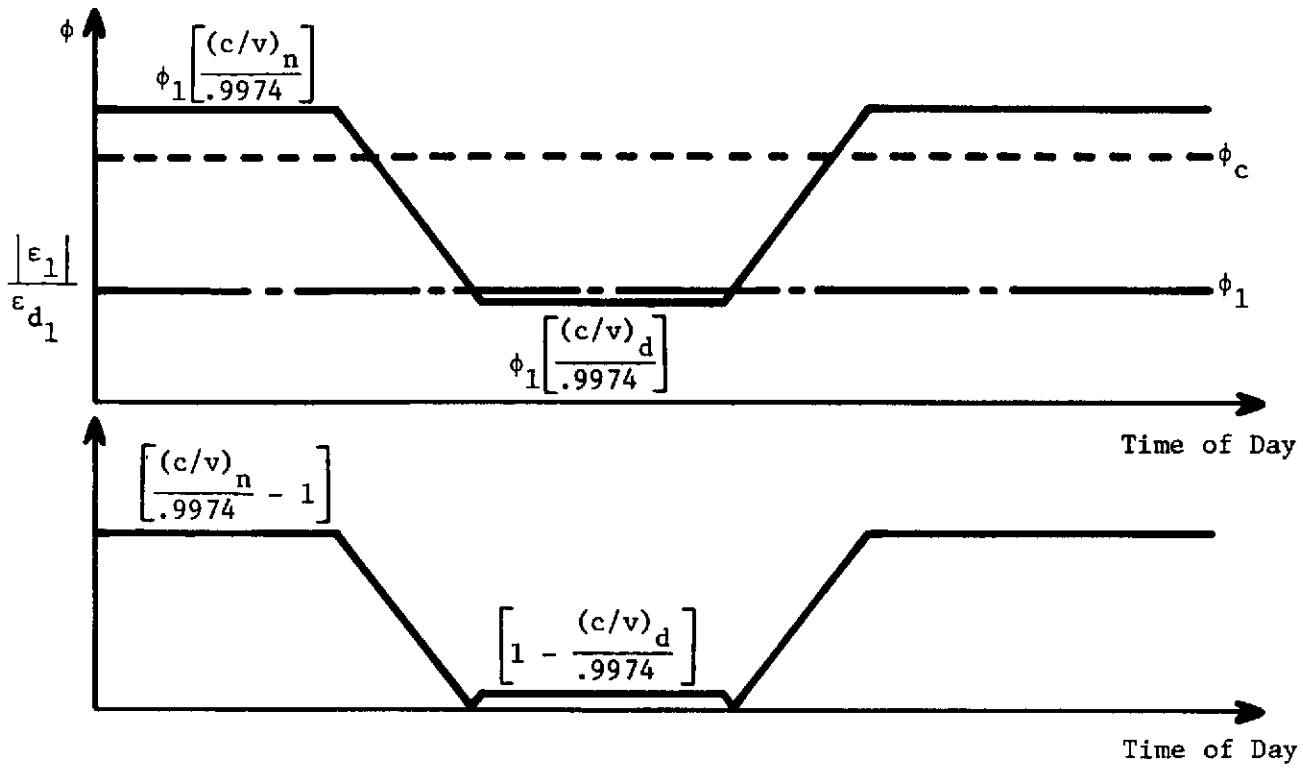

Fig. 15. Position error as a function of time of day for receiver-transmitter path 1.

Consider a transmitter pair where there is uncertainty in each of the receiver-transmitter distance measurements. Figure 16 represents the phase difference prediction using the trapezoidal method and the associated position error standard deviation using the transmitter pair.

As can be seen in Fig. 16, the maximum error in position estimate using trapezoidal SWC as a function of receiver-transmitter distance measurements is during the total nighttime period. The rms error is given by

$$\sigma_{\Delta_{12}} = \left[\frac{\left(\frac{c}{v}\right)_n}{.9974} - 1\right]\left[\sigma^2_{\varepsilon_{d_1}} + \sigma^2_{\varepsilon_{d_2}}\right]^{1/2} \tag{11}$$

where $\sigma^2_{\varepsilon_{d_1}}$ = variance of distance error in path 1,

$\sigma^2_{\varepsilon_{d_2}}$ = variance of distance error in path 2, and

σ_{Δ_2} = standard deviation of position estimation error based on phase difference measurements.

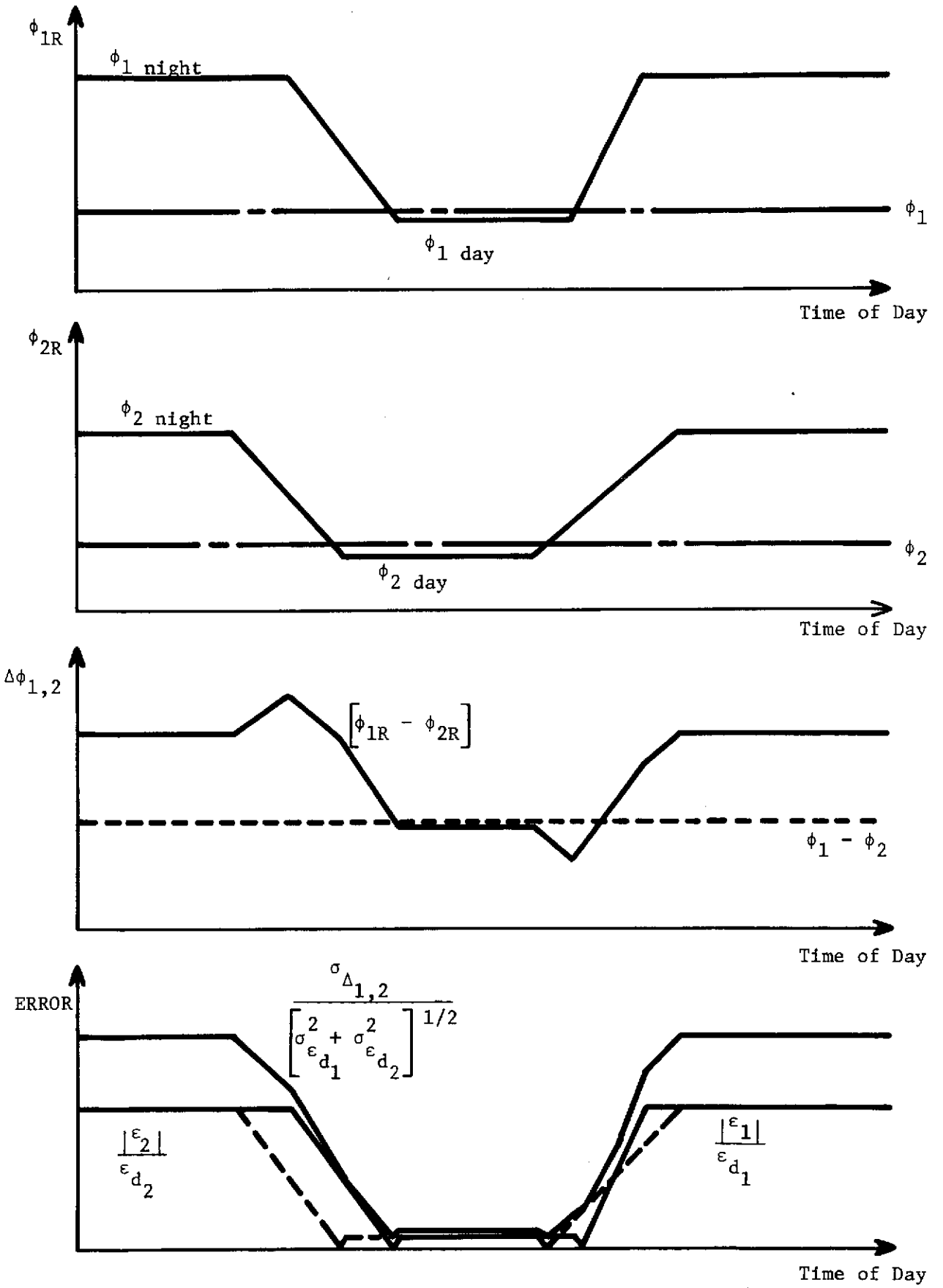

Fig. 16. Trapezoidal prediction of phase difference between two transmitters at a receiver and the associated error standard deviation as a function of error in receiver-transmitter distance measurements.

4.6.3 Analysis.— As can be seen from this analysis, the error in position estimation from phase difference measurement employing trapezoidal SWC at a receiver is relatively insensitive to errors in distance measurement between the receiver and the transmitters used. (Trapezoidal SWC are thus relatively insensitive to error in receiver-transmitter distance measurement.) The maximum error occurs during nighttime conditions, where nominally the ratio of $(c/v)_n = 1.0004$ so that the standard deviation of position error

$$\sigma_{\Delta_{12}} = \left[.003\ \sigma^2_{\varepsilon_{d_1}} + \sigma^2_{\varepsilon_{d_2}} \right]^{1/2} . \qquad (12)$$

Thus, an rms error of 18 n. mi. can be sustained in estimates of receiver-transmitter distance and yields less than 1 cec position error at 10.2 kHz at the receiver.

During daytime, an rms error of 560 n. mi. can be sustained in estimates of receiver-transmitter distance and yields less than 1 cec position error at 10.2 kHz at the receiver.

To illustrate confidence in the method discussed in Section 4.5 for calculating distances between points on the earth's surface, the distances from the four present Omega stations to Cambridge were computed and compared with values determined in ref. 13. These calculations are in terms of SWC chart wavelengths.

	Latitude	Longitude	Pierce's Distance (in Chart cec)	Geodesic Distance
Cambridge	42°22'39"N (42.3775°N)	71°07'03"W (71.1175°W)		
Norway	66°25'15"N (66.420833°N)	13°09'10"E (346.847222°W)	18792.16	18819.12
Trinidad	10°42'6.22"N (10.701728°N)	61°38'20.30"W (61.638972°W)	12316.34	12311.34
Hawaii	21°24'20.67"N (21.405742°N)	157°49'47.75"W (157.829931°W)	27747.83	27753.84
New York	43°26'40.92"N (43.4447°N)	75°05'09.80"W (75.086056°W)	1170.86	1171.47

These calculations were made with the following constants:

$$\text{one chart wavelength} = \frac{\text{Free space wavelength at 10.2 kHz}}{.9974}$$

$$= 2.946641 \times 10^4 \text{ meters}$$

one mean earth radius = 6371 km

= 216.212271 chart wavelengths.

The largest difference between the geodesic and the Pierce values is in the Norway-Cambridge distance, which is off by 26.96 cec, or 7.944 km. The largest (daytime) error that this can cause when computing sky-wave corrections using the T-model is, from (5),

$$\varepsilon = \left[1 - \frac{\frac{c}{v_{p_{day}}}}{.9974}\right] \varepsilon_{distance} = .0001 \times 26.96 \approx .0027 \text{ cec} \quad .$$

4.7 Summary

To obtain the T-model phase correction at a particular receiver site, the latitudes and longitudes of the receiver and transmitter are needed. The ephemeris of the sun, along with an estimate of the receiver-transmitter distance, can then provide all the information needed to get the sky-wave correction at a particular frequency. Constants needed are relative daytime, nighttime, and nominal phase velocities and estimates of the earth radius.

The T-model method offers a very simple scheme for generating sky-wave corrections. The resulting correction is constant during the receiver-transmitter path daytime and nighttime periods. During the transition periods, the correction is essentially the daytime correction modified according to the percentage of the path in darkness. The change in phase correction as a function of the percentage of the path in darkness is assumed linear.

Appendix D provides a flow chart description of a computer program to generate phase corrections using the T-model scheme.

5.0 COMPARISON OF TRAPEZOIDAL MODEL, NAVY MODEL, AND ACTUAL DATA

This chapter provides a comparison of predicted phase difference measurements at 10.2 kHz over a one-year period with actual phase measurements made by J. A. Pierce at Harvard University in Cambridge, Massachusetts. Phase difference predictions are provided from two sources. The published Navy sky-wave corrections have been used to obtain one set of predicted phase difference measurements by applying the published corrections to the nominal* phase prediction in the Cambridge area using the Trinidad-Hawaii (B-C) transmissions. A second set of phase difference predictions has been obtained using the trapezoidal model described in Chapter 3.0. Since the Navy predictions are provided as two-week averages, the T-model predictions used are 15-day average phase difference predictions. The daily phase measurement Pierce data have also been averaged over 15-day periods. One 15-day period for each month from October 1970 through September 1971 is considered. All periods are the first 15 days of the month except for May 1971, when the Pierce data were incomplete. For May 1971 the average of the last 15 days of Pierce data is used.

Figures 17-25 compare phase difference predictions from the published Navy tables (N), the T-model (T), and the Pierce data (P) for the months Jan.-Sept. 1971. Figures 26-28 provide the same comparison for the period Oct.-Dec. 1970. Predictions and measurements are provided in centicycles at 10.2 kHz averaged over 15 days for each hour of the 24-hour period. Lines have been drawn between points to assist in reading the plots.

Figures 29-40 provide pairwise differences between the curves given in Figs. 17-28. In each of Figs. 29-40, the curve defined by points labeled "X" represents the difference between the Pierce average measurements and the T-model average predictions for each hour of the 24-hour day. Curve "Y" represents the difference between the Pierce average measurements and the Navy predictions. Curve "Z" represents the difference between the two predictions. Relative phase difference is indicated in centicycles of 10.2 kHz.

Plots of the monthly mean difference between each pairwise comparison are given in Figs. 41-43. The monthly mean is determined by computing the 24-hour average of the hourly values given in Figs. 29-40.

---

*Nominal phase is based on chart velocity.

PRECEDING PAGE BLANK NOT FILMED

Figure 41 illustrates the mean difference between the Pierce measurements and the T-model predictions for each 15-day period. Figure 42 shows the mean differences between the Pierce measurements and the Navy predictions, while Fig. 43 provides the mean differences between the T-model and Navy phase predictions. Additionally, these three figures show three-month average differences for each pair to indicate seasonal variations.

Figures 44-46 provide monthly and quarterly rms difference for each pairwise comparison. These rms values for each month are determined with respect to the monthly means given in Figs. 41-43 for pairs X, Y, and Z, respectively. The quarterly rms difference is provided to indicate seasonal variations.

5.1 Analysis

In Figures 17-28 it can be seen that the T-model phase predictions do provide a generally accurate representation of what the phase difference readings will be. The diurnal shifts are definitely present; however, the largest error seems to be in prediction of the time of day when the diurnal effects occur. The all-daytime and all-nighttime periods are illustrated by the horizontal straight lines on the trapezoidal predictions. Variations within these periods as evidenced by the actual data and as accounted for by the Navy predictions are, of course, not obtainable with the T-model predictions. After some examination, it appears that some simple filtering of the T-model predictions to smooth out the "sharp corners" might improve these predictions.

Analyzing Figures 29-40, it is clearly evident that the largest errors in the T-model predictions occur during the transition regions. The largest errors are on the order of 25 cec, occurring in Jan., Feb., and Mar. during the nighttime-daytime transition on the Cambridge-Hawaii path. A shift in the calculated sunrise times at Hawaii and Cambridge could improve this error considerably.

Generally, from Figure 41, the T-model predictions are too low in the winter months (Jan.-Feb.) and are high for the remainder of the year. Closest agreement occurs in Jun. and Jul. and shows very small average error (less than .3 cec) with the summertime predictions less than 1 cec on the average. Considering the mean values above, the T-model predictions do as well or better than the Navy predictions (Figure 42) with the yearly average

deviation from the measured value less than 3 cec for both. Comparison of the Navy and T-model predictions in Fig. 43 shows that the trapezoidal predictions are generally higher than the Navy predictions.

The rms error in the T-model predictions in Fig. 44 illustrates why the T-model predictions have been objected to previously (see ref. 14). The rms error as compared to that of the Navy predictions (Fig. 45) is some 3 cec higher comparing the yearly average rms error. This error is the error when comparing the predictions with the measured phase values. As illustrated in Fig. 46, the rms error between the two predictions averages out to approximately 8 cec. However, comparison of each method of phase prediction to the measured phase is a more valid comparison.

5.2 Conclusions

The T-model phase predictions account for the most significant Omega phase perturbations caused by diurnal ionospheric variations. The greatest advantage of this method is the inherent simplicity of generating the predictions and/or corrections. As has been illustrated, the incurred first-order error is comparable to that achieved with the complex Navy sky-wave correction method. Although the second-order error of the T-model is not as good as the Navy predictions, it appears that there may be a possibility of filtering the trapezoidal predictions to improve the second-order errors. Furthermore, the simplicity of generating the T-model predictions enhances the possibility of real-time employment in the SWC gradient corrected mode of differential Omega (see Section 6.3).

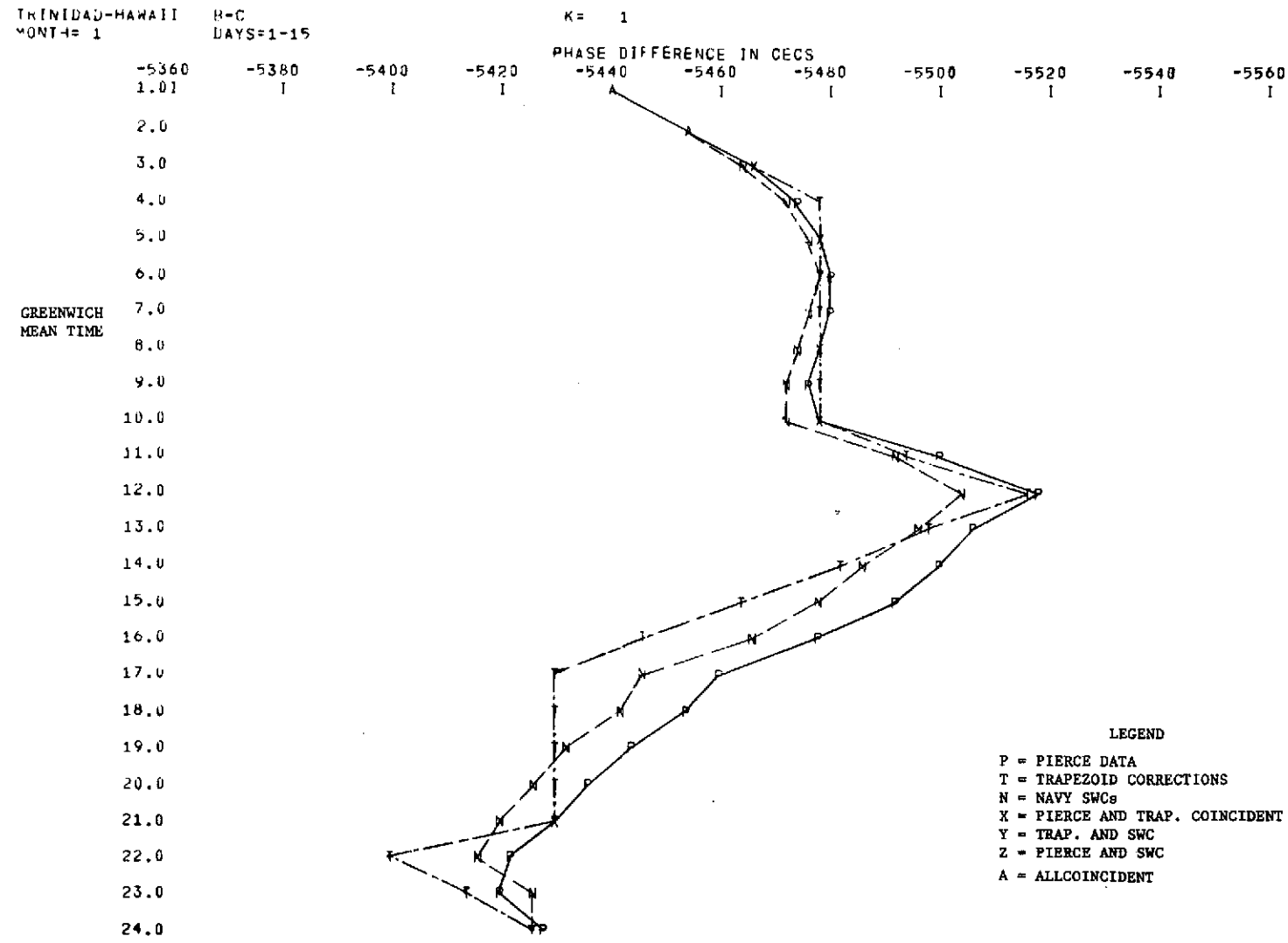

Fig. 17. 10.2 kHz Omega phase predictions for B-C at Cambridge, Mass., using Navy SWC Tables (N), Trapezoidal Model (T), and Pierce Measurements (P) for period 1-15 January 1971.

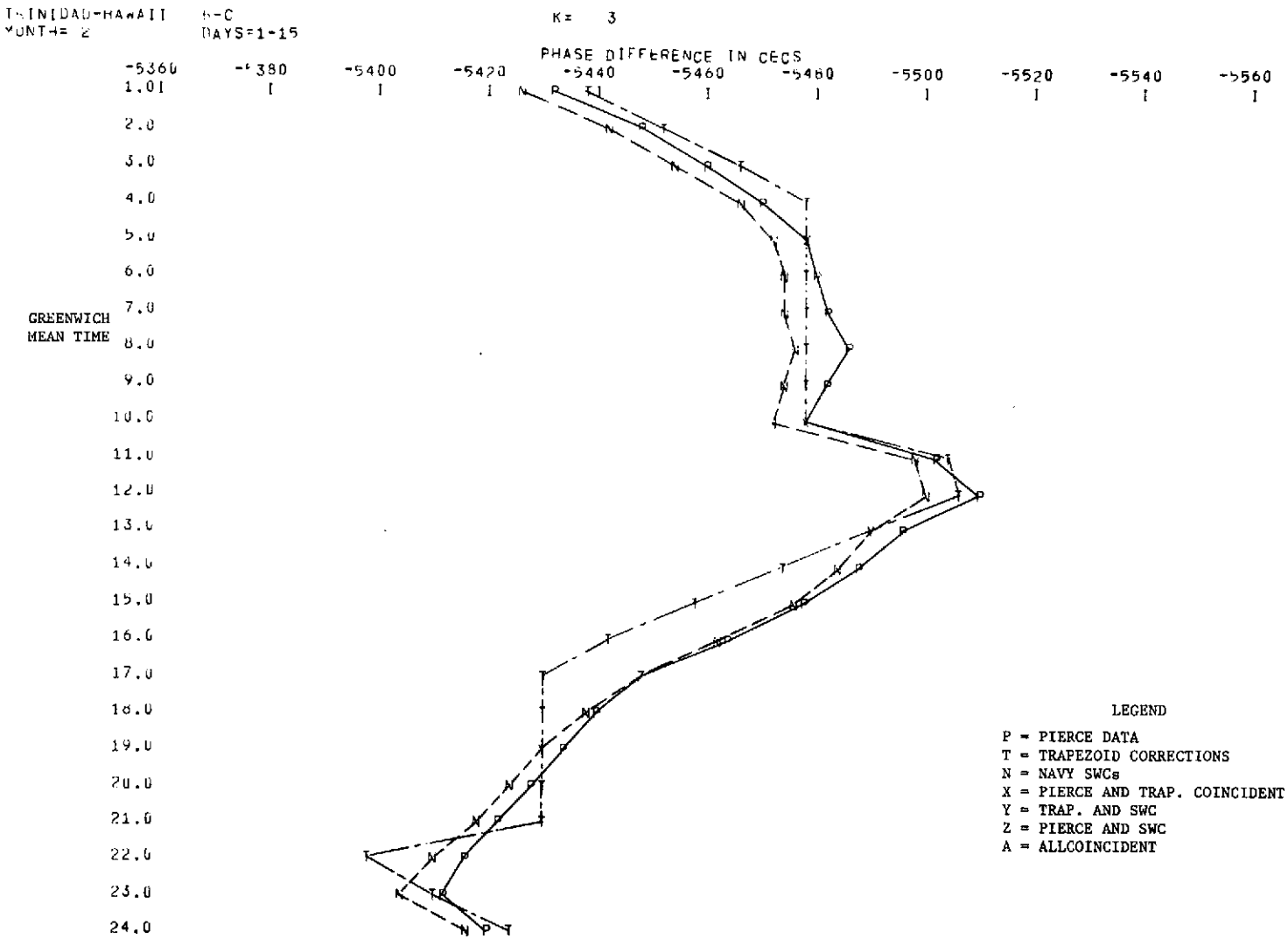

Fig. 18. 10.2 kHz Omega phase predictions for B-C at Cambridge, Mass., using Navy SWC Tables (N), Trapezoidal Model (T), and Pierce Measurements (P) for period 1-15 February 1971.

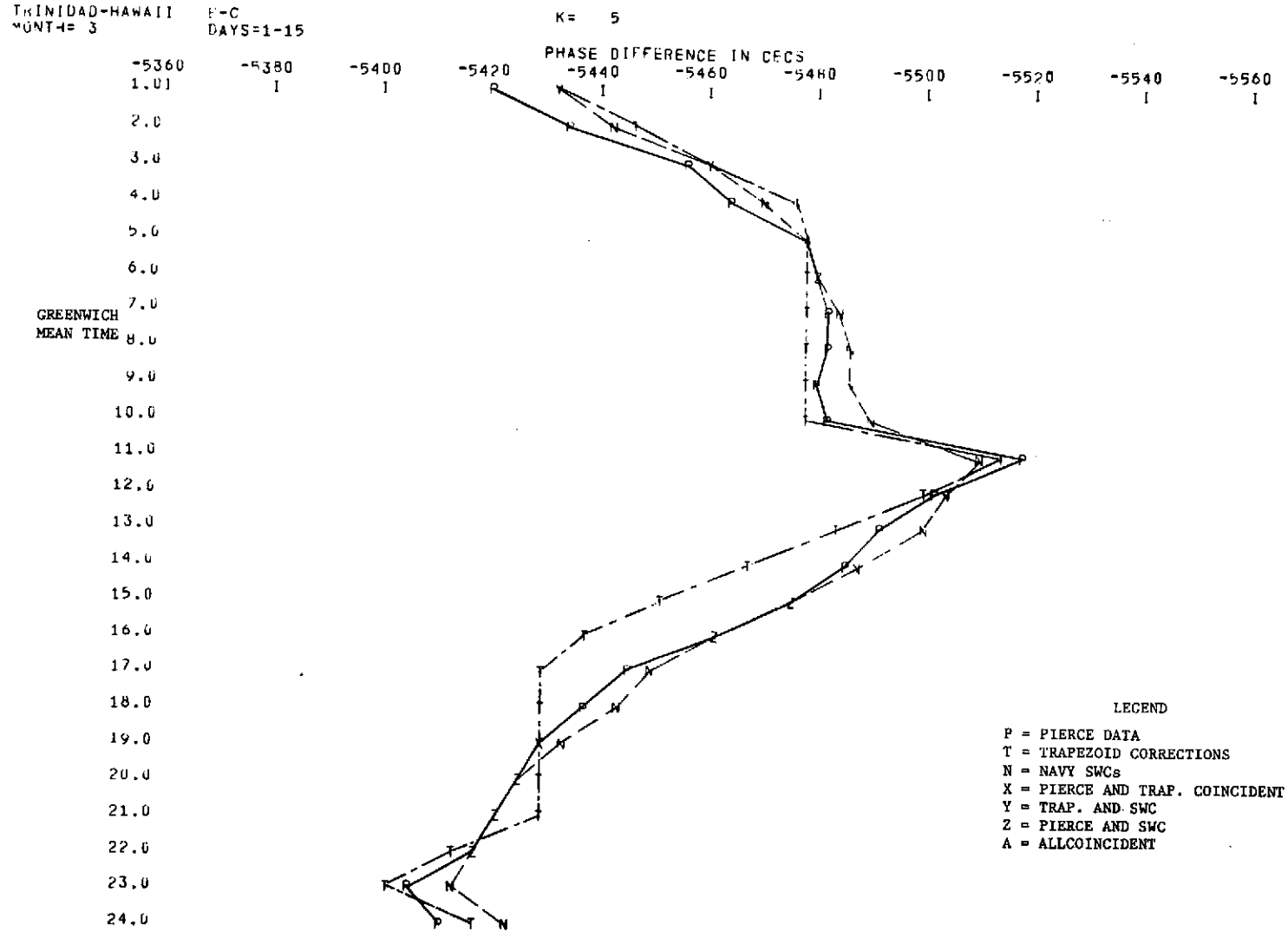

Fig. 19. 10.2 kHz Omega phase predictions for B-C at Cambridge, Mass., using Navy SWC tables (N), Trapezoidal Model (T), and Pierce measurements (P) for period 1-15 March 1971.

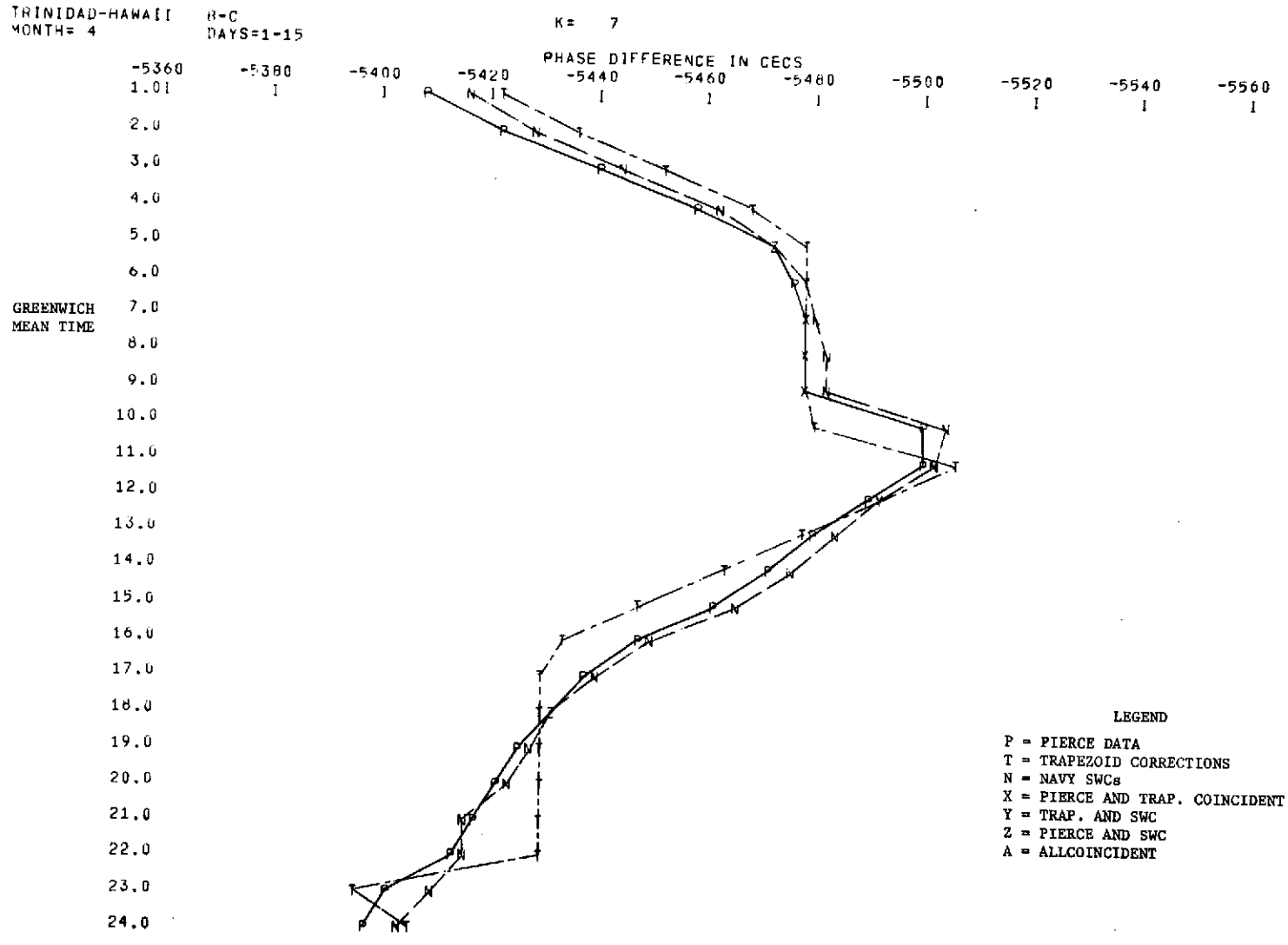

Fig. 20. 10.2 kHz Omega phase predictions for B-C at Cambridge, Mass., using Navy SWC tables (N), trapezoidal model (T), and Pierce measurements (P) for period 1-15 April 1971.

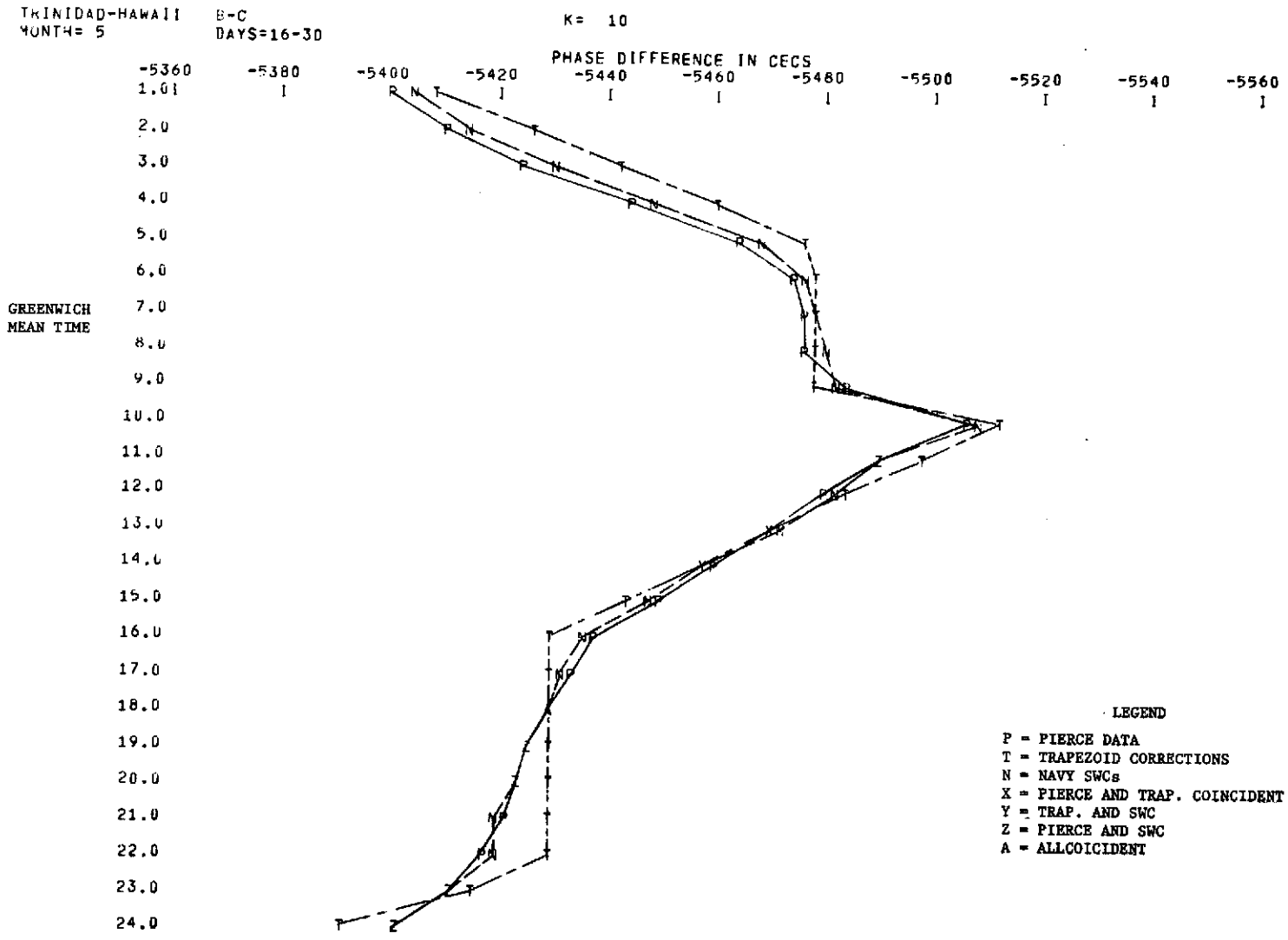

Fig. 21. 10.2 kHz Omega phase predictions for B-C at Cambridge, Mass., using Navy SWC tables (N), trapezoidal model (T), and Pierce measurements (P) for period 16-30 May 1971.

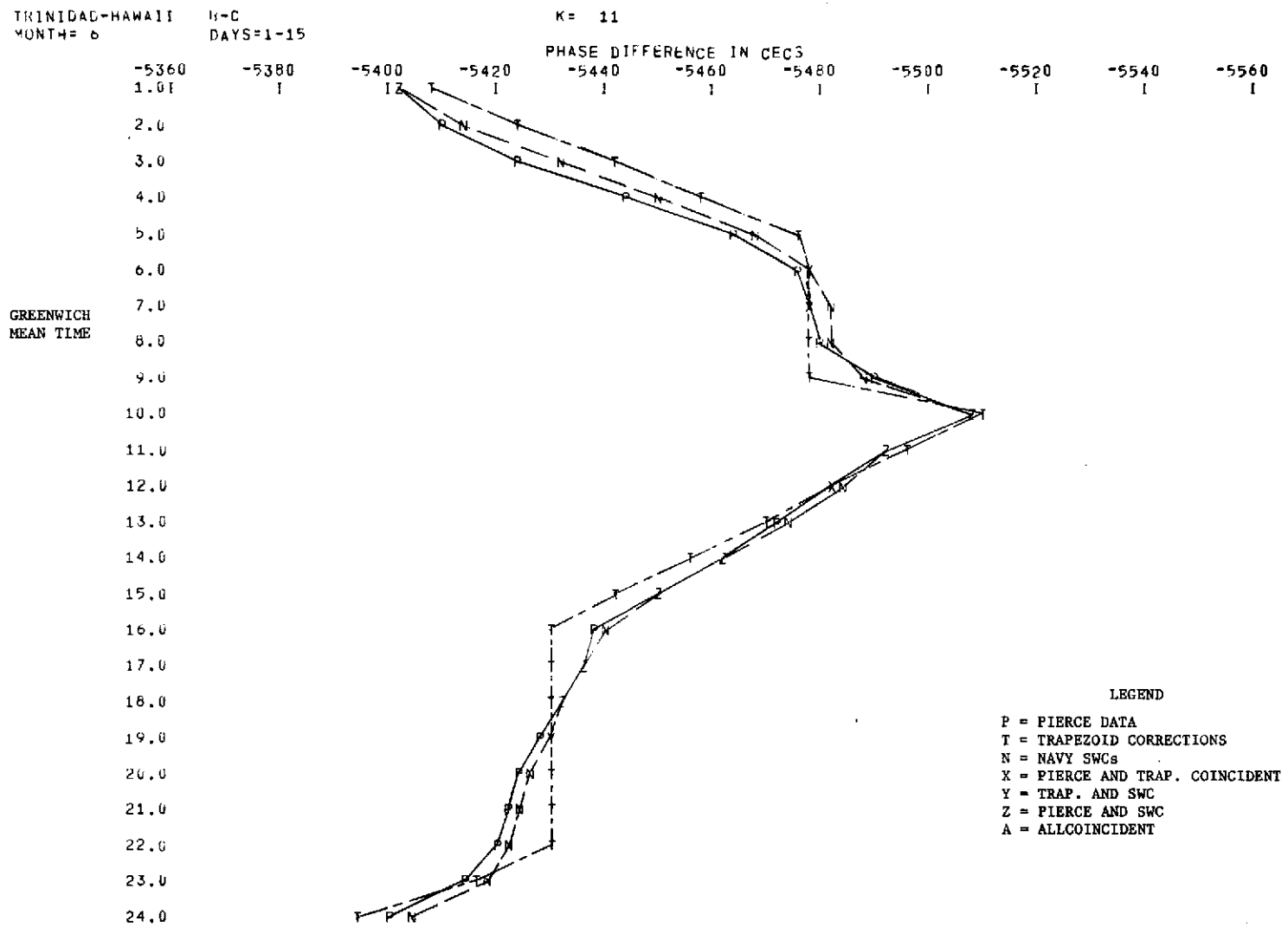

Fig. 22. 10.2 kHz Omega phase predictions for B-C at Cambridge, Mass., using Navy SWC tables (N), trapezoidal model (T), and Pierce measurements (P) for period 1-15 June 1971.

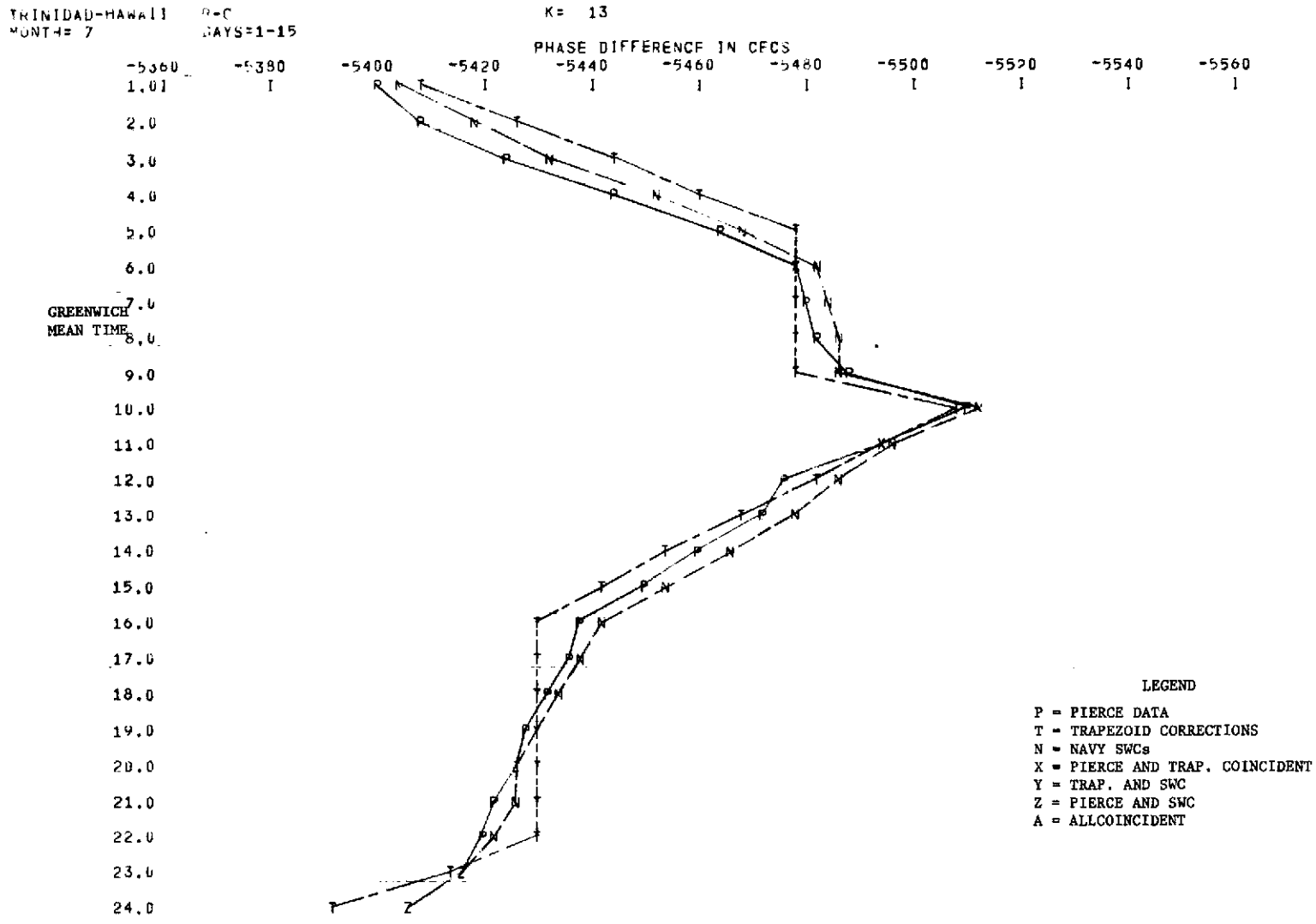

Fig. 23. 10.2 kHz Omega phase predictions for B-C at Cambridge, Mass., using Navy SWC tables (N), trapezoidal model (T), and Pierce measurements (P) for period 1-15 July 1971.

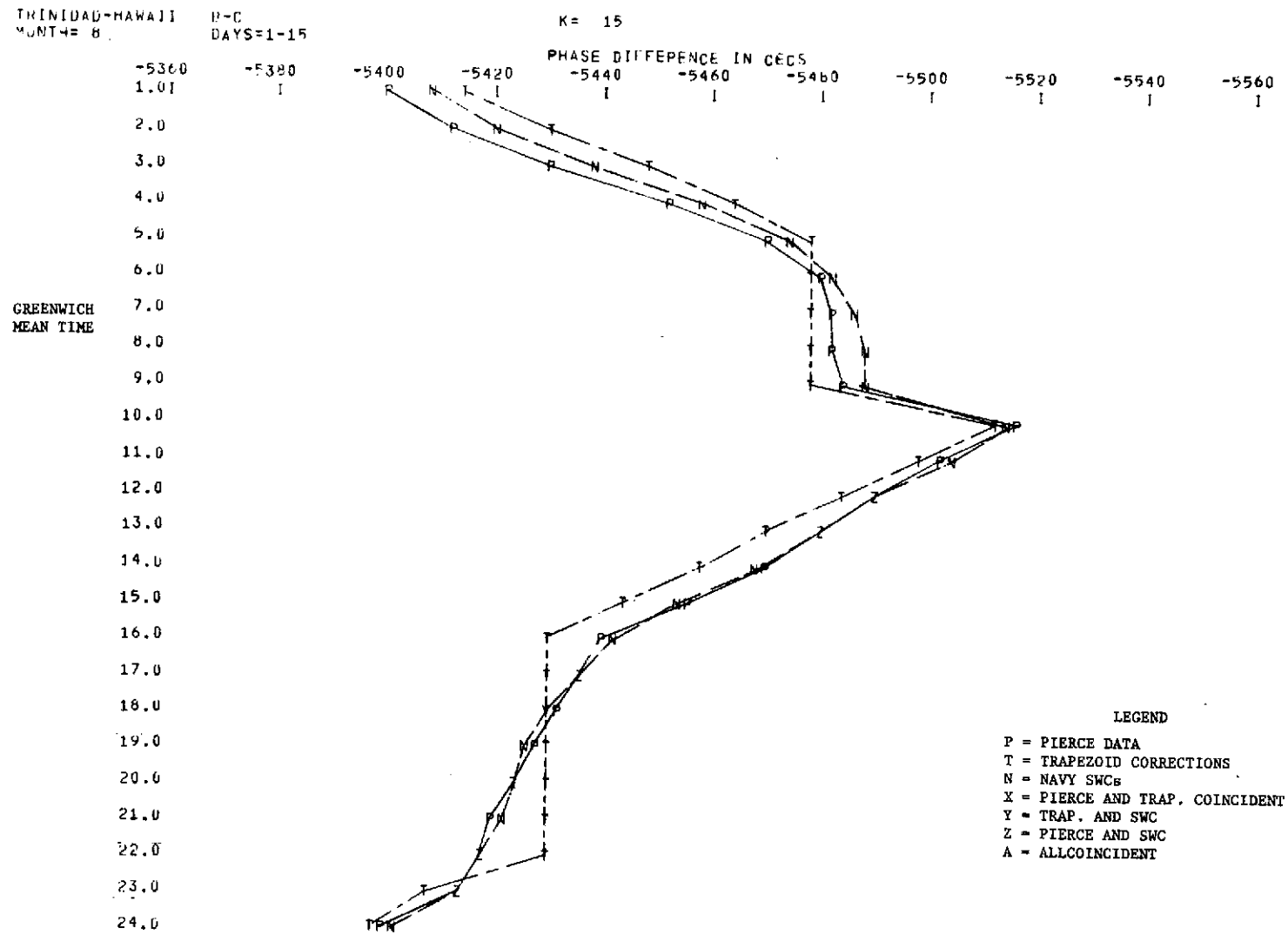

Fig. 24. 10.2 kHz Omega phase predictions for B-C at Cambridge, Mass., using Navy SWC tables (N), trapezoidal model (T), and Pierce measurements (P) for period 1-15 August 1971.

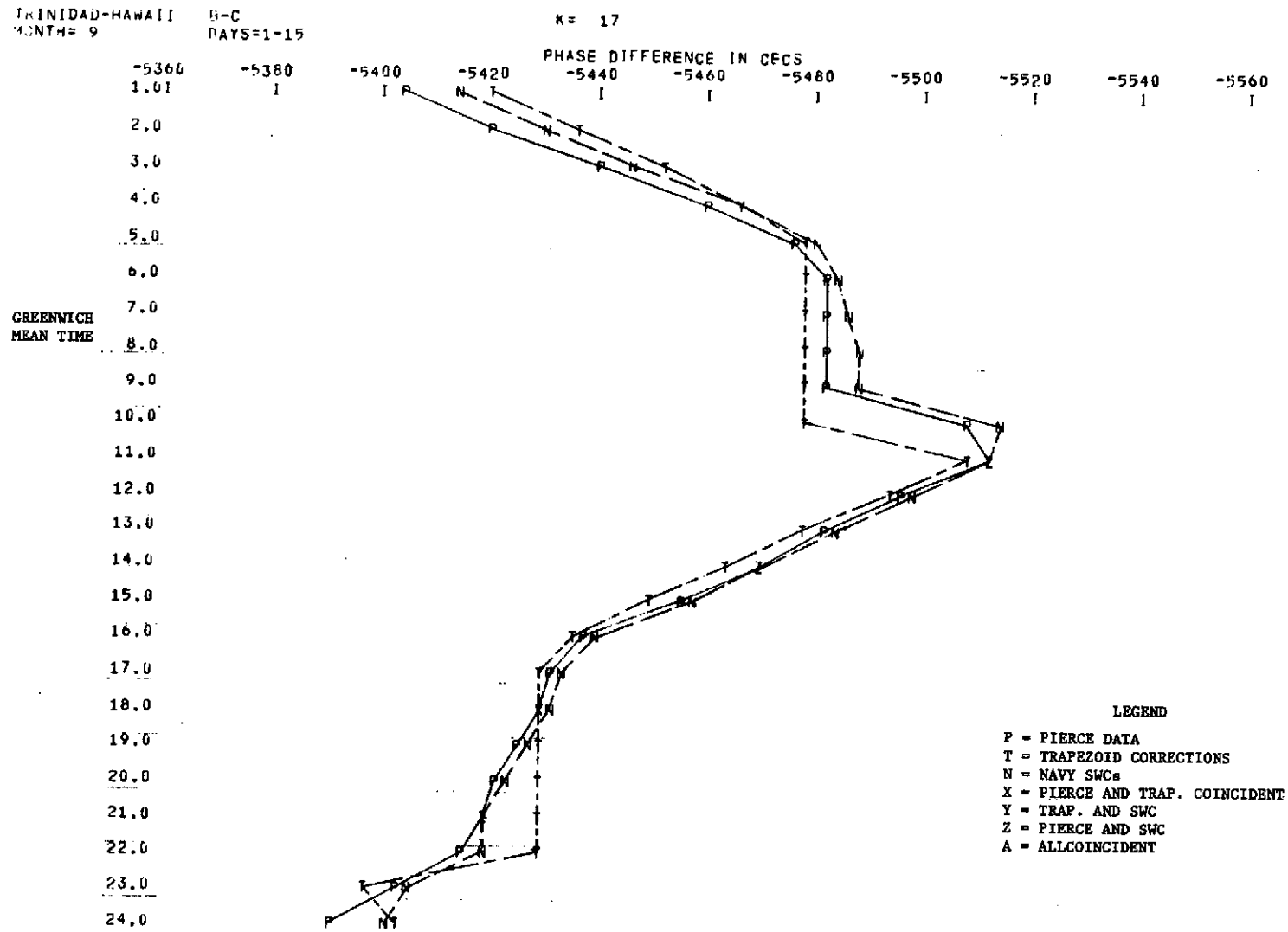

Fig. 25. 10.2 kHz Omega phase predictions for B-C at Cambridge, Mass., using Navy SWC tables (N), trapezoidal model (T), and Pierce measurements (P) for period 1-15 September 1971.

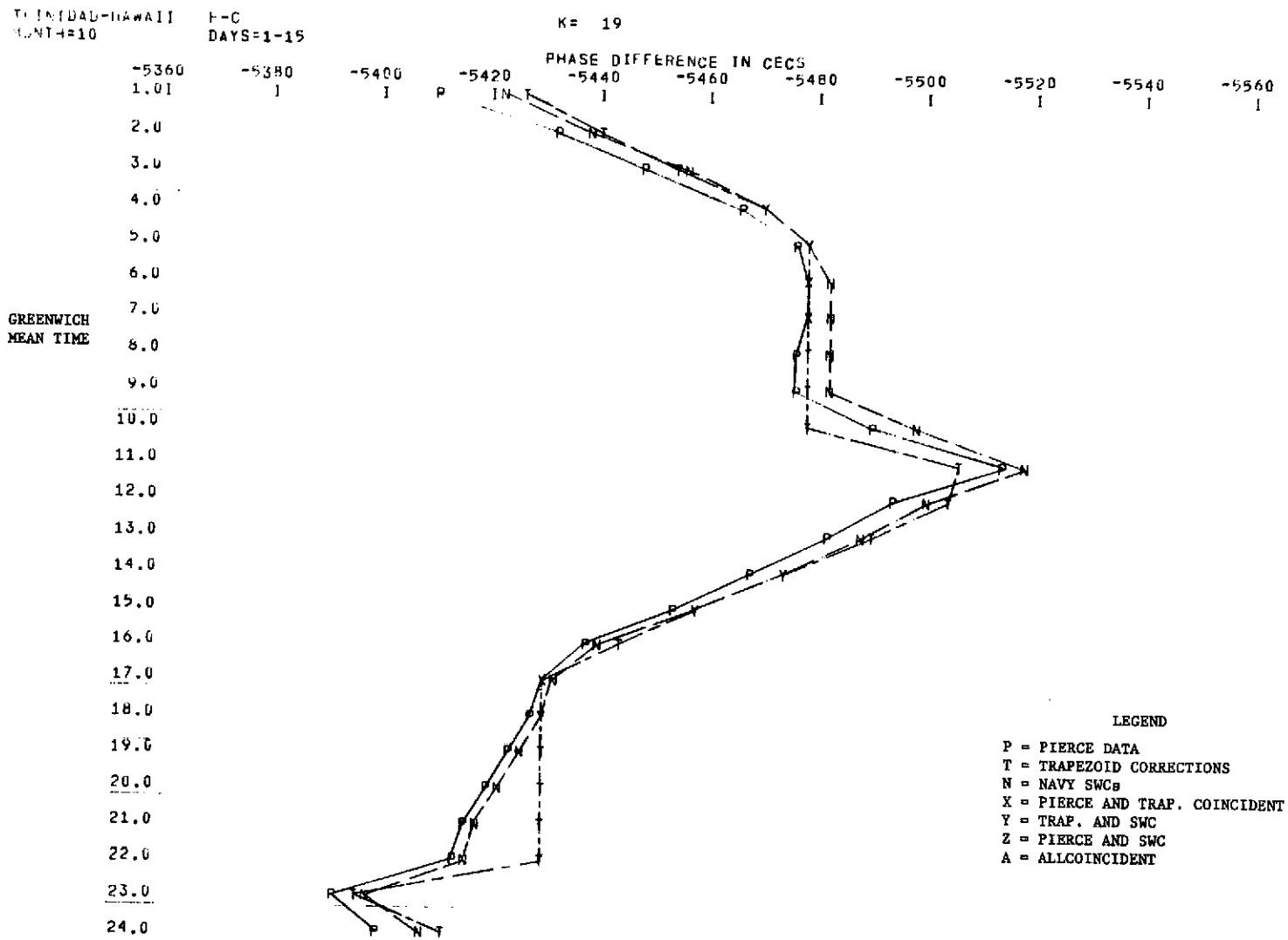

Fig. 26. 10.2 kHz Omega phase predictions for B-C at Cambridge, Mass., using Navy SWC tables (N), trapezoidal model (T), and Pierce measurements (P) for period 1-15 October 1970.

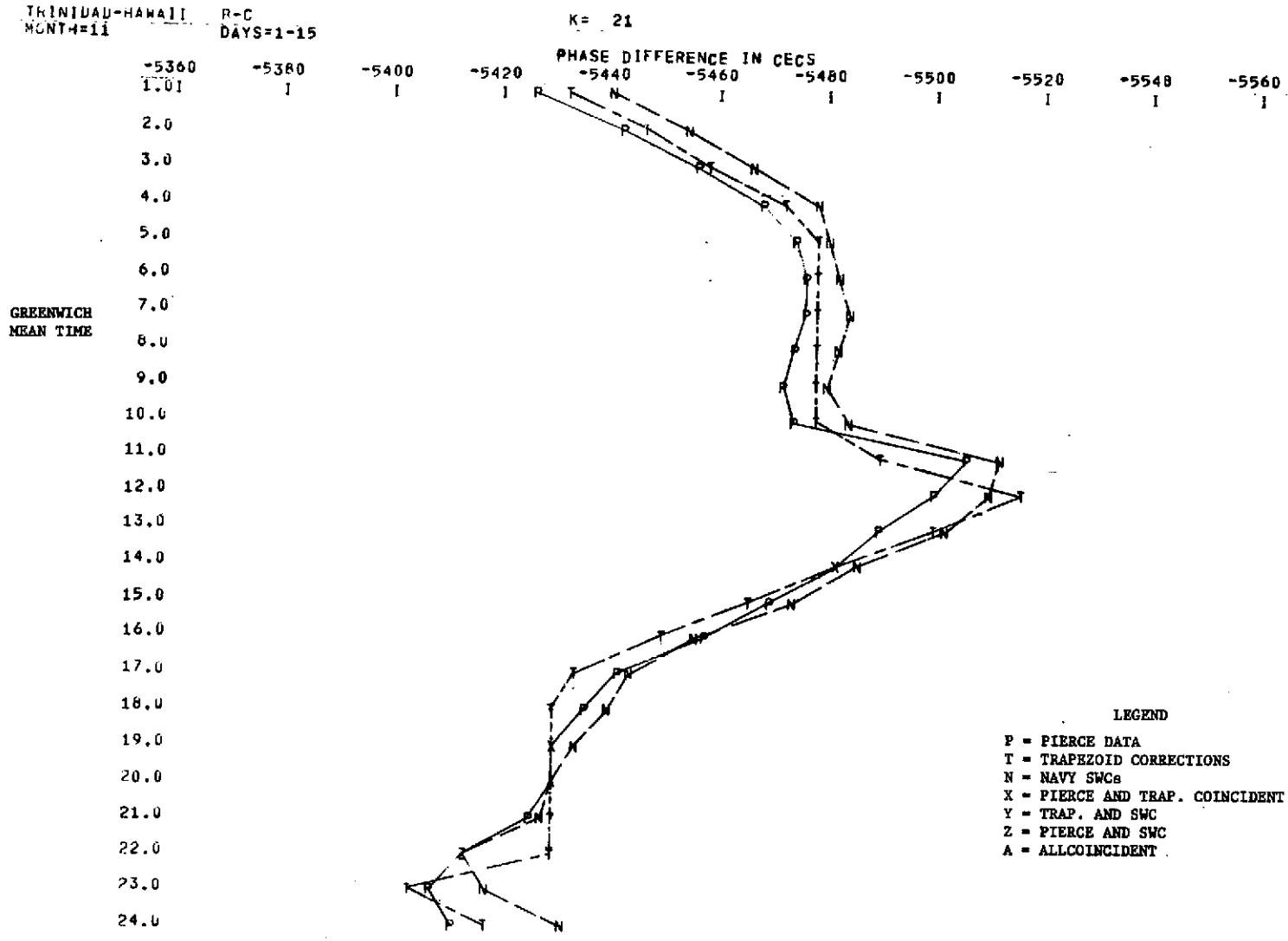

Fig. 27. 10.2 kHz Omega phase predictions for B-C at Cambridge, Mass., using Navy SWC tables (N), trapezoidal model (T), and Pierce measurements (P) for period 1-15 November 1970.

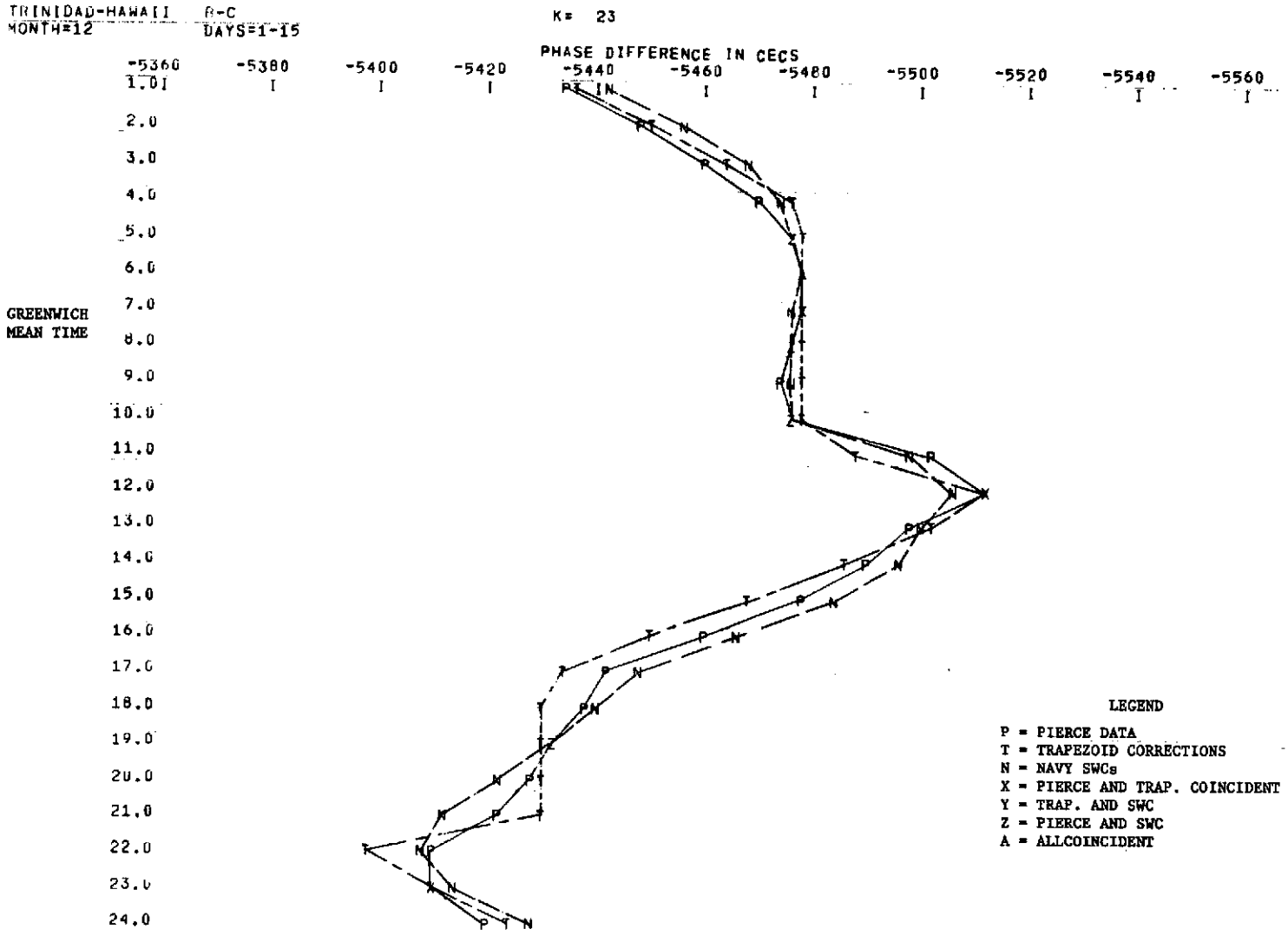

Fig. 28. 10.2 kHz Omega phase predictions for B-C at Cambridge, Mass., using Navy SWC tables (N), trapezoidal model (T), and Pierce measurements (P) for period 1-15 December 1970.

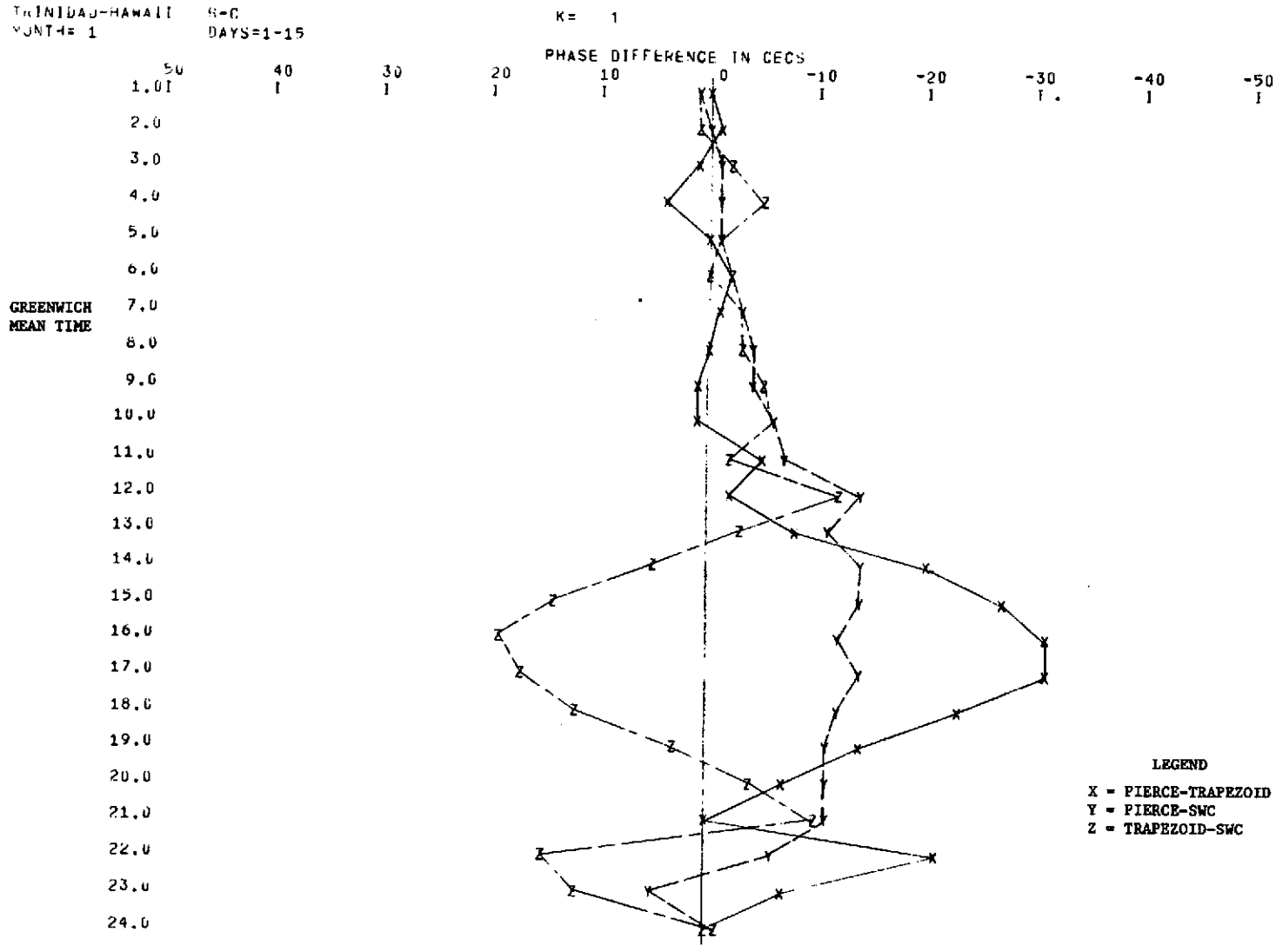

Fig. 29. B-C 10.2 kHz Omega phase difference comparison of Pierce measurement minus trapezoidal prediction (X), Pierce measurement minus Navy prediction(Y), and trapezoidal prediction minus Navy prediction (Z) at Cambridge, Mass., for period 1-15 January 1971.

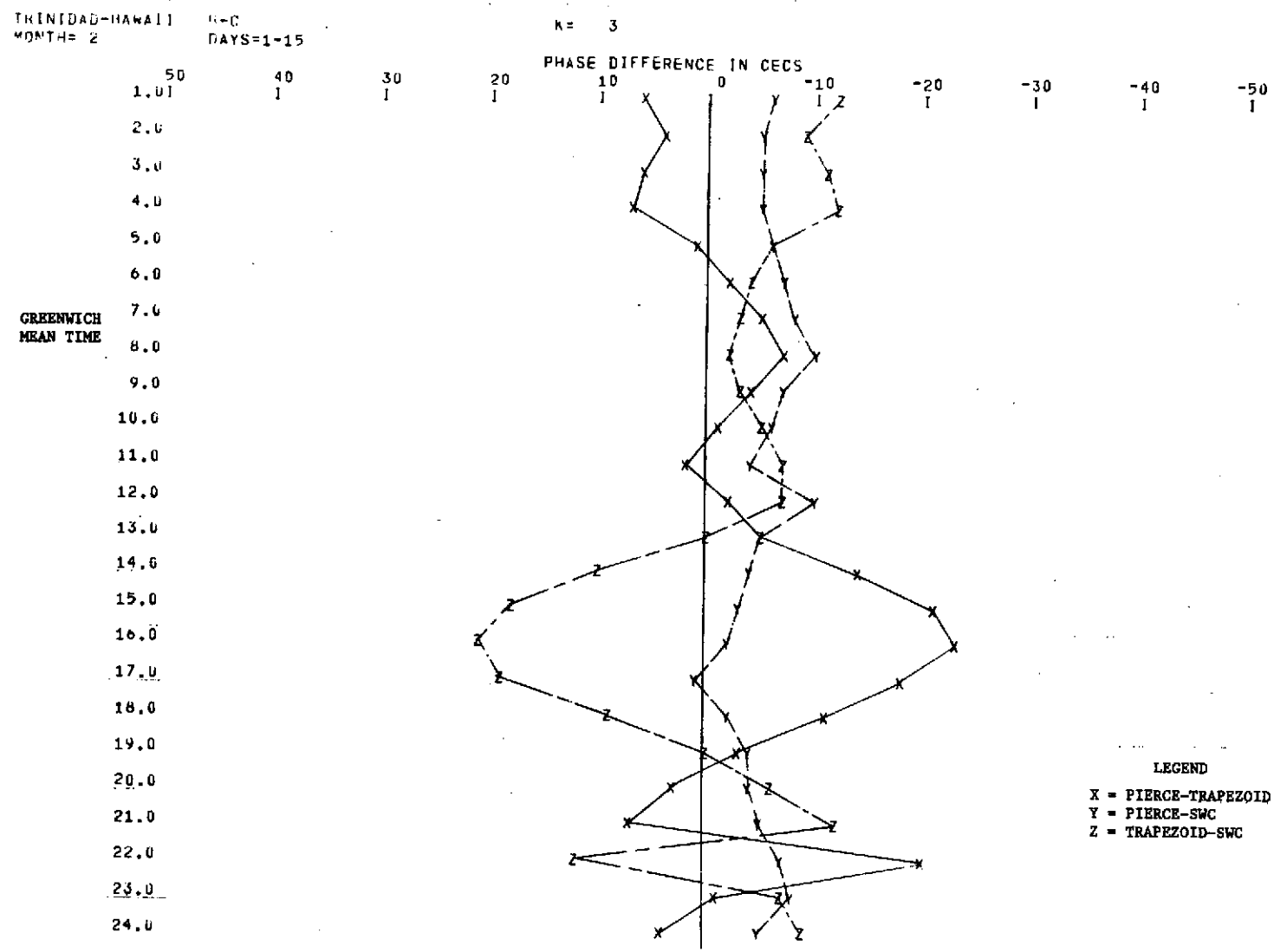

Fig. 30. B-C 10.2 kHz Omega phase difference comparison of Pierce measurement minus trapezoidal prediction (X), Pierce measurement minus Navy prediction (Y), and trapezoidal prediction minus Navy prediction (Z) at Cambridge, Mass., for period 1-15 February 1971.

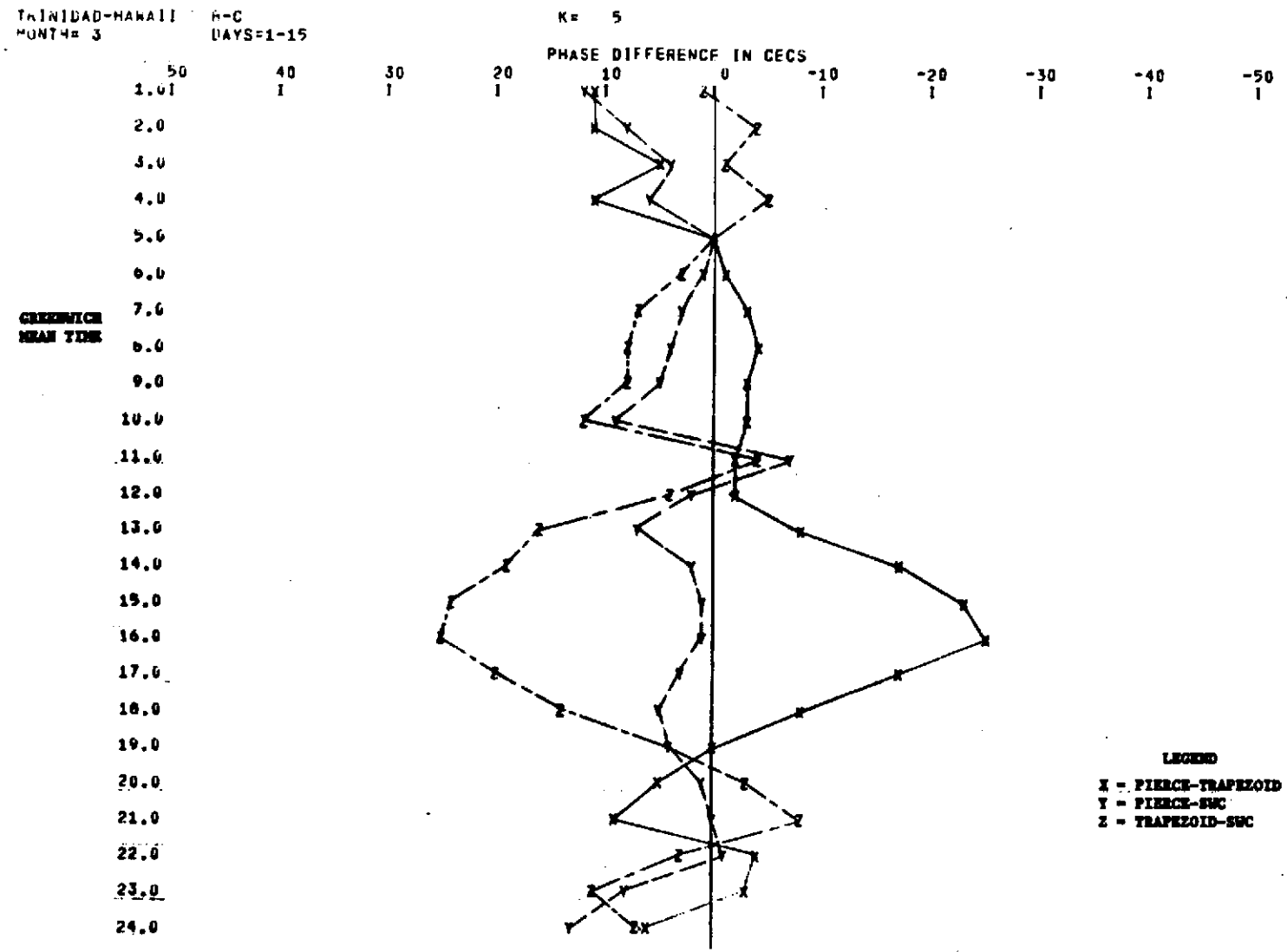

Fig. 31. B-C 10.2 kHz Omega phase difference comparison of Pierce measurement minus trapezoidal prediction (X), Pierce measurement minus Navy prediction (Y), and trapezoidal prediction minus Navy prediction (Z) at Cambridge, Mass., for period 1-15 March 1971.

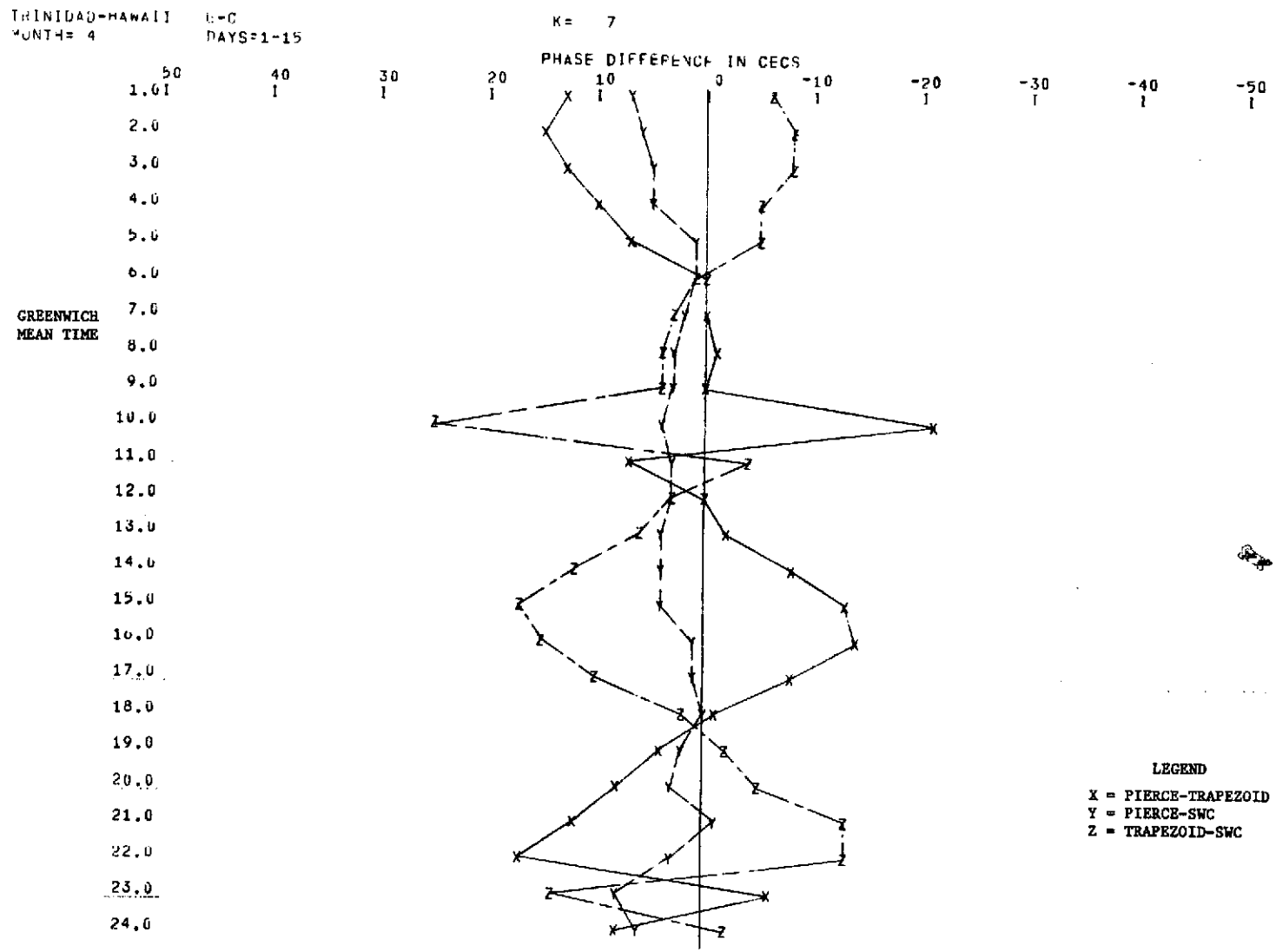

Fig. 32. B-C 10.2 kHz Omega phase difference comparison of Pierce measurement minus trapezoidal prediction (X), Pierce measurement minus Navy prediction (Y), and trapezoidal prediction minus Navy prediction (Z) at Cambridge, Mass., for period 1-15 April 1971.

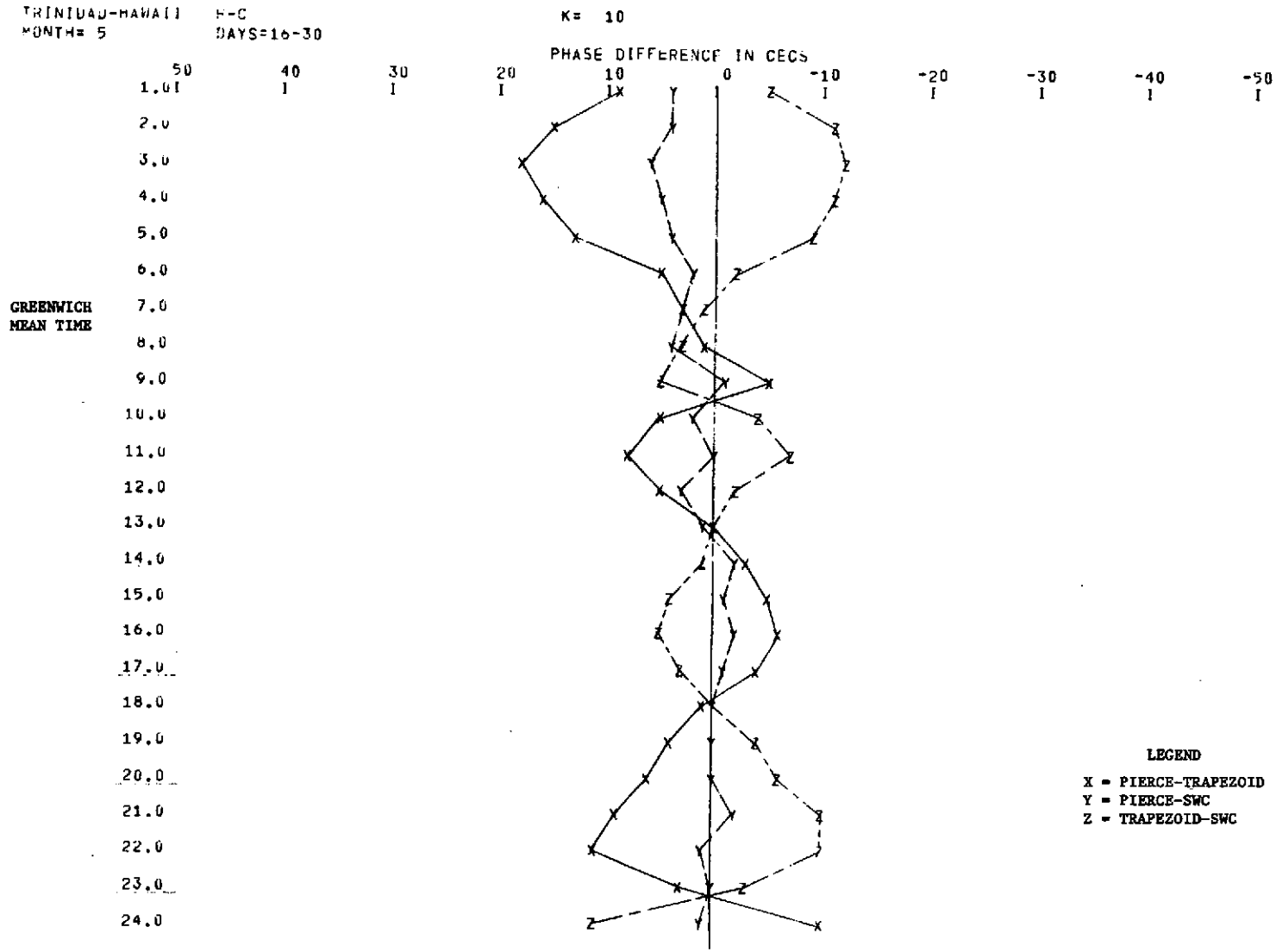

Fig. 33. B-C 10.2 kHz Omega phase difference comparison of Pierce measurement minus trapezoidal prediction (X), Pierce measurement minus Navy prediction (Y), and trapezoidal prediction minus Navy prediction (Z) at Cambridge, Mass., for period 16-30 May 1971.

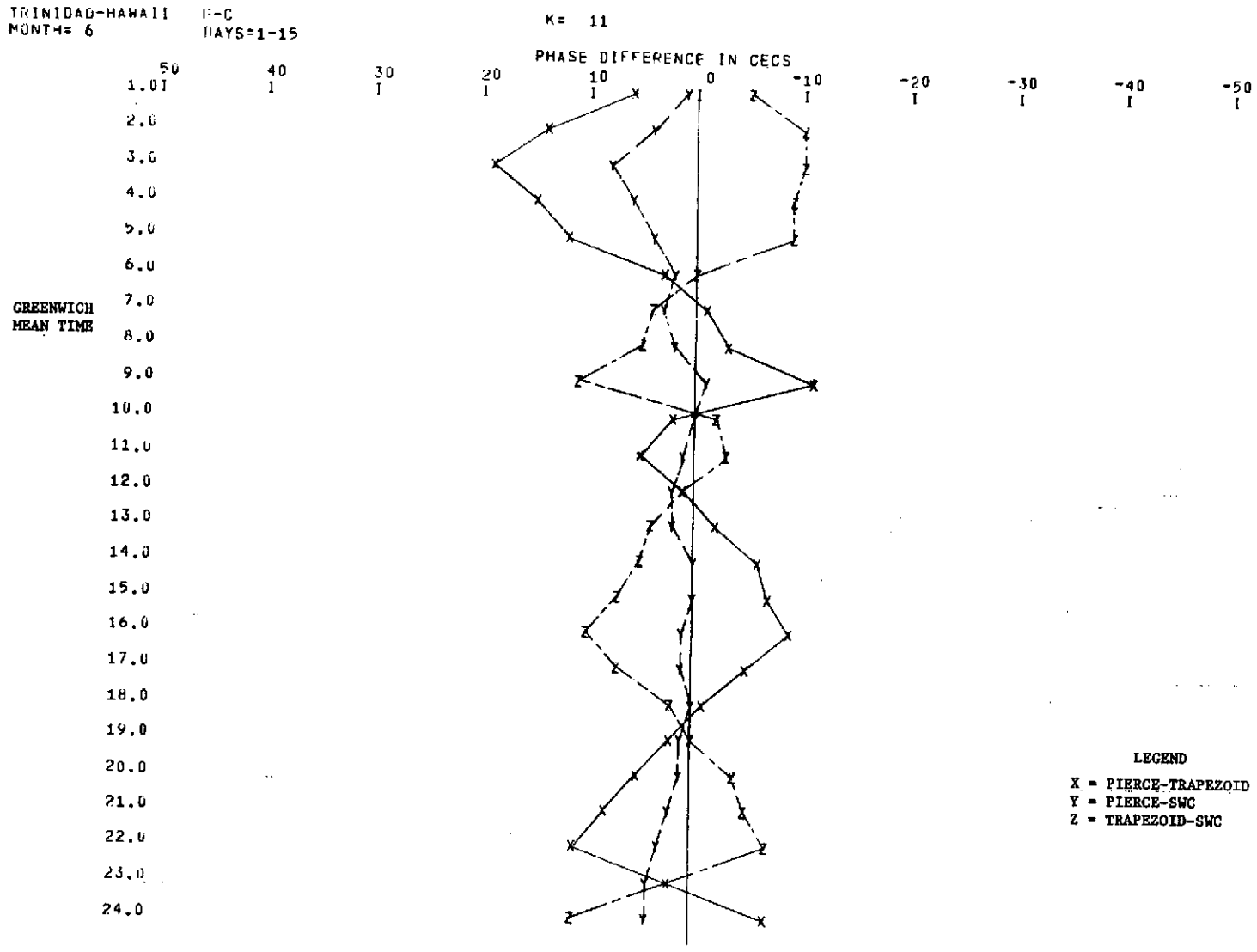

Fig. 34. B-C 10.2 kHz Omega phase difference comparison of Pierce measurement minus trapezoidal prediction (X), Pierce measurement minus Navy prediction (Y), and trapezoidal prediction minus Navy prediction (Z) at Cambridge, Mass., for period 1-15 June 1971.

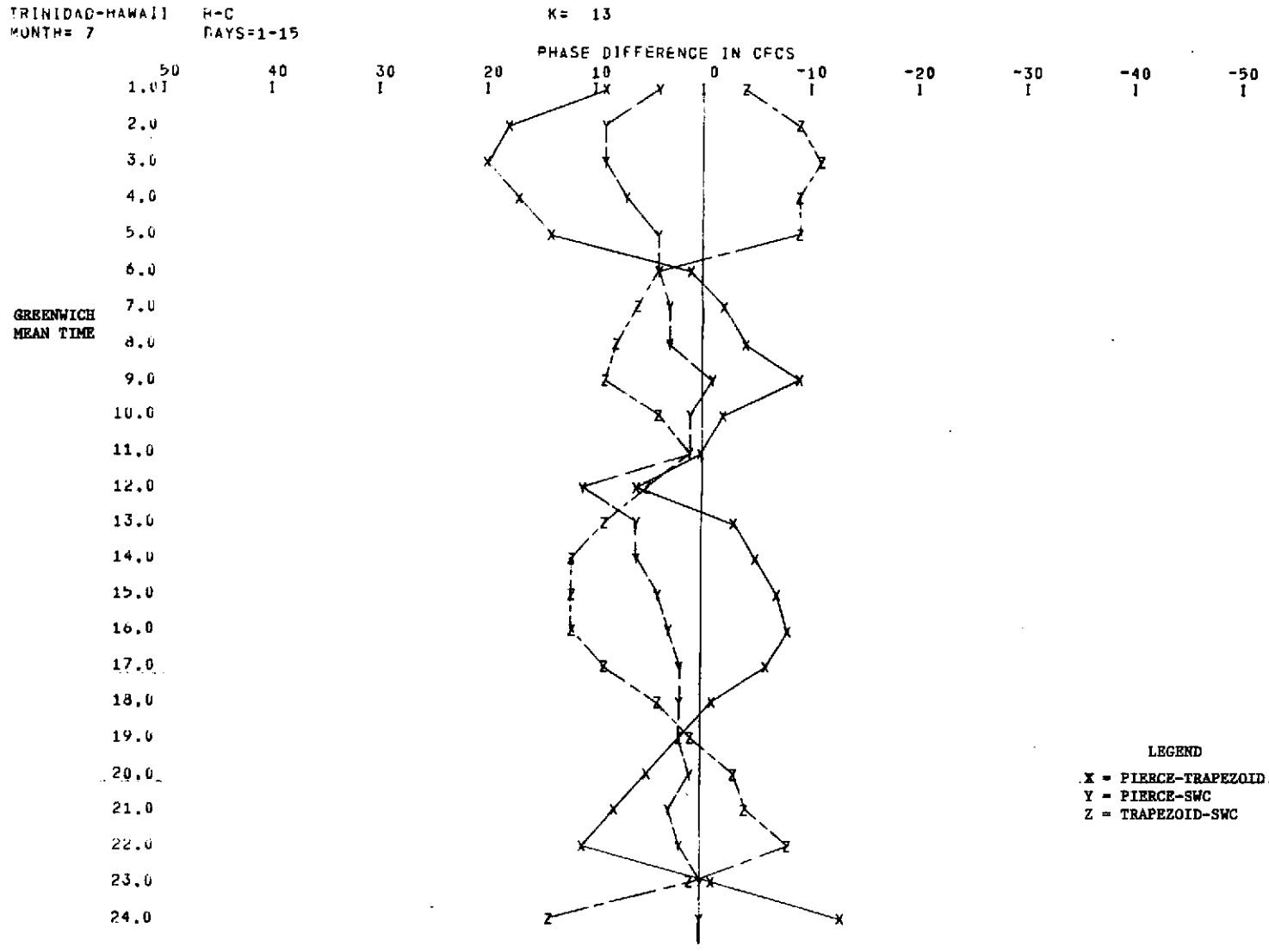

Fig. 35. B-C 10.2 kHz Omega phase difference comparison of Pierce measurement minus trapezoidal prediction (X), Pierce measurement minus Navy prediction (Y), and trapezoidal prediction minus Navy prediction (Z) at Cambridge, Mass., for period 1-15 July 1971.

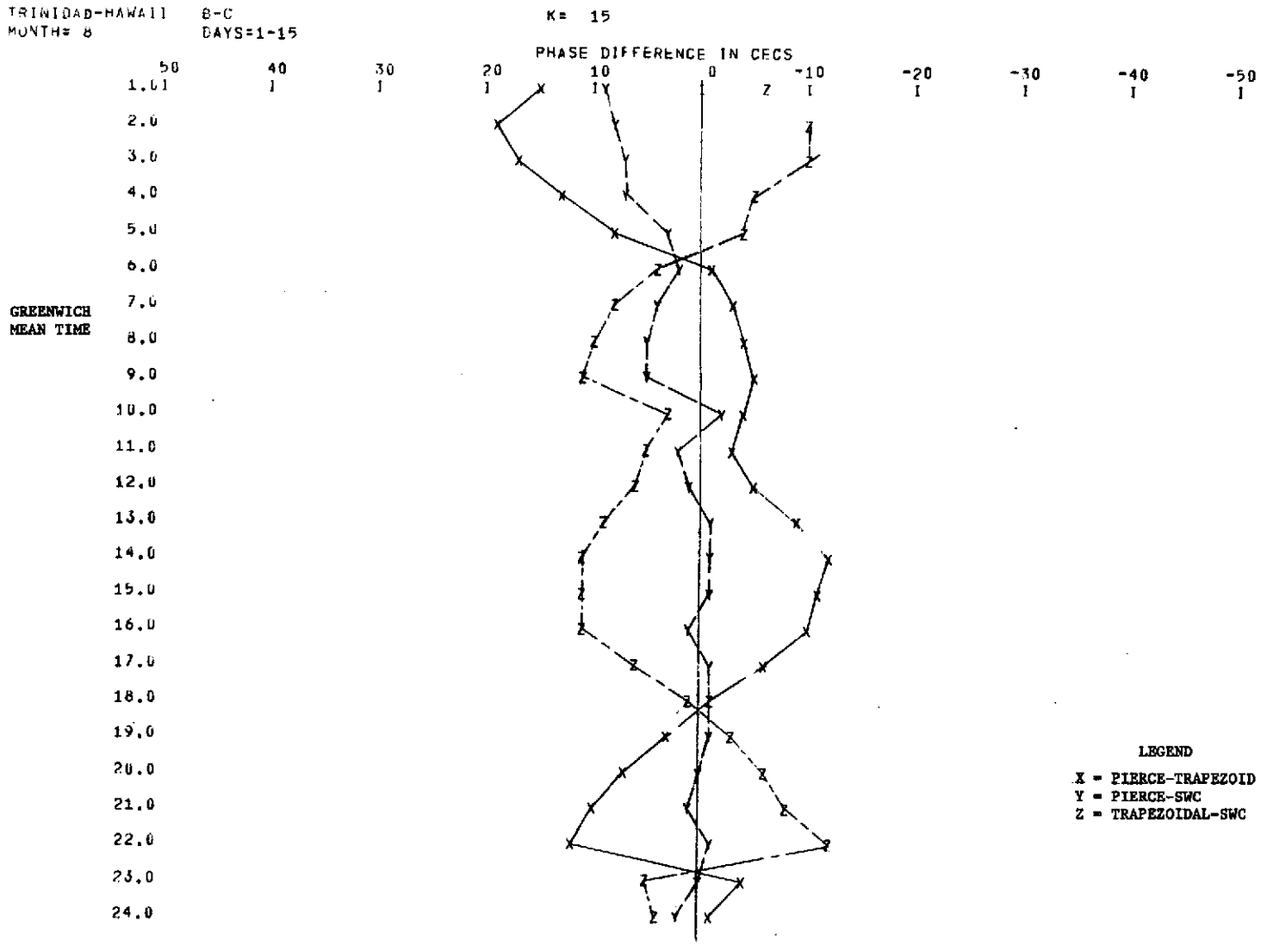

Fig. 36. B-C 10.2 kHz Omega phase difference comparison of Pierce measurement minus trapezoidal prediction (X), Pierce measurement minus Navy prediction (Y), and trapezoidal prediction minus Navy prediction (Z) at Cambridge, Mass., for period 1-15 August 1971.

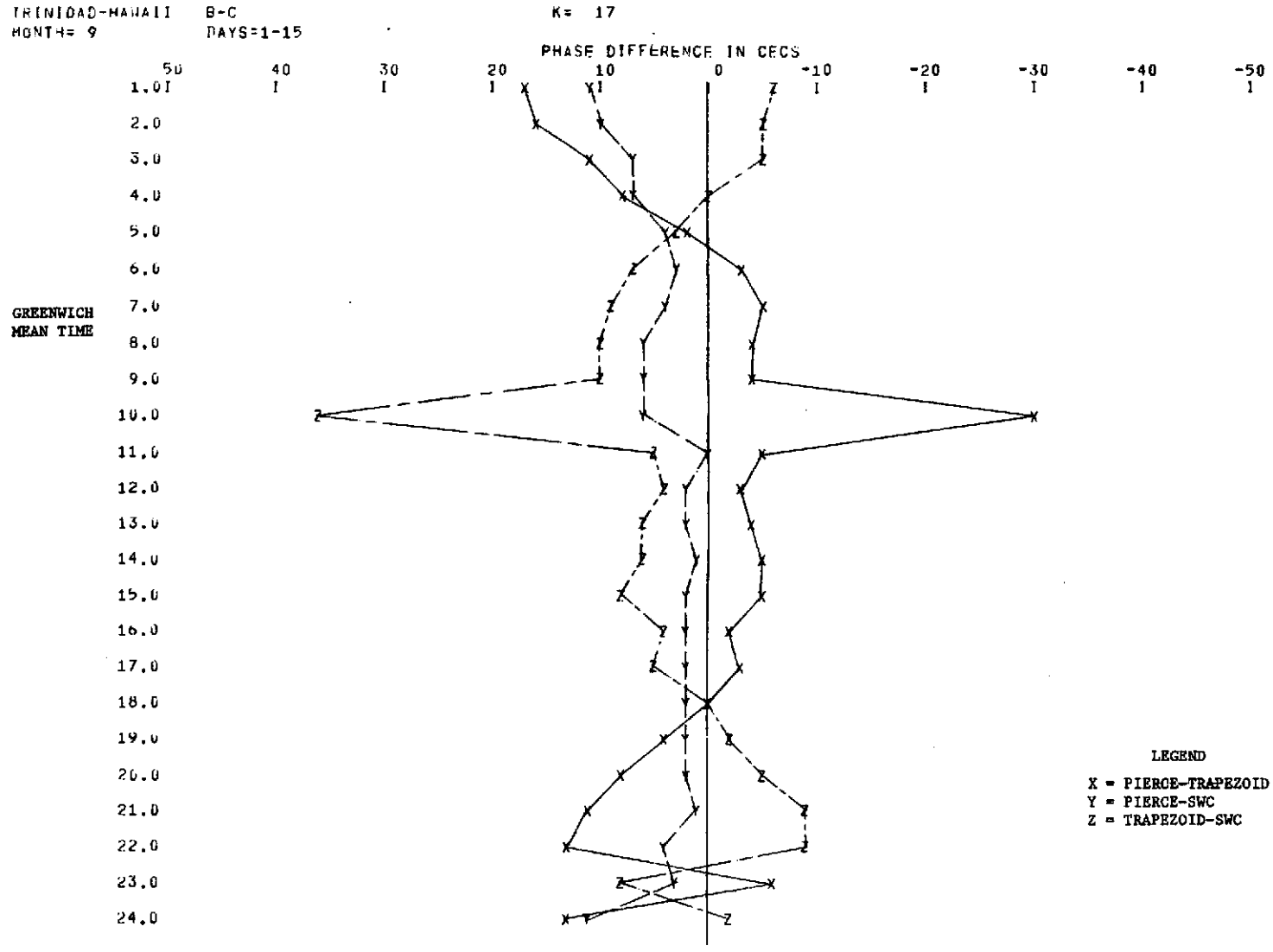

Fig. 37. B-C 10.2 kHz Omega phase difference comparison of Pierce measurement minus trapezoidal prediction (X), Pierce measurement minus Navy prediction (Y), and trapezoidal prediction minus Navy prediction (Z) at Cambridge, Mass., for period 1-15 September 1971.

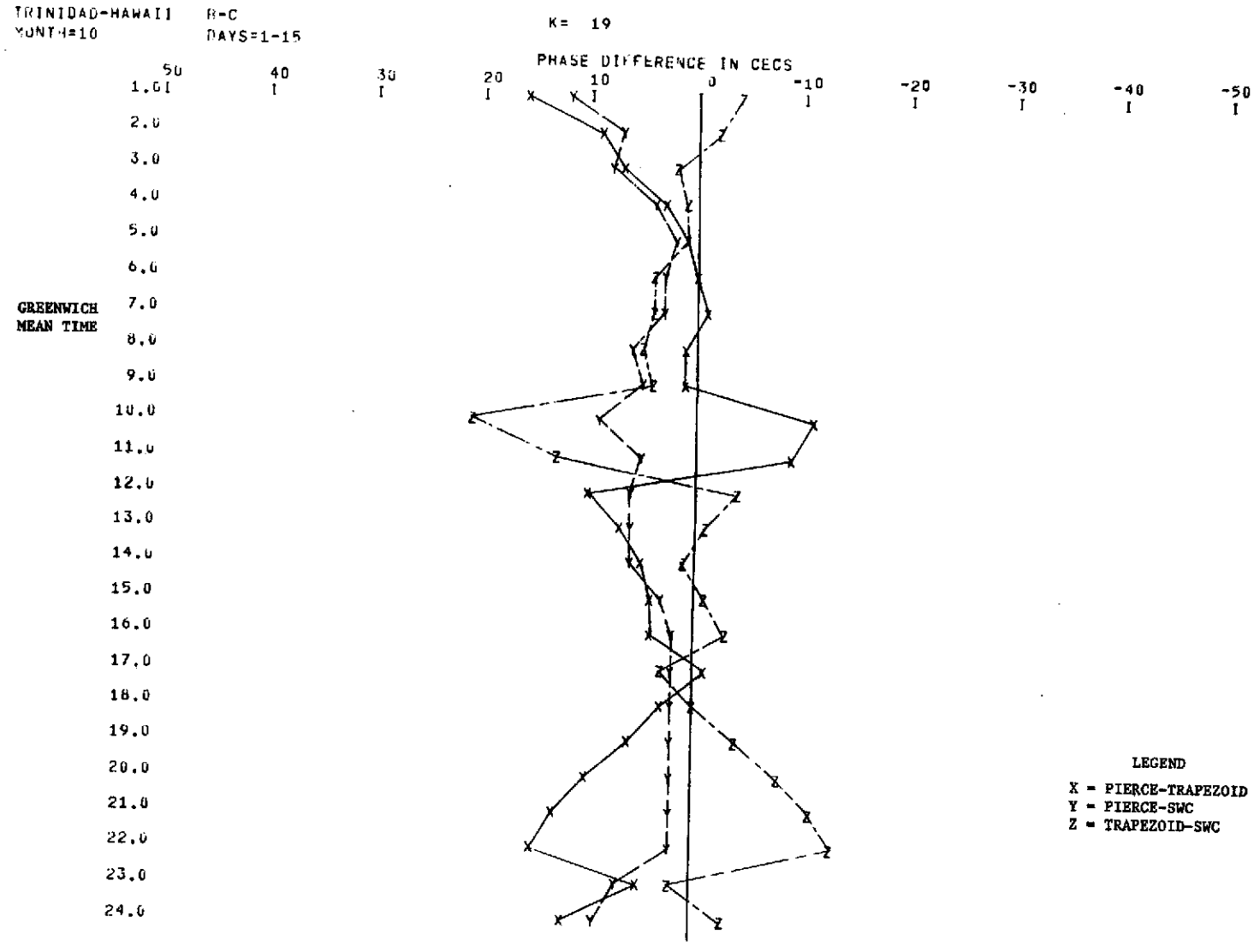

Fig. 38. B-C 10.2 kHz Omega phase difference comparison of Pierce measurement minus trapezoidal prediction (X), Pierce measurement minus Navy prediction (Y), and trapezoidal prediction minus Navy prediction (Z) at Cambridge, Mass., for period 1-15 October 1970.

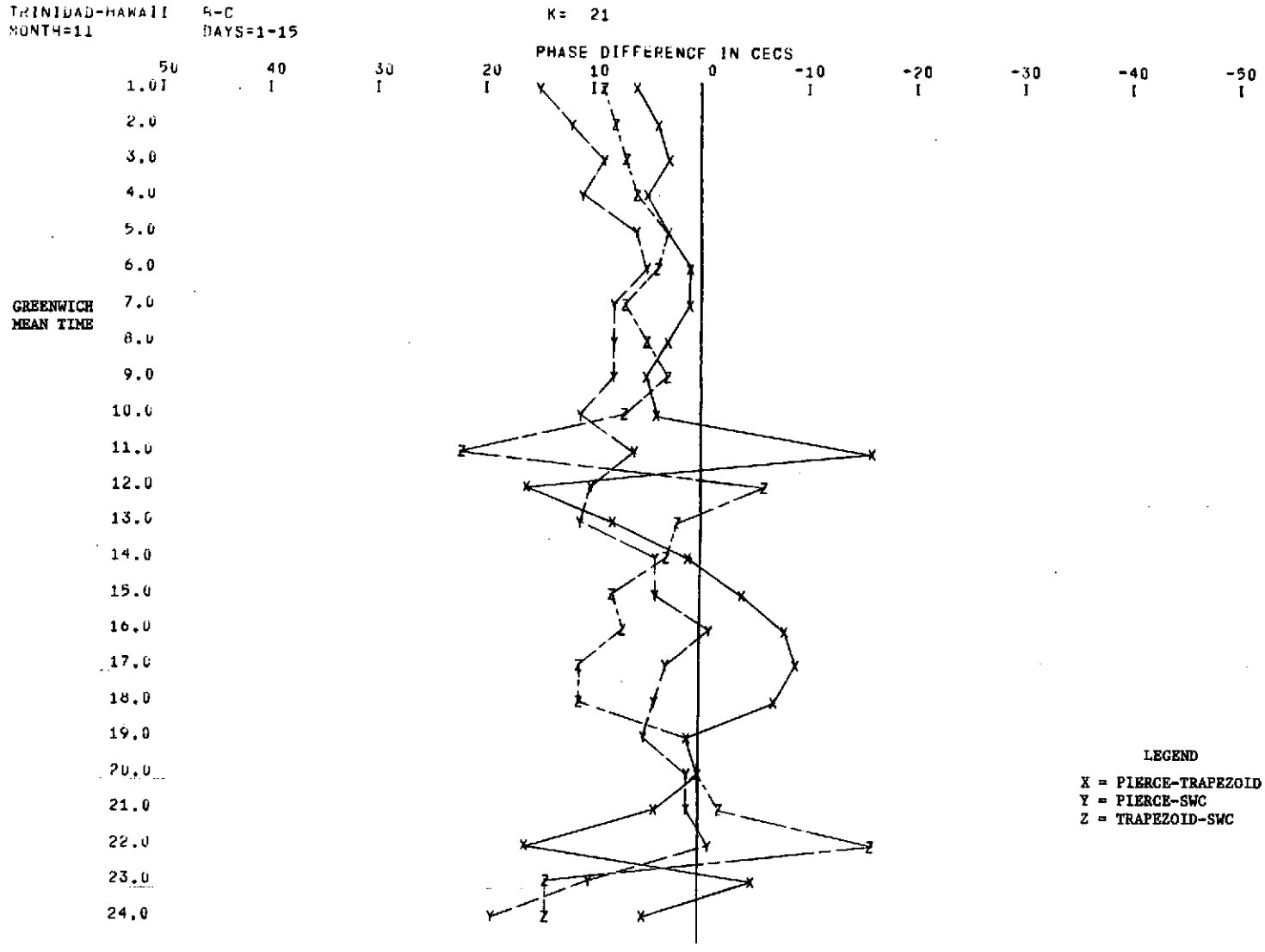

Fig. 39. B-C 10.2 kHz Omega phase difference comparison of Pierce measurement minus trapezoidal prediction (X), Pierce measurement minus Navy prediction (Y), and trapezoidal prediction minus Navy prediction (Z) at Cambridge, Mass., for period 1-15 November 1970.

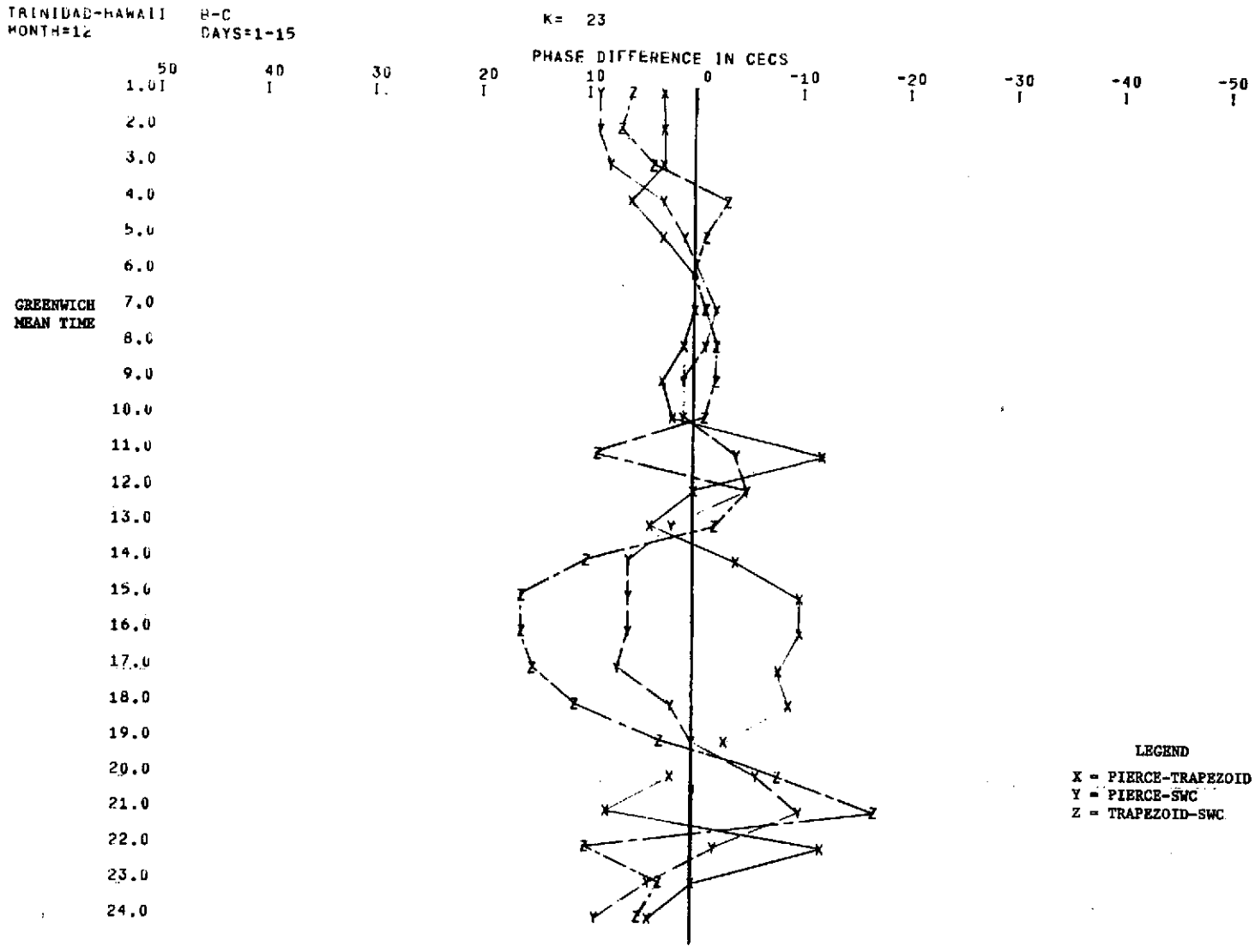

Fig. 40. B-C 10.2 kHz Omega phase difference comparison of Pierce measurement minus trapezoidal prediction (X), Pierce measurement minus Navy prediction (Y), and trapezoidal prediction minus Navy prediction (Z) at Cambridge, Mass., for period 1-15 December 1970.

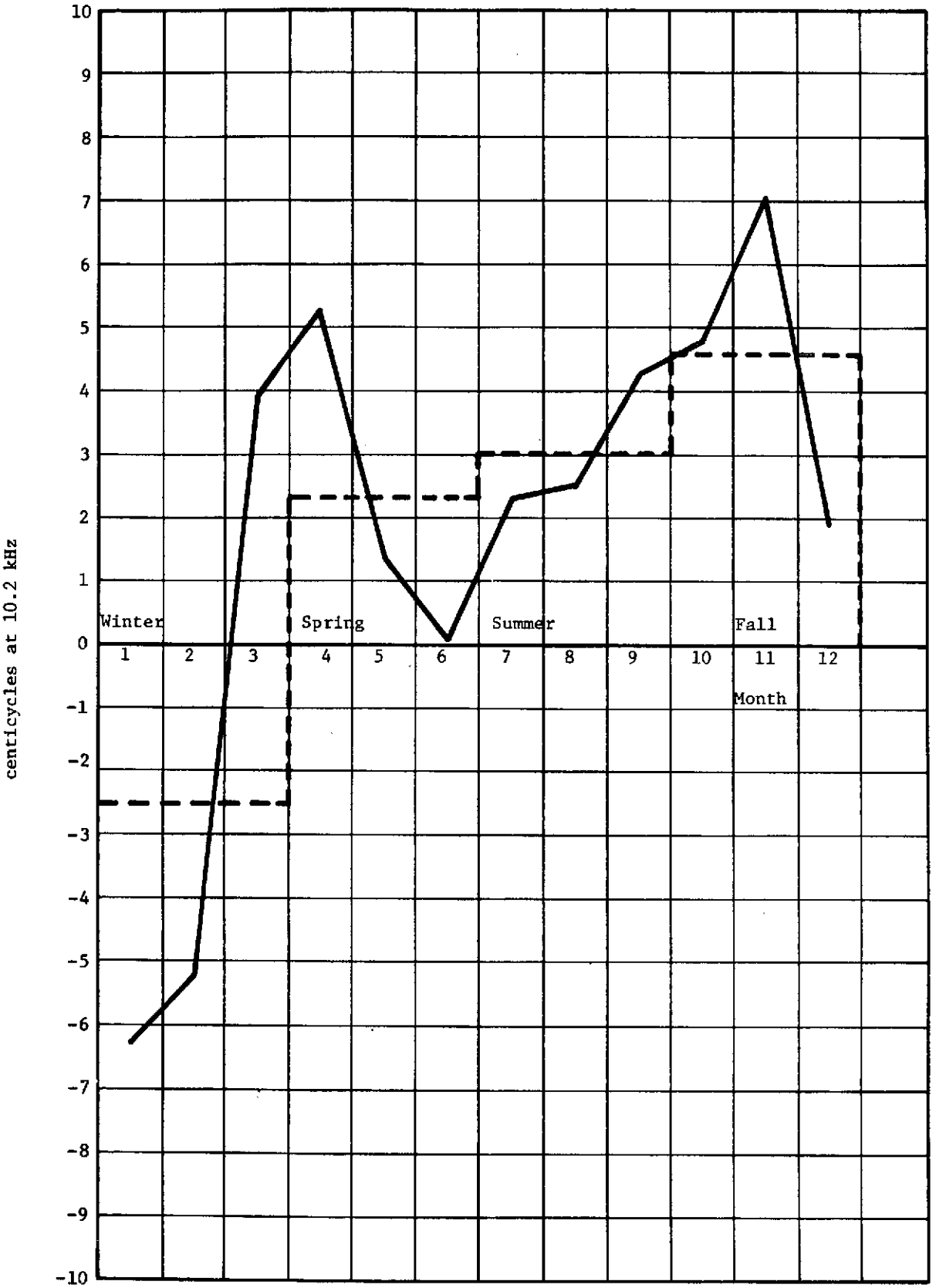

Fig. 41. Monthly averages (using one 15-day period per month) B-C phase difference for Pierce measurements minus trapezoidal predictions of 10.2 kHz Omega phase at Cambridge, Mass., for Jan.-Sept. 1971 and Oct.-Dec. 1970.

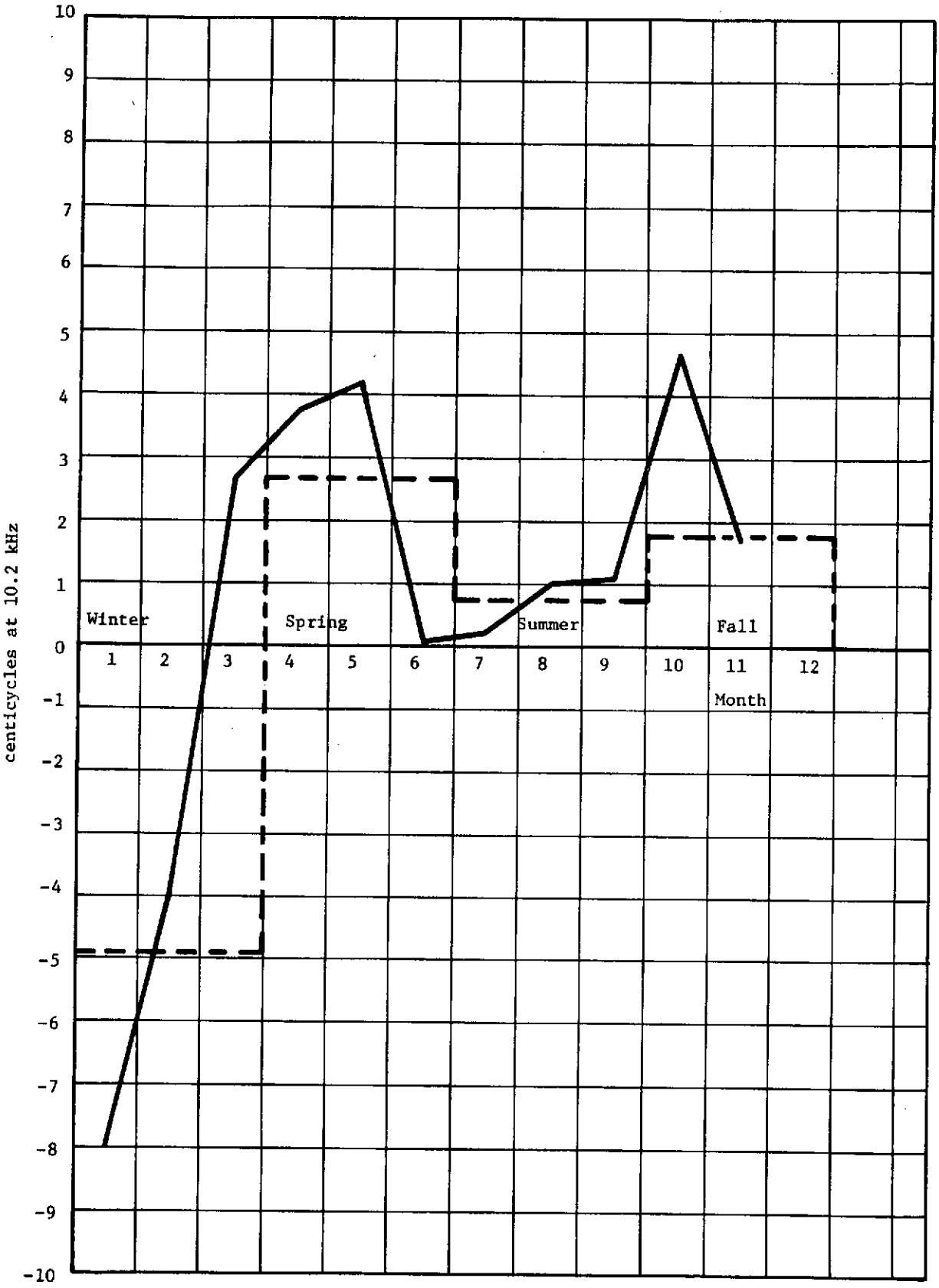

Fig. 42. Monthly averages (using one 15-day period per month) B-C phase difference for Pierce measurements minus Navy predictions of 10.2 kHz Omega phase at Cambridge, Mass., for Jan-Sept. 1971 and Oct.-Dec. 1970.

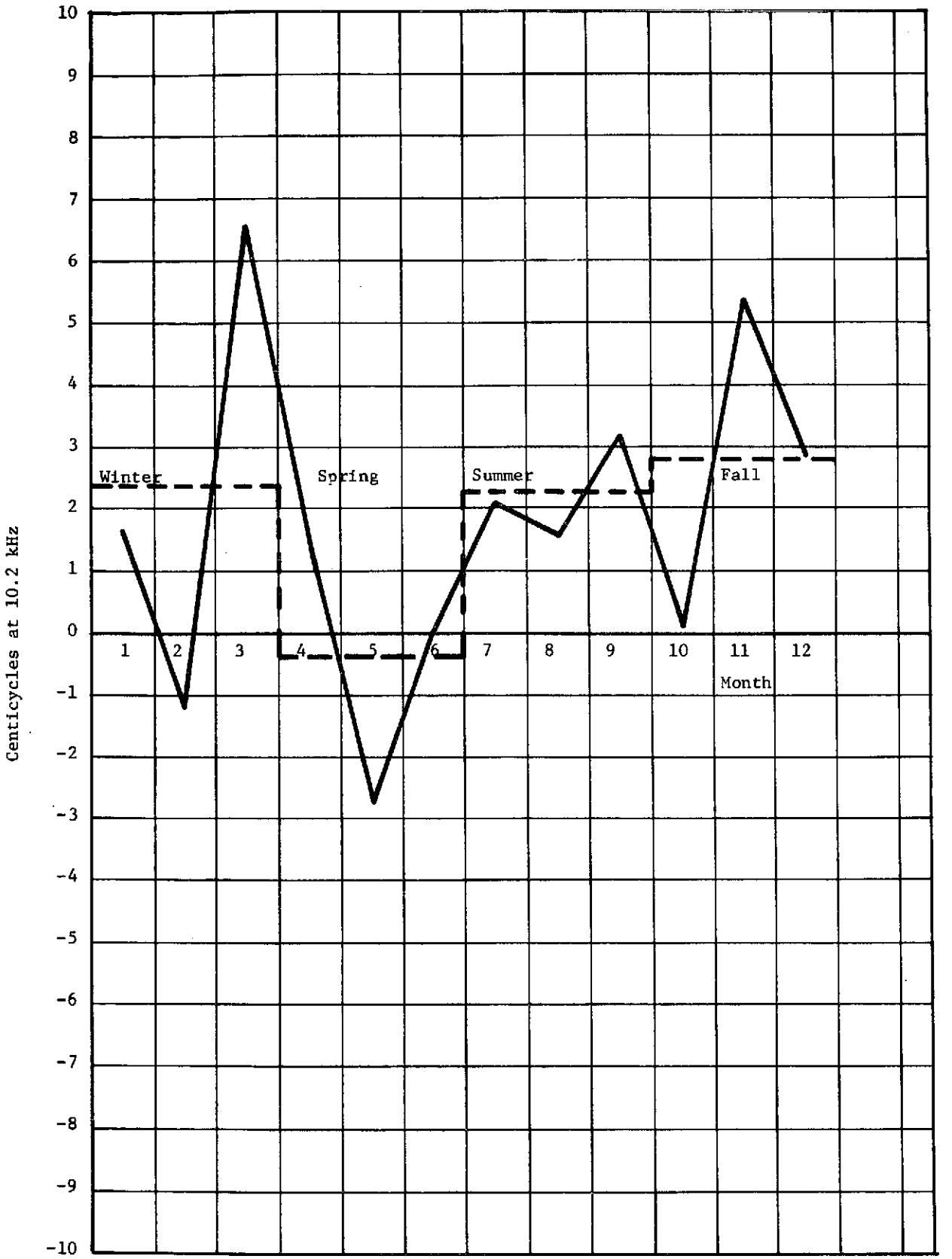

Fig. 43. Monthly averages (using one 15-day period per month) B-C phase difference for trapezoidal predictions minus Navy predictions of 10.2 kHz Omega phase at Cambridge, Mass., for Jan.-Sept. 1971 and Oct.-Dec. 1970.

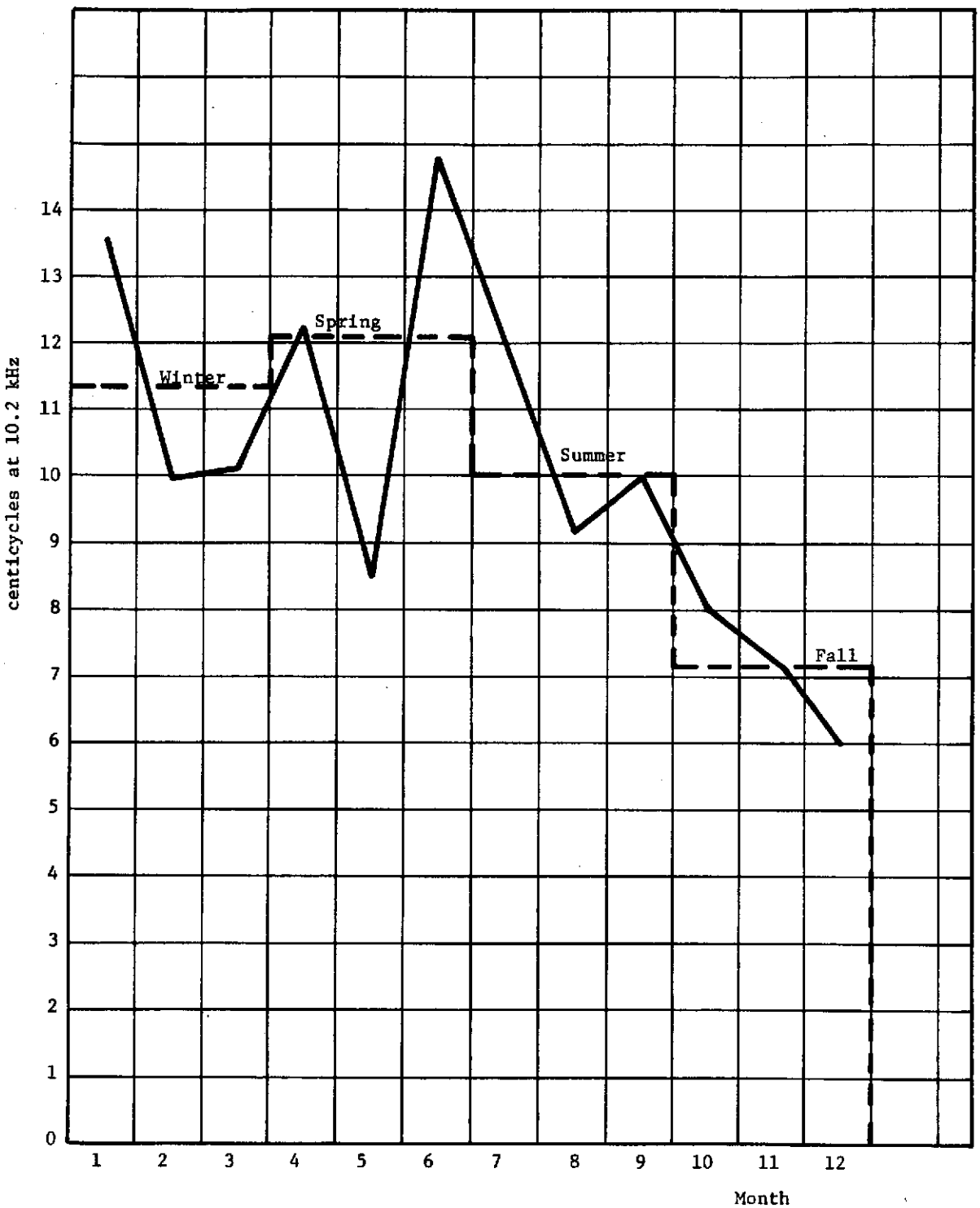

Fig. 44. Monthly rms (using one 15-day period per month) B-C phase difference for Pierce measurements minus trapezoidal predictions of 10.2 kHz Omega phase at Cambridge, Mass., for Jan.-Sept. 1971 and Oct.-Dec. 1970.

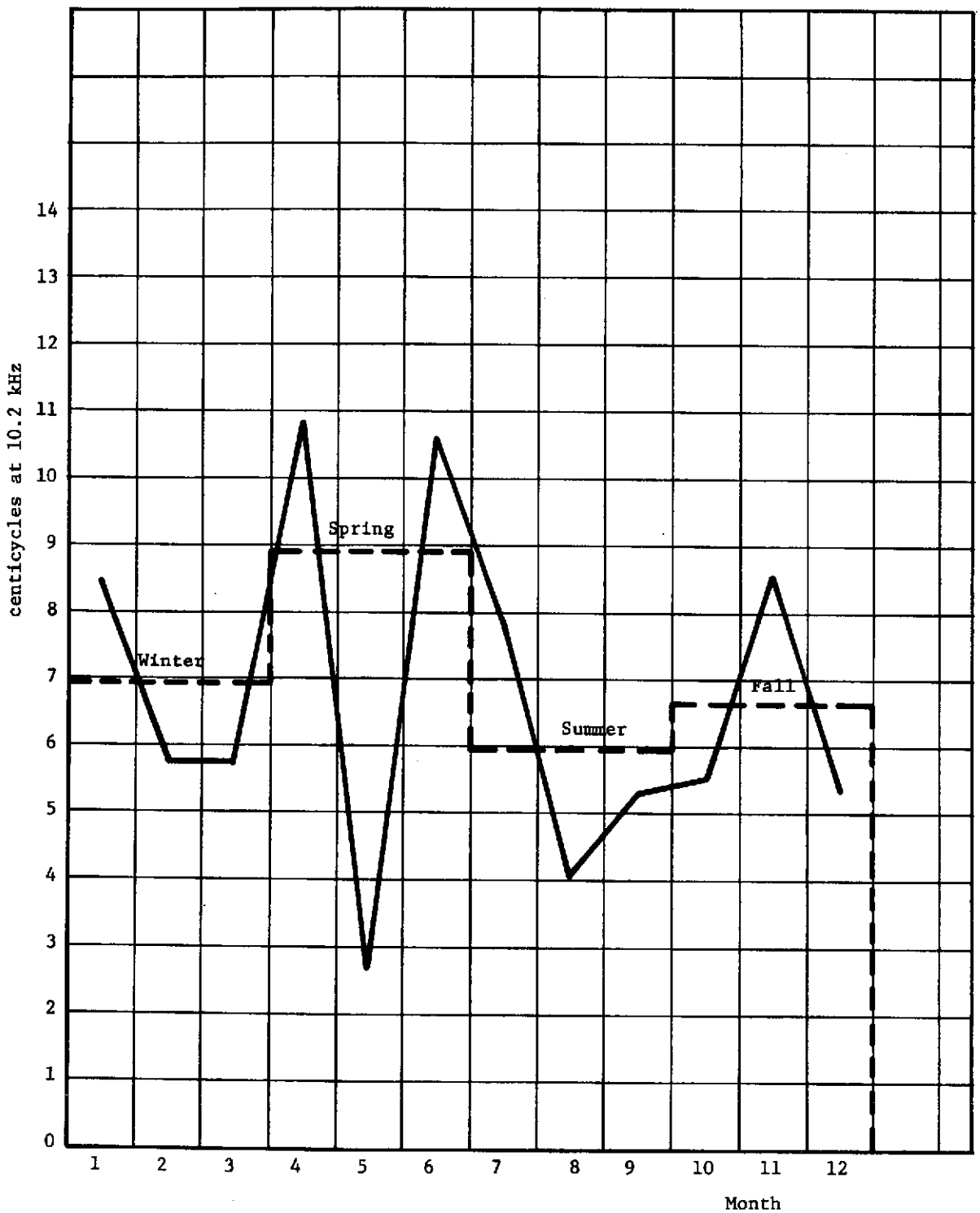

Fig. 45. Monthly rms (using one 15-day period per month) B-C phase difference for Pierce measurements minus Navy predictions of 10.2 kHz Omega phase at Cambridge, Mass., for Jan.-Sept. 1971 and Oct.-Dec. 1970.

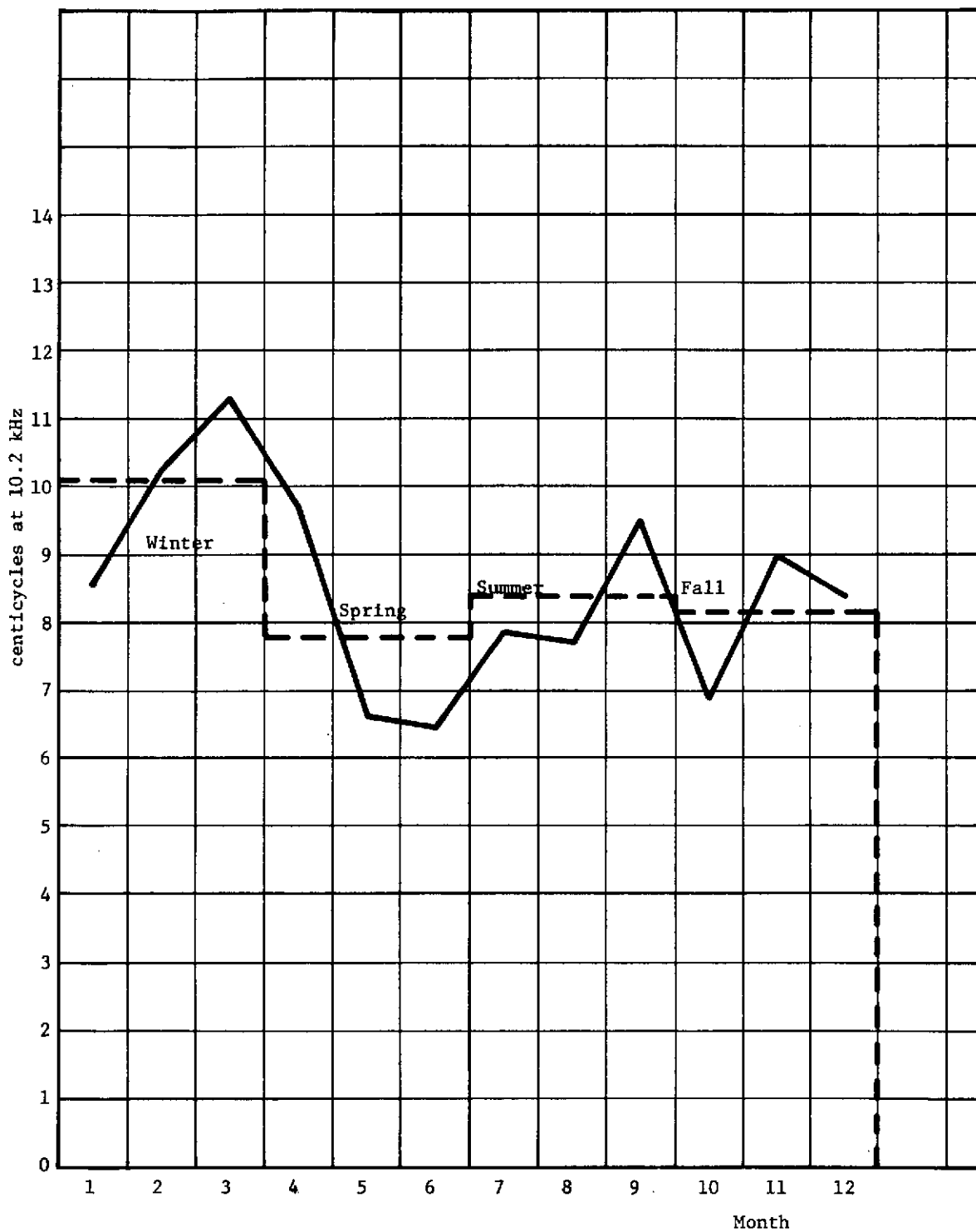

Fig. 46. Monthly rms (using one 15-day period per month) B-C phase difference for trapezoidal predictions minus Navy predictions of 10.2 kHz Omega phase at Cambridge, Mass., for Jan.-Sept. 1971 and Oct.-Dec. 1970.

6.0 DIFFERENTIAL OMEGA

6.1 Differential Omega Concept

The concept of Differential Omega was first formally proposed in 1966 by the Omega Implementation Committee set up by the Department of the Navy (see ref. 18). The assumption made is that the phase difference error of the Omega signals within any small region (approximately 300 n. mi. in radius) will be very nearly constant. The assumption that sky-wave corrections are constant over a 240 n. mi. square region is made in the published tables, where one correction applies over a 4° x 4° area.

One mode of operation would be to locate a base receiver at a fixed known position so that true Omega phase is known. This receiver can then at any time make an actual phase difference measurement and obtain a phase difference measurement correction applicable to other receivers in the differential region. Some auxiliary means of communications could then be used to transmit the correction information from the base receiver to other receivers within the differential region.

The method offers a real-time measurement of the phase perturbations within a relatively small area of operation about the base receiver. This should serve to reduce navigation error over the ordinary Omega navigation procedure where phase perturbation predictions are used. Differential Omega studies, including refs. 19-28, have shown that the differential method can achieve better navigation accuracies than ordinary Omega.

6.2 Navy SWC Table Analysis

To gain insight into the nature of time and space correlation of Omega phase differences, a simple analysis of the Navy sky-wave correction (SWC) tables has been carried out. Using the tables, lines of constant phase correction for given transmitters and lines of constant phase difference correction for various pairs of transmitters have been plotted in the North American region. Figures 47 and 48 provide plots of constant Navy SWC for transmitters B and D, respectively, at 0700 GMT for the 1-15 July period. The value of phase correction given in the SWC tables is assumed to hold at the center of the 4° x 4° lattice square. Linear interpolation is used between lattice regions in determining where these isolines are plotted. Figure 49

PRECEDING PAGE BLANK NOT FILMED

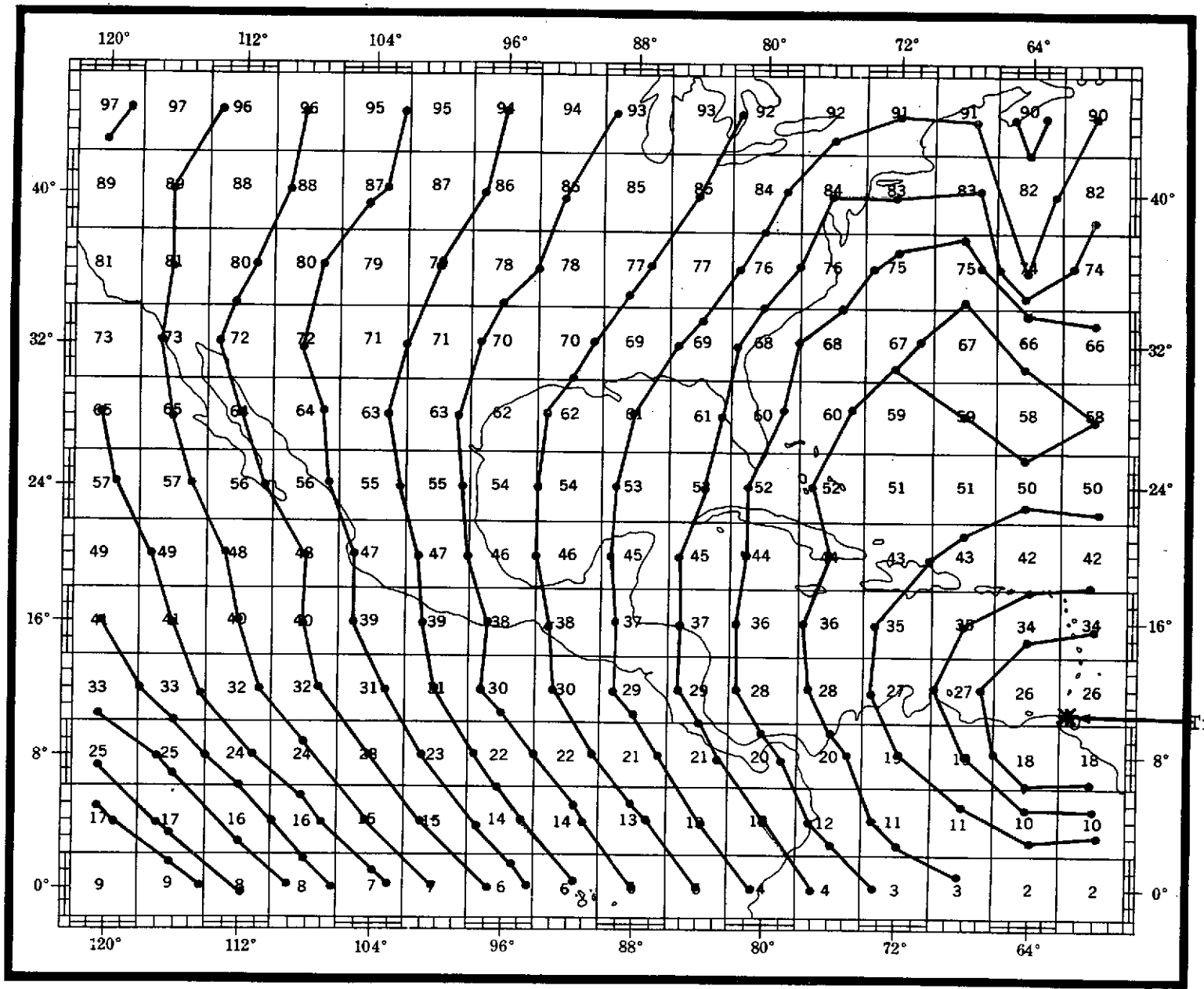

Fig. 47. Isoline plot of 10.2 kHz Omega phase corrections in centicycles for Trinidad (Station B) transmissions at 0700 GMT for period 1-15 July obtained using linear interpolation of Navy SWC table values for each 4°x4° lattice grid.

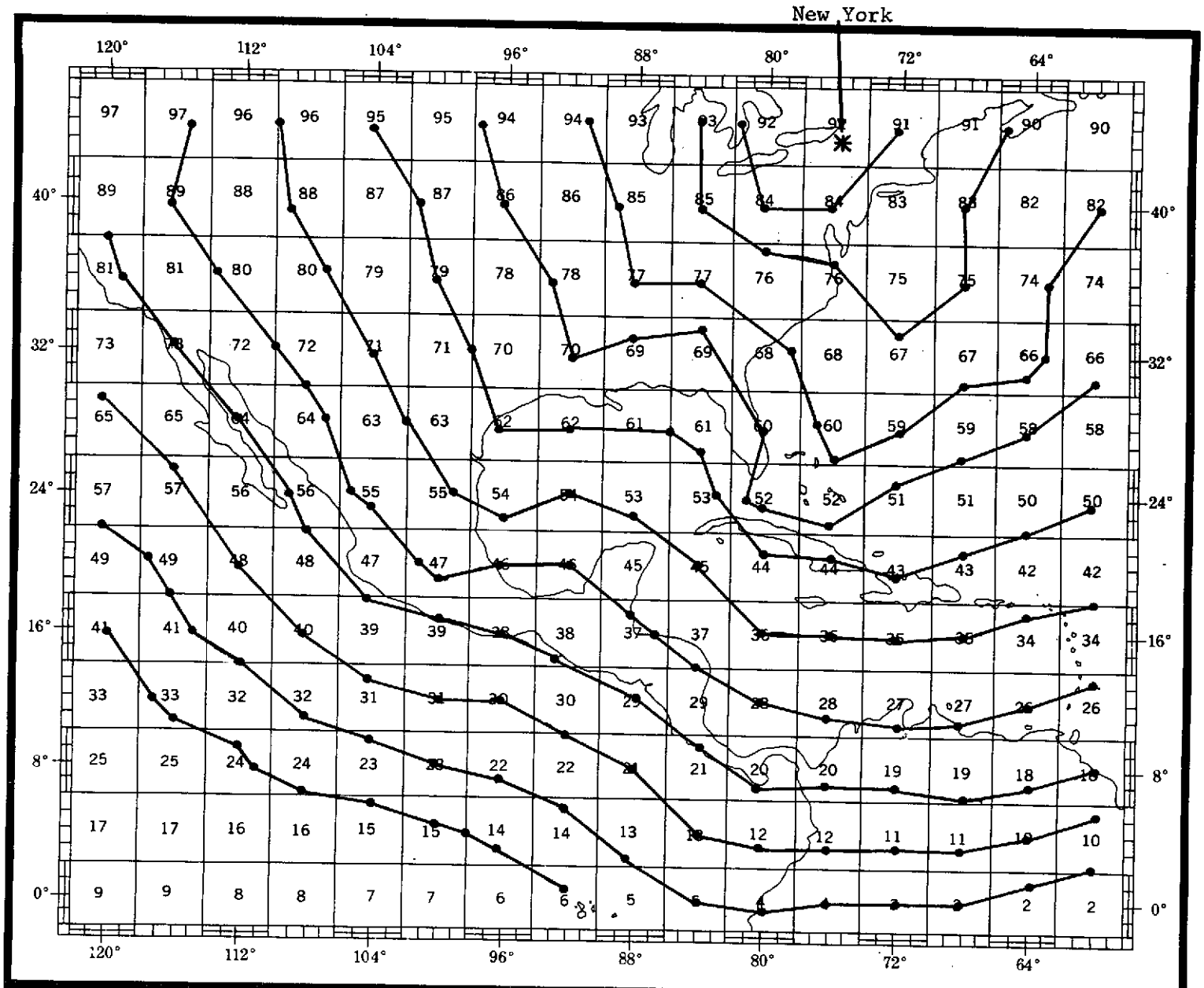

Fig. 48. Isoline plot of 10.2 kHz Omega phase corrections in centicycles for New York (Station D) transmissions at 0700 GMT for period 1-15 July obtained using linear interpolation of Navy SWC table values for each 4°x4° lattice grid.

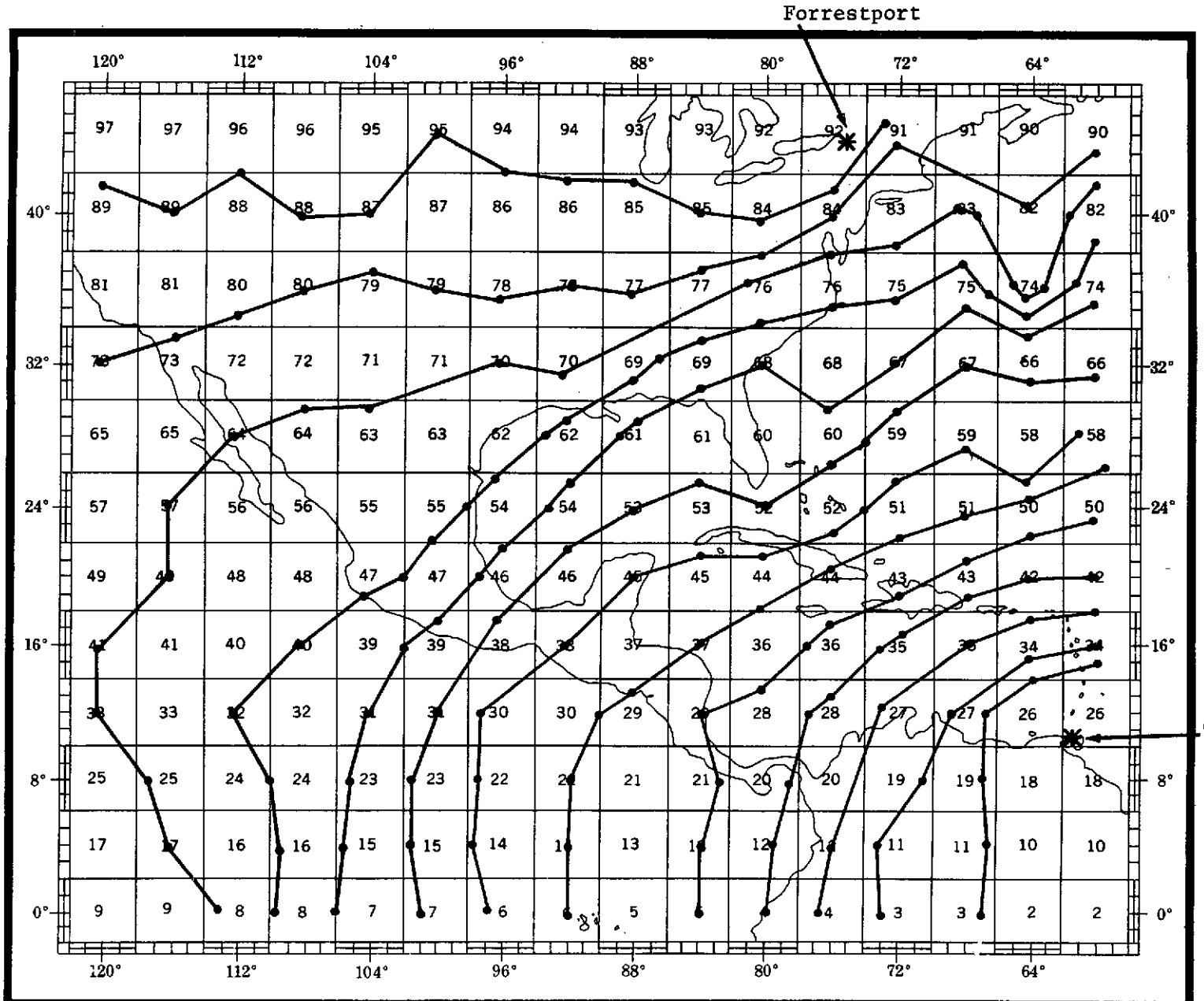

Fig. 49. Isoline plot of 10.2 kHz Omega phase difference correcting in centicycles for B-D LOP measurements at 0700 GMT for period 1-15 July obtained using linear interpolation of Navy SWC table values for each 4°x4° lattice grid.

shows isolines of phase difference correction for the station pair B-D obtained from Figs. 47 and 48. Figures 51 and 52 show isolines of phase difference correction for station pair A-C at 0600 GMT and 1700 GME, respectively, for the period 1-15 July. Isolines are shown for the area immediately around Langley Research Center (LRC) only. From these plots it can be seen that changes in phase difference corrections vary with direction and are generally non-linear in any given direction. Further analysis has been carried out in the immediate area of LRC by calculating the gradient of phase difference correction for each hour of the day using the published SWC tables for 1-15 July. The gradient as used here is defined as the vector which represents the magnitude and direction of greatest phase difference correction change for the SWC table region in which LRC is located. The following illustrates the technique used.

The set of 9 regions in Fig. 50 represents the sky-wave correction region containing LRC (a_{22}) and the 8 surrounding it. For each d x d region and each Omega transmitter, there is a published SWC. The a_{ij}'s represent the difference between any two corrections. It is desirable to find the gradient of a field represented by the a_{ij}'s and centered at a_{22}; i.e., the direction and magnitude of the largest change in the a_{ij}'s around a_{22}.

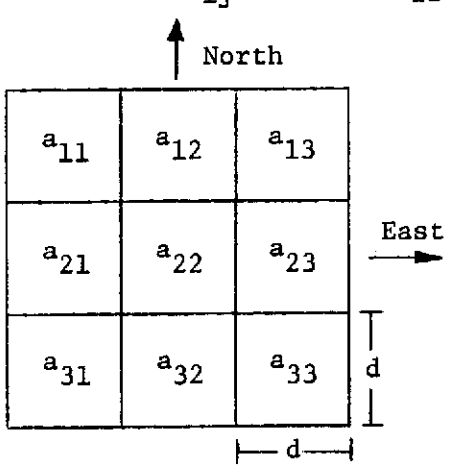

Fig. 50. Localized Omega SWC grid for determining gradient of sky-wave corrections at center grid.

If we consider a surface containing points raised from the center of each region by an amount equal to a_{ij} for that region, then the closest approximation to the partial derivatives in the gradient will be for the East coordinate

$$\text{Grad}_E = \frac{a_{23} - a_{21}}{2d}$$

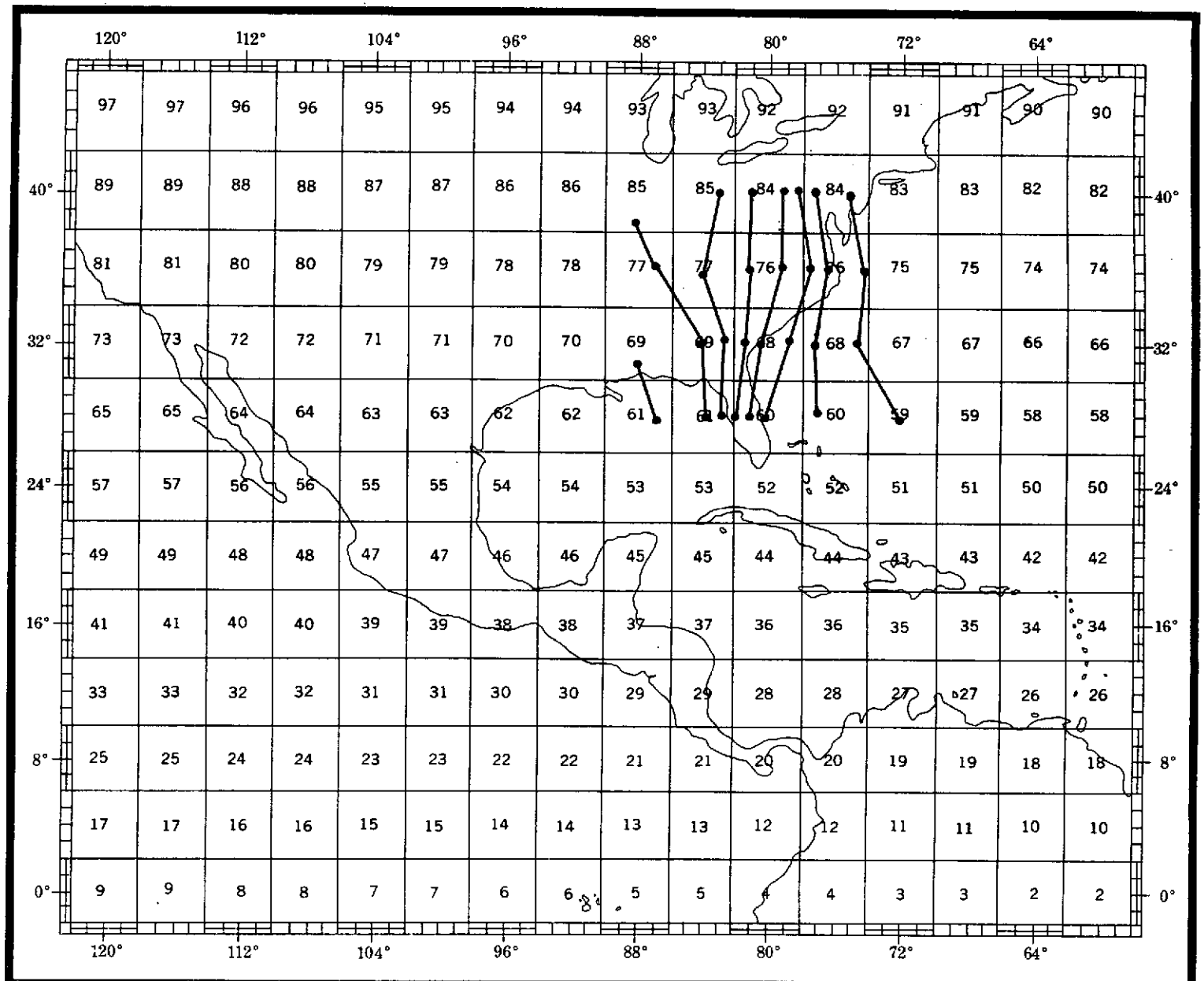

Fig. 51, Isoline plot of 10.2 kHz Omega phase difference corrections in centicycles for Southeastern U.S. for A-C LOP measurements at 0600 GMT for period 1-15 July obtained using linear interpolation of Navy SWC table values for each 4°x4° lattice grid.

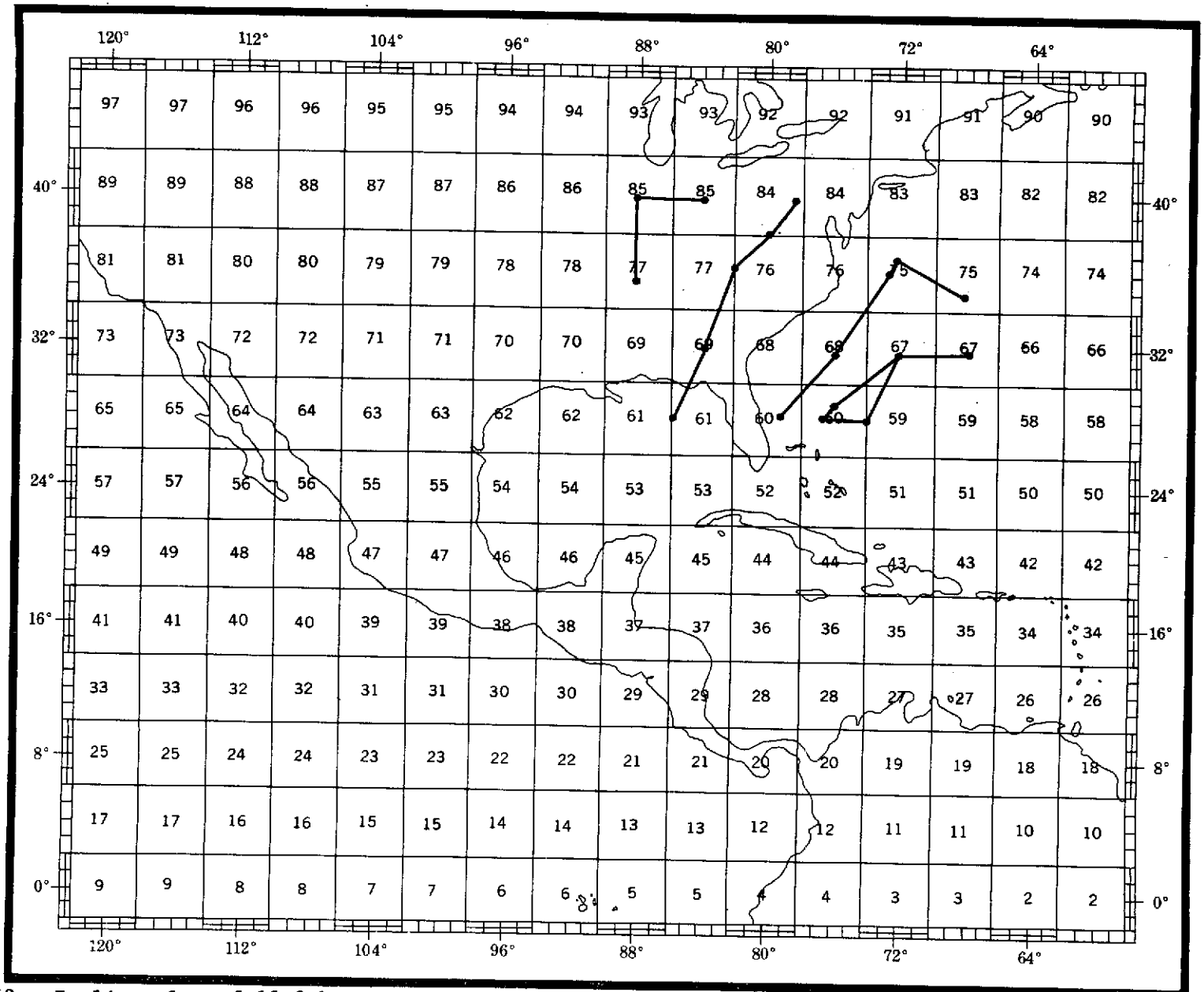

Fig. 52. Isoline plot of 10.2 kHz Omega phase difference corrections in centicycles for Southeastern U. S. for A-C LOP measurements at 1800 GMT for period 1-15 July obtained using linear interpolation of Navy SWC values for each 4°x4° lattice grid.

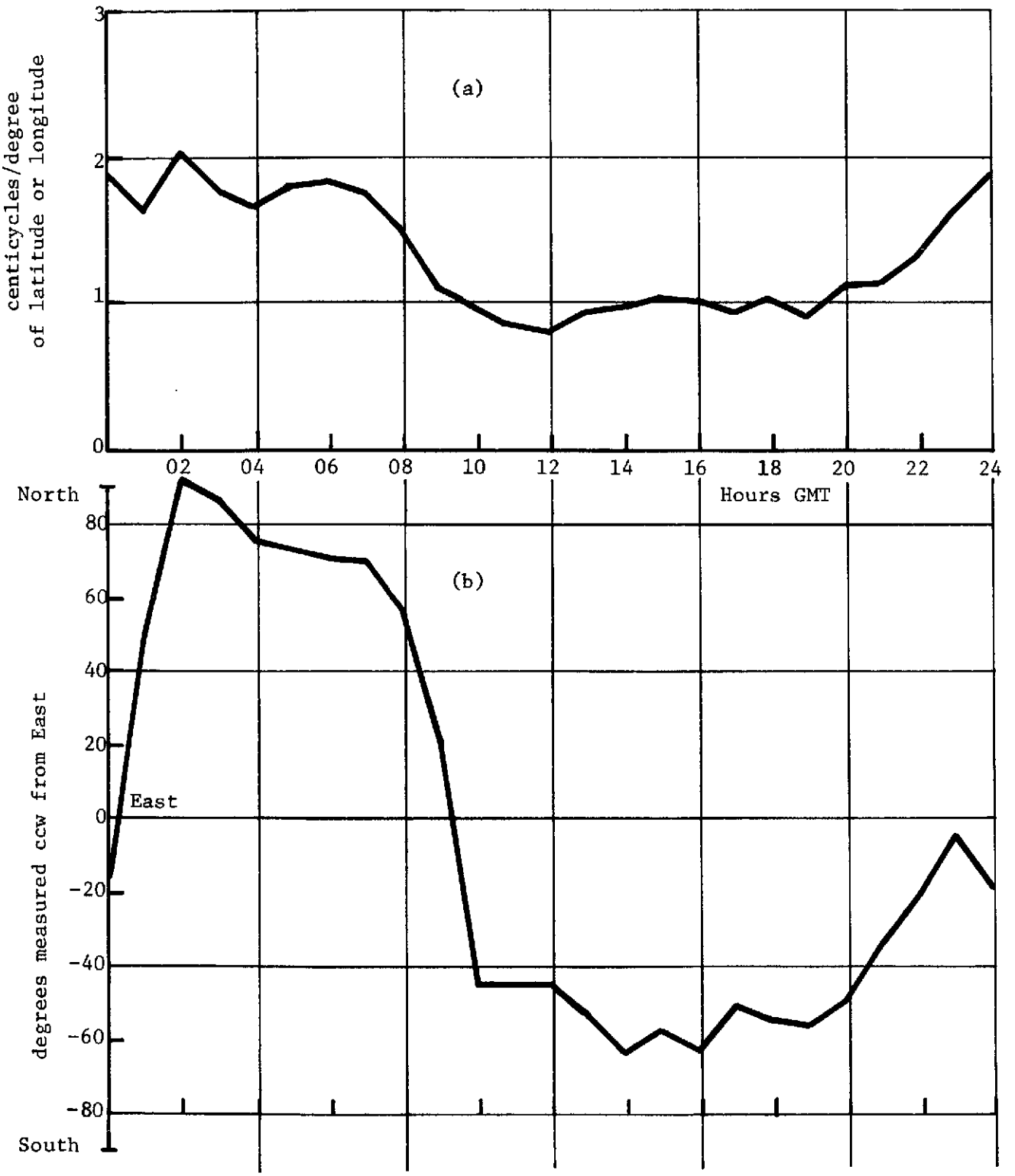

Fig. 53. Magnitude (a) and direction (b) of gradient of 10.2 kHz Omega SWC difference for A-B phase difference measurements for area centered at Hampton, Va., for each hour during the period 1-15 July.

and for the North coordinate

$$\text{Grad}_N = \frac{a_{12} - a_{32}}{2d} \quad .$$

These orthogonal components then determine the magnitude and direction of the resultant vector which is the gradient. The above approximation is considered to be a good one, since the gradient varies slowly with distances on the order of d.

Figures 53 through 58 are plots of the magnitude and the direction of the gradient centered at Hampton, Virginia, for the 10.2 kHz SWC differences for each hour of the 24-hour day. All possible pairs for stations A, B, C, and D are shown. The magnitude of the gradient is shown in centicycles (cec) per degree of latitude or longitude, while gradient direction is given in degrees measured ccw from East. It can be seen that for most station pairs a diurnal variation is evident in the gradient magnitude and direction. This is most pronounced with pair B-C in Fig. 57, where the baseline between the Trinidad and New York transmitters is parallel to the sunrise-sunset line and Langley Research Center is located very near the baseline.

This same information is presented in Figs. 59 through 64 in polar form, superimposed on an Omega map of part of the Eastern United States. In these figures, individual points indicate the termini of each hourly gradient for the two-week period analyzed. As mentioned previously, each hourly gradient vector has a magnitude and direction as indicated in Figs. 53 through 58. The vectors actually drawn in the figures represent median gradients for various periods in the day where the gradient remains relatively stationary. Additionally, the daily average gradient, Σ, is shown. This is calculated by determining the average East coordinate and the average North coordinate for all hourly gradients over the 24-hour period. A trend is evident in that the average gradient is generally almost perpendicular to the station pair LOP at LRC for each station pair; this is not necessarily the situation for given individual hourly gradient directions. (Note that the Omega map only shows LOP's for A-C, A-D, B-C and B-D, which are considered the most usable pairs in the area.)

The magnitude of the gradients is generally less than about 2 cec per degree of latitude or longitude, which means that variations of phase difference measurement of less than 10 cec (.8 n. mi.) would be generally true within a 300 n. mi. radius of LRC. This would allow for differential Omega navigation

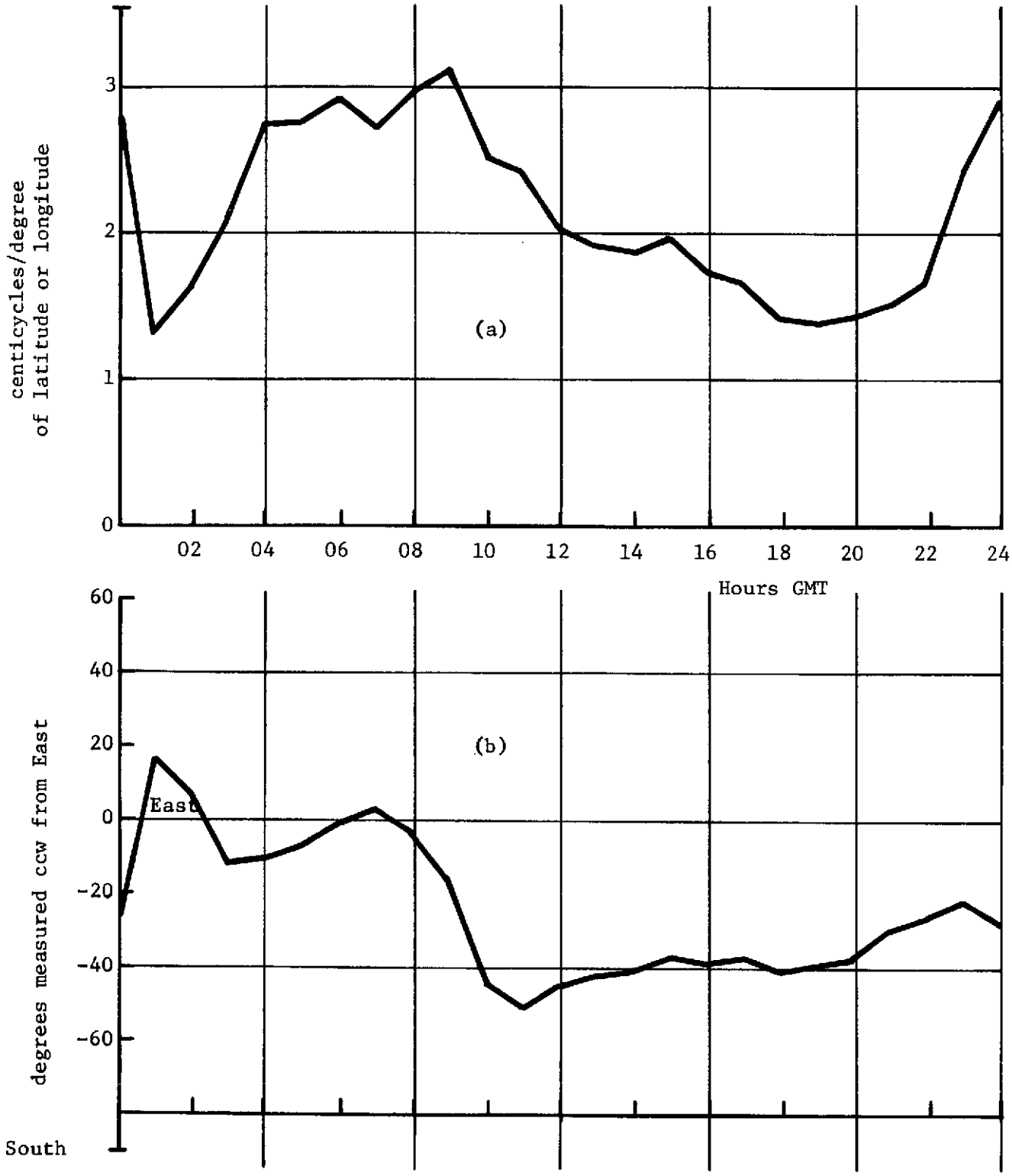

Fig. 54. Magnitude (a) and direction (b) of gradient of 10.2 kHz Omega SWC difference for A-C phase difference measurements for area centered at Hampton, Va., for each hour during the period 1-15 July.

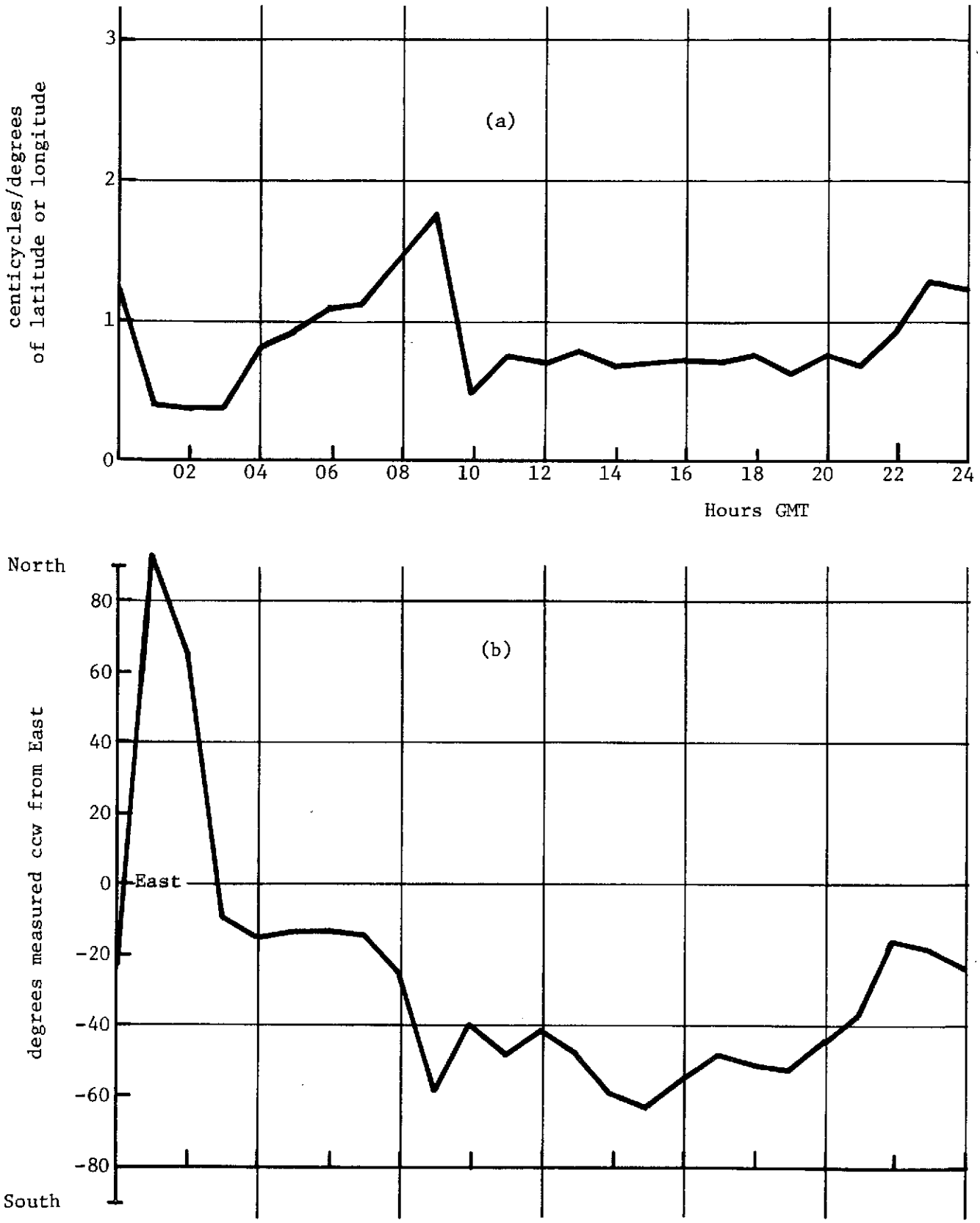

Fig. 55. Magnitude (a) and direction (b) of gradient of 10.2 kHz Omega SWC difference for A-D phase difference measurements for area centered at Hampton, Va., for each hour during the period 1-15 July.

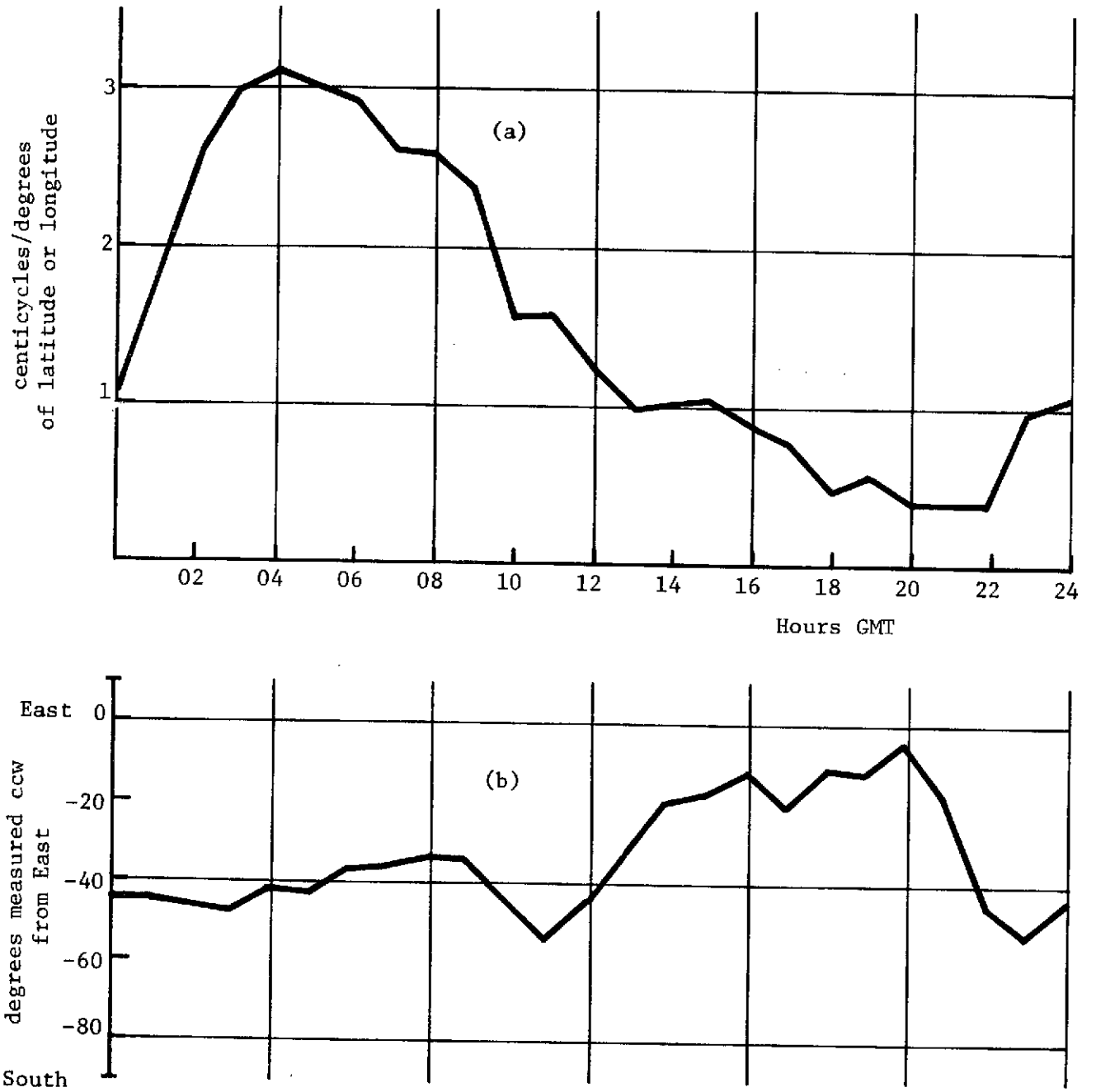

Fig. 56. Magnitude (a) and direction (b) of gradient of 10.2 kHz Omega SWC difference for B-C phase difference measurements for area centered at Hampton, Va., for each hour during the period 1-15 July.

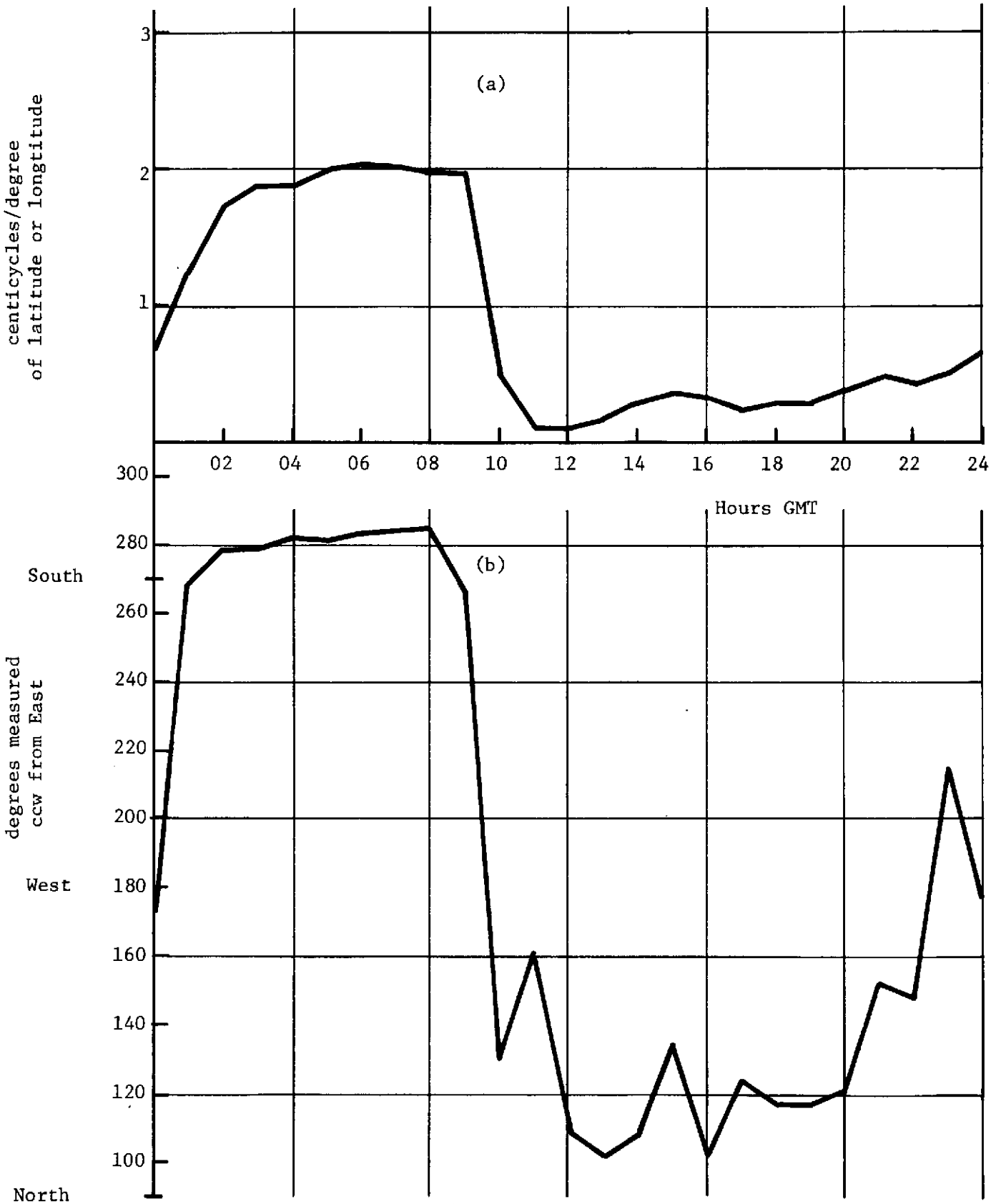

Fig. 57. Magnitude (a) and direction (b) of gradient of 10.2 kHz Omega SWC difference for B-D phase difference measurements for area centered at Hampton, Va., for each hour during the period 1-15 July.

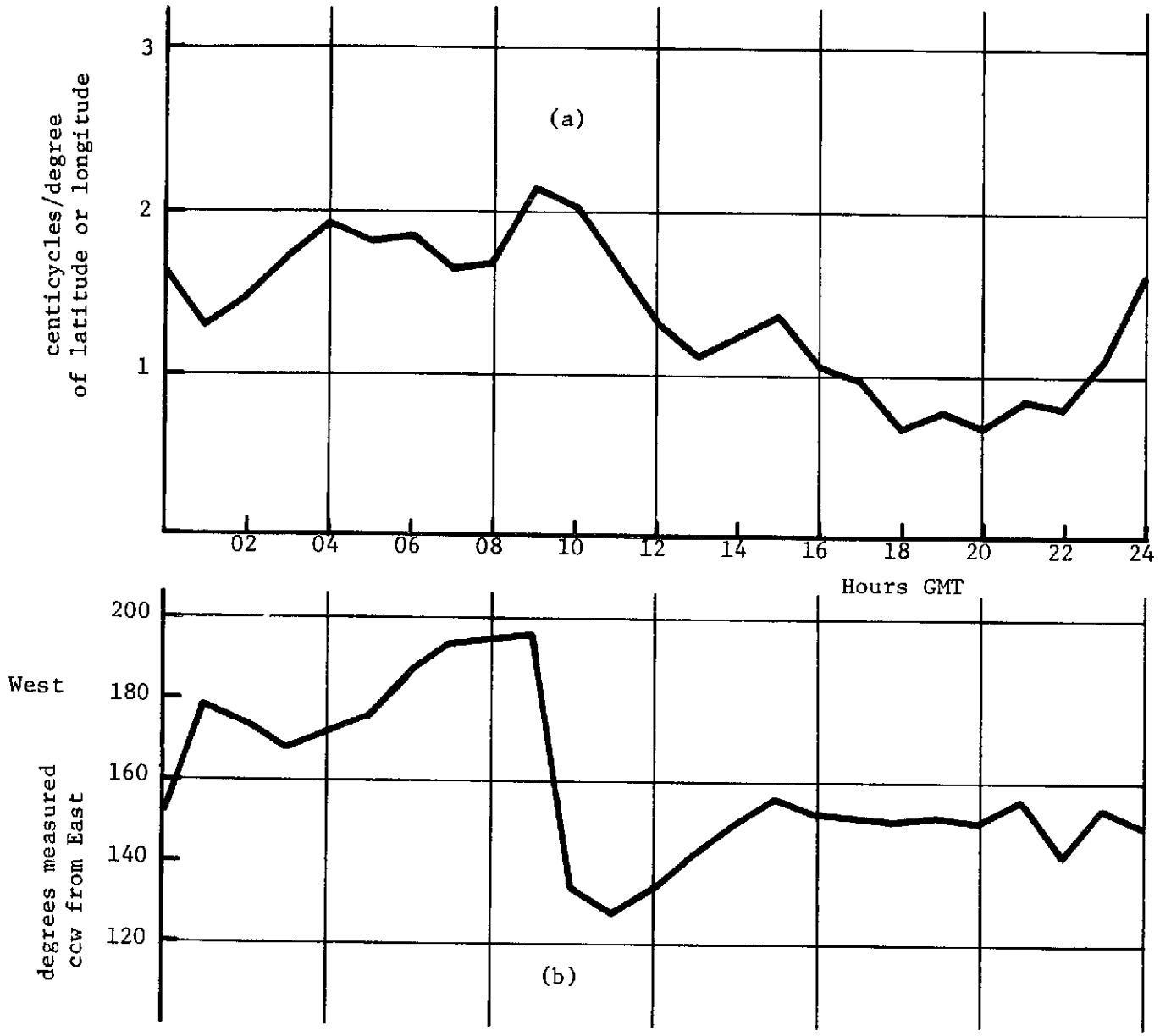

Fig. 58. Magnitude (a) and direction (b) of gradient of 10.2 kHz Omega SWC difference for C-D phase difference measurements for area centered at Hampton, Va., for each hour during the period 1-15 July.

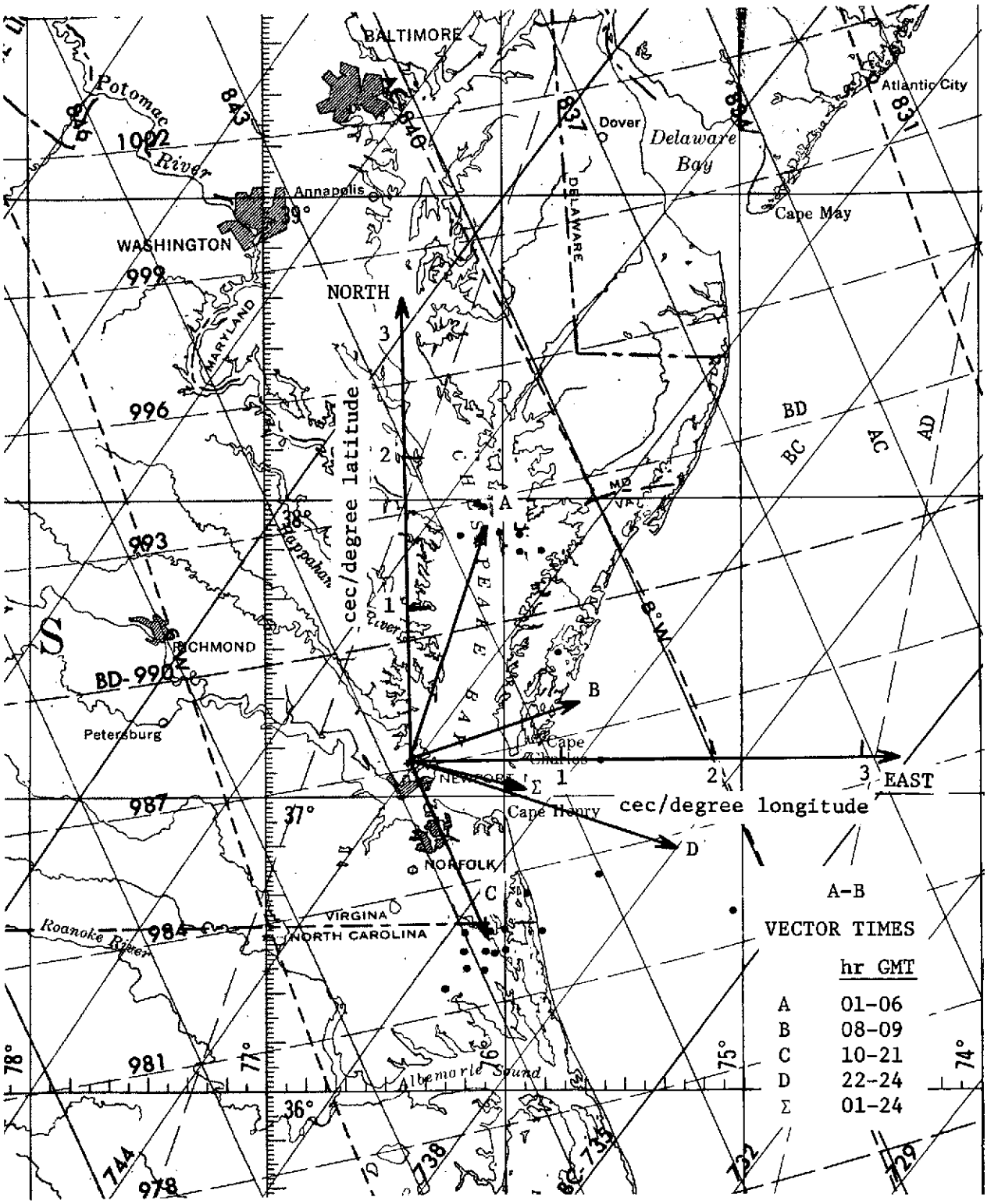

Fig. 59. Median gradients of 10.2 kHz Omega SWC differences for A-B phase difference measurements for indicated hourly periods for area centered at Hampton, Virginia, during the period 1-15 July. Mean gradient for the period is shown as Σ. Vector plots are superimposed on Omega LOP chart.

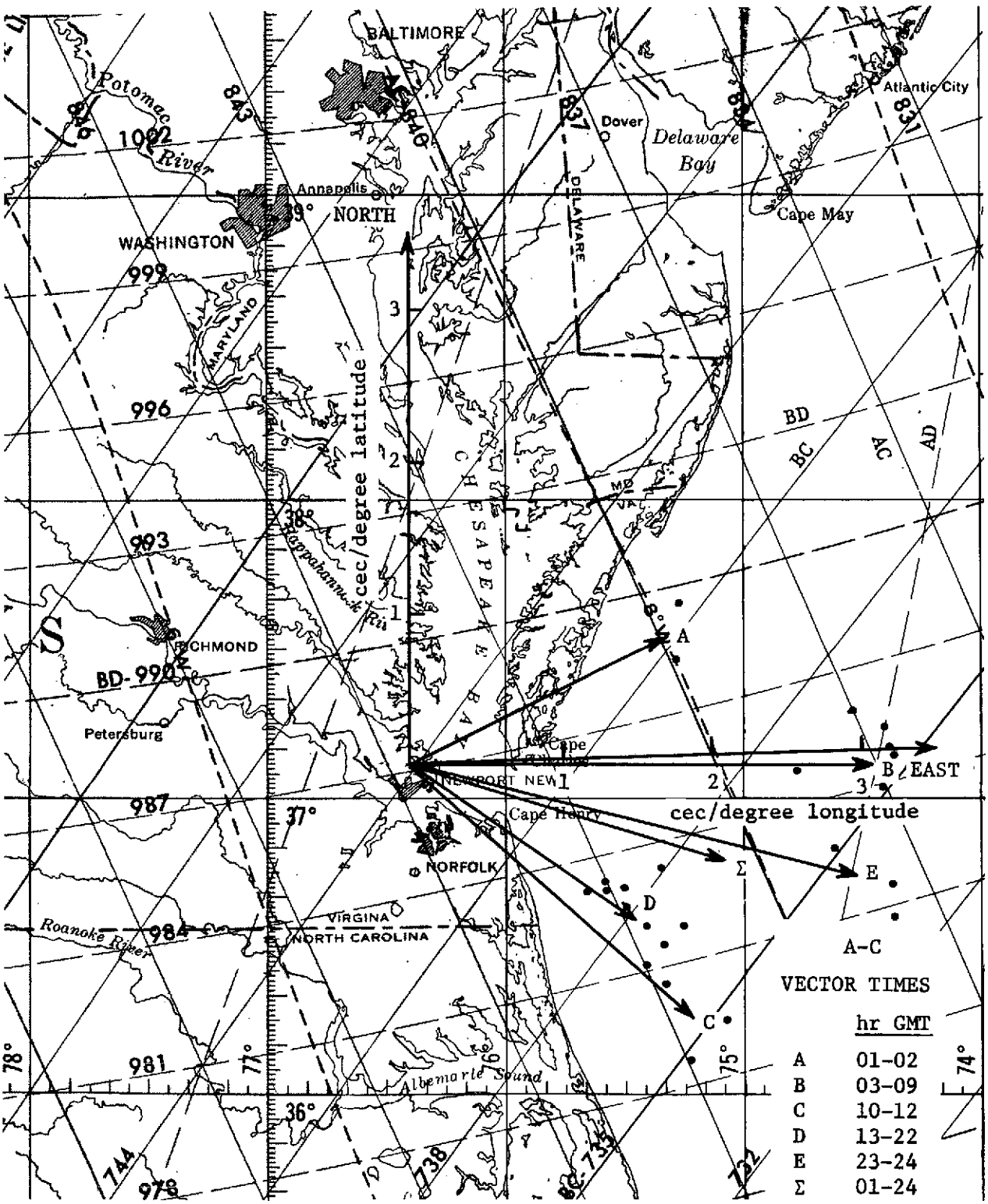

Fig. 60. Median gradients of 10.2 kHz Omega SWC differences for A-C phase difference measurements for indicated hourly periods for area centered at Hampton, Virginia, during the period 1-15 July. Mean gradient for period is shown as Σ. Plots superimposed on Omega LOP chart.

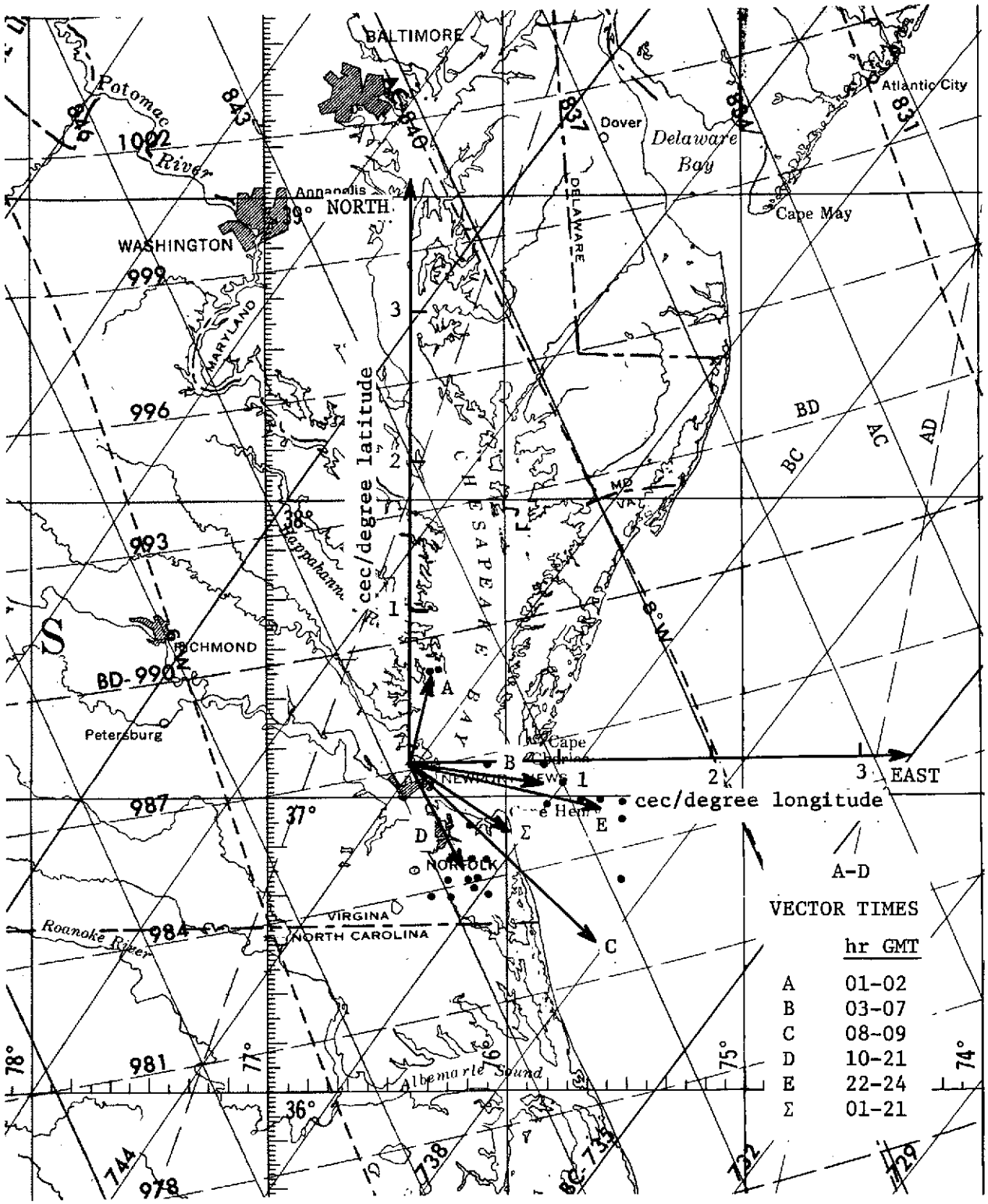

Fig. 61. Median gradients of 10.2 kHz Omega SWC differences for A-D phase difference measurements for indicated hourly periods for area centered at Hampton, Virginia, during the period 1-15 July. Mean gradient for the period is shown as Σ. Plots superimposed on Omega LOP chart.

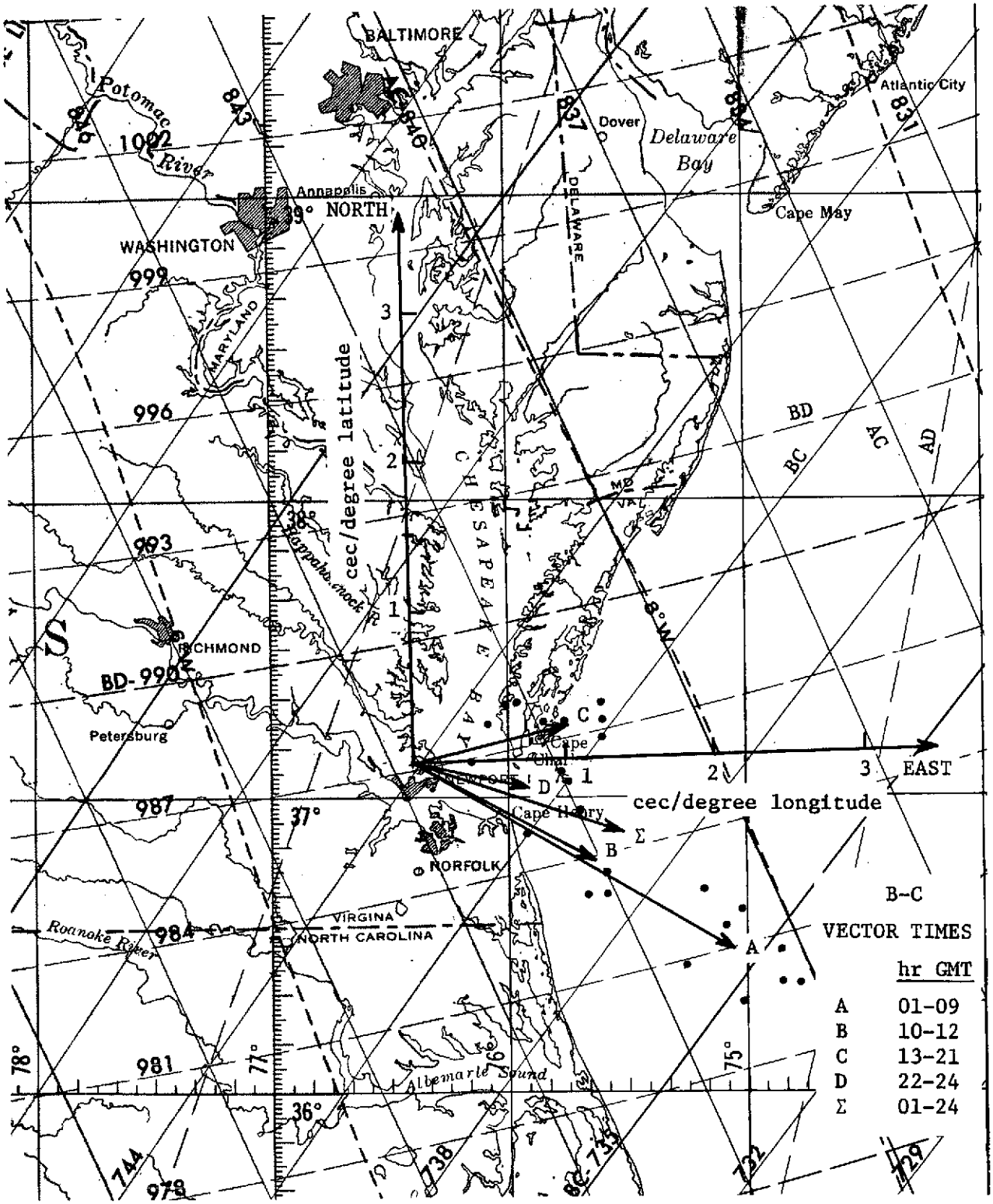

Fig. 62. Median gradients of 10.2 kHz Omega SWC differences for B-C phase difference measurements for indicated hourly periods for area centered at Hampton, Virginia, during the period 1-15 July. Mean gradient for the period is shown as Σ. Plots superimposed on Omega LOP chart.

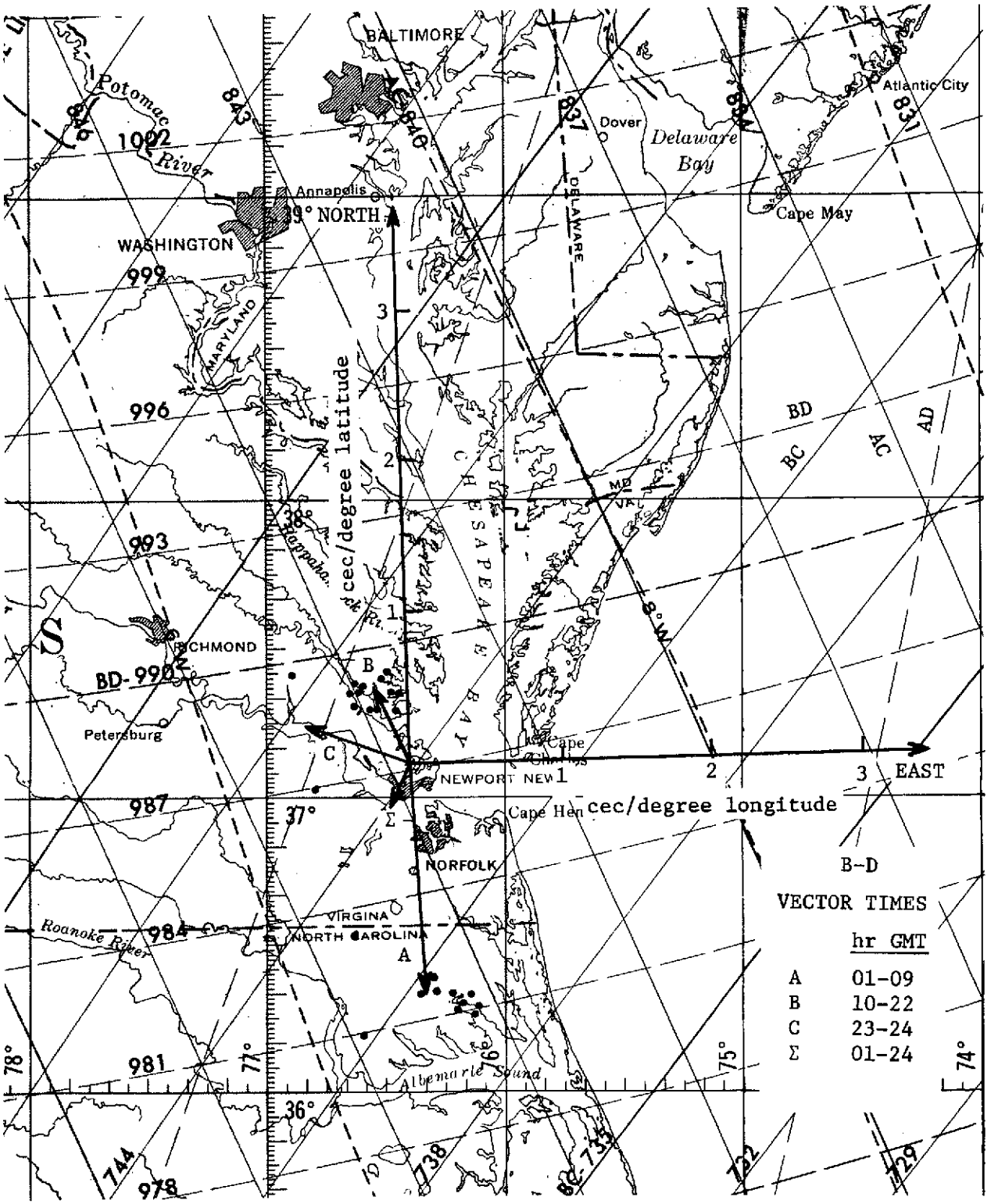

Fig. 63. Median gradients of 10.2 kHz Omega SWC differences for B-D phase difference measurements for indicated hourly periods for area centered at Hampton, Virginia, during the period 1-15 July. Mean gradient for the period is shown as Σ. Plots superimposed on Omega LOP chart.

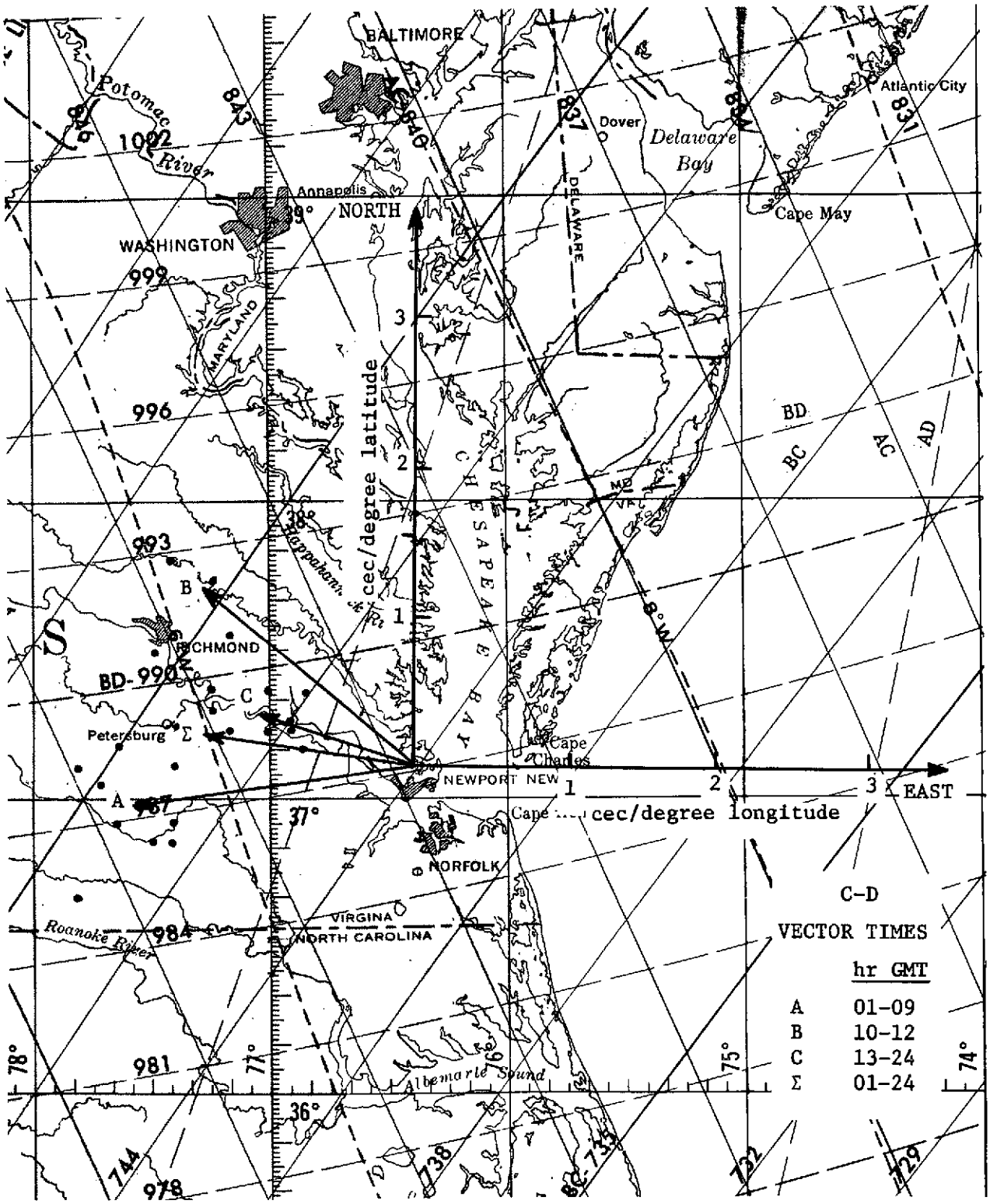

Fig. 64. Median gradients of 10.2 kHz Omega SWC differences for C-D Phase difference measurements for indicated hourly periods for area centered at Hampton, Virginia, during the period 1-15 July. Mean gradient for the period is shown as Σ. Plots superimposed on Omega LOP chart.

errors of less than 1 n. mi. within this "differential region."

Although this analysis may not provide a reliable quantitative measure of the navigational accuracy obtainable with differential Omega, it does provide some qualitative measure of the spatial and temporal correlation of Omega corrections within a relatively small area. As an example, for station pair B-D, SWC differences may be adequately accounted for by measuring a daytime value and a nighttime value, whereas for another pair, B-C, more frequent phase difference corrections would be needed to maintain good navigational accuracy.

6.3 Modes of Differential Omega

There are several modes of operation with differential Omega that have been conceptualized. Common to these modes is the need for a base station which is in a precisely-known position and which is able to determine the difference between the actual received phase difference and the charted phase difference for a given transmitter pair.

For aircraft usage, ref. 22 has defined a differential mode and a sky-wave corrected differential mode. In the differential mode, the difference between the measured phase difference and the charted phase difference can be communicated from the base station receiver to all subscribers within the differential region. These subscribers could then directly apply the phase corrections to measured phase differences. In the sky-wave corrected mode, a larger area of operation might be possible. Here, the base station applies the published SWC to the measured phase difference for any given transmitter pair and then determines the difference between the corrected phase difference and the charted phase difference. This difference is then communicated to subscribers who would first apply the appropriate published SWC to their measured phase difference and then apply the base station-determined correction. This might have application over fairly large regions to improve navigational accuracies, particularly during times when anomalies such as sudden ionospheric disturbances (SID's) occur.

Another mode of operation involves use of differential Omega to track drones. (See ref. 28.) Here, the vehicle requiring position location is equipped with an Omega receiver and a transmitter to telemeter the phase measurements to a base tracking station. The tracking station then applies the measured Omega phase difference correction to the telemetered phase difference measurements and can use differential Omega to track the drone.

This particular mode might also have application in a Search and Rescue system.

A variation of the SWC differential mode, the "sky-wave correction gradient corrected differential Omega," is conceivable particularly for large-area usage of differential Omega. In this mode, the gradient of sky-wave corrections at the base station receiver is used to adjust the differential correction at the mobile receiver according to the distance between the two receivers and the azimuth from base to mobile receiver. This mode is equivalent to the SWC differential mode; however, the actual sky-wave correction at either site is not required--only the difference in the sky-wave correction at the two receivers is needed.

Various telemetry schemes for communication between base and mobile receivers have been discussed and experimented with, including VHF and UHF radio systems with possible use of satellite relays. Appendix A includes some reports pertaining particularly to studies involving application of the differential Omega technique.

7.0 APPENDICES

APPENDIX A

BIBLIOGRAPHY

ACF Industries: Platform Electronics Package, Omega Position Location Equipment (OPLE). First Quarterly Report, NASA CR-80941, 30 July-30 Sept. 1966.

Agy, V.: Ionospheric Forecasting. N70-23112, Presented at Avionics Panel 15th Technical Symposium, Quebec, 2-5 Sept. 1969.

Alberts, W. S.: Transmitting Facilities for Omega. Westinghouse Engineer, July 1970, pp. 98-107.

Ambroseno, B.; Davidson, D.; Spears, M.; Woodward, R. H.: VLF Airborne System Noise and Antenna Study and Study of Lane Identification for Omega. Final Report, Vol. 2, N68-34748, Pickard and Burns Electronics, Waltham, Mass.

Anon.: The Endless Signal. FAA Aviation News, March 1972, pp. 6-7.

Argo, P. E.: Electrom-Production Rate of Solar and Galactic Cosmic Rays. NELC TR 1783, August 1971.

Avion Electronics, Inc.: Platform Electronics Package, Omega Position Location Equipment (OPLE). Quarterly Report, NASA CR-85473, 15 Feb.-31 Mar. 1967.

Bahar, E.: Model Studies of the Influence of Ionospheric Perturbations on VLF Propagation. ARPA Order No. 183-62, U. of Colorado, May 5, 1964.

Baltzer, O. J.: Final Technical Report: Differential Omega Test and Evaluation Program. A68-36444, TRACOR Publ. No. 68-135-U, 18 Jan. 1967.

_____: Omega Test Results: DC-6 Aircraft Flight to Bermuda. TRACOR, Inc., Austin, Texas, Sept. 1968.

_____: Omega Navigational Instrumentation for Special Shipping Applications. Marine Sciences Instrumentation, Vol. 4, 1968.

Barad, M. L.: NATO Advanced Study Institute on Structure of the Lower Atmosphere. November 1967.

Barnard, C. R. N.: The Use of Phase Modulations in Radio Navigation Aids. A64-12856, IEE Conference on Electronics Research and Development for Civil Aviation, London, Oct. 2-4, 1963, pp. 197-200.

Bauss, W. (ed.): Radio Navigation System for Aviation and Maritime Use. Pergamon Press, Oxford, London, 1963.

Beukers, John M.: Windfinding Using the LORAN-C and Omega Long Range Navigational Systems. IEEE Trans. on Aerospace and Electronic Systems, vol. AES-3, no. 6, Nov. 1967, pp. 290-299.

 PRECEDING PAGE BLANK NOT FILMED

Bickel, J. E.; Britt, J. E.; Freres, C. H.; Gossard, E. E.; Ortwein, N. R.; and Swanson, E. R.: A Proposed Method for Over the Horizon Location of Friendly Tactical Units. NELC TM 1105(C), May 1967.

Bickel, J. E.; Ferguson, J. A.; and Stanley, G. V.: Experimental Observation of Magnetic Field Effects on VLF Propagation at Night. Radio Science, vol. 5, no. 1, Jan. 1970, pp. 19-25.

Blackband, W. T. (ed.): Advanced Navigational Techniques. Royal Aircraft Establishment, AGARD Conference Proceedings No. 28, Technivision Services, Slough, England, Jan. 1970. Available through CIRCA Publications, 415 5th Ave., Pelham, NY 10803.

Blackband, W. T.: The Effects of the Ionosphere on VLF Navigation Aids. J. Res. Nat. Bur. Std., vol. 65D, no. 6, June 1961, pp. 575-579.

_____: Propagation of Radio Waves at Frequencies Below 300 kc/s. Pergamon Press, 1964.

Bos, H. J.: Preliminary Report on the State-of-the-Art of Omega. A VLF Long-Range Hyperbolic Radio-Navigation Technique for Present and Future Air-Transport and Sea-Transport Requirements. N67-10030, Technisch Documentatie en Informatie Centrum Voor de Krijgsmacht, The Hague, Netherlands, August 1966.

_____: Third Report on Omega, Differential Omega, and OPLE. Future Sea Transport, Air Transport and Meteorological Prediction Needs. N70-16719, Technisch Documentatie en Informatie Centrum Voor de Krijgsmacht, The Hague, Netherlands. In Dutch.

Bowhill, S. A.: Ionospheric Irregularities Causing Random Fading of Very Low Frequencies. J. Atmospheric and Terrestrial Physics, vol. 11, 1957, p. 91.

Bradford, W. R.: Desk Top Calculator Program Used for Diurnal Phase Variation Study. NELC TN 1921, 30 August 1971.

_____: Freznel Zone Theory of VLF Coupling into the Earth-Ionosphere Waveguide. NELC TN 1896, 22 July 1971.

Braff, R.; and Braverman, N.: VLF Range-Range Navigation Error Contours. J. Inst. Nav., vol. 12, no. 1, Spring 1965, pp. 36-48.

_____: VLF Multirange Navigation Errors. IEEE Trans. Aerospace and Electronic Systems, vol. AES-5, no. 3, May 1969, pp. 396-416.

Bremmer, H.: Terrestrial Radio Waves. Elsevier Publishing Company, 1949.

Britt, J. E.: Accuracy Tests on Tracor 3-599R Omega Receivers. NELC TN-1529, 21 August 1969.

Brogden, J. W.: The Omega Navigation System. A68-20753, ION National Marine Navigation Meeting on Status of New Developments in Marine Navigation, Annapolis, Maryland, 11-12 October 1967.

Brogden, J. W.; Coven, A. W.; and Williams, M. F.: The Omega Navigation System. N62-16678, Naval Res. Lab., Report of NRL Progress, August 1962, pp. 1-11.

Brogden, J. W.; and Luken, K. O. L.: Differential OMEGA. AD 640 013, Interim Report, Naval Research Laboratory, 8 August 1966.

_____: Lane Identification in the Omega System. Naval Research Laboratory. Interim Report, AD 659 959, 28 July 1967.
Final Report, AD 672 587, 2 May 1968.

Brown, R. P.; and Swanson, E. R.: Omega Data Program: A Computer Program for Monthly Blocks of Hourly Phase Difference Data. NELC.

Budden, K. G.: The Waveguide Theory of the Propagation of VLF Radio Waves. Proc. I. R. E., vol. 45, no. 6, 1957, pp. 772-774.

Burgess, B.: Experimental Observations on the Phase Variability of 200 Hz Difference Frequencies Derived from VLF Transmissions Obtained over Large Distances. R. A. E. Tech. Report 68150, N70-26341, June 1968.

_____: Navigation Errors Using OMEGA at Ranges Close to a Transmitter. A70-19222, Proc. IEE, vol. 117, no. 1, Jan. 1970, pp. 51-55.

_____: Propagation Effects and Lane Ambiguity Resolution in Omega. AD 683 075, A69-38756, Proc. IEE, vol. 116, June 1968, pp. 1297-1303.

_____: Some Aspects of VLF Propagation as Appropriate to Omega in the Arctic Environment. RAE TR-68142, Farnborough, England, June 1968.

_____: VLF Phase Delay Variability and the Design of Long-Range Navigation Aids. RAE TR-68145, Farnborough, England, June 1968.

_____: VLF Radio Wave Propagation and its Influence in Position Fixing. A70-13614, Paper Presented at Deutsche Gesellschaft Für Ortung und Navigation, Internationale Navigationstagung, Hamburg, W. Ger., Oct. 28-30, 1969.

Burgess, B.; and Walker, D.: Effects in Omega from Propagation Variations. A70-21564, J. Inst. Nav. (Brit.), vol. 23, no. 1, Jan. 1970, pp. 49-59.

Burt, W. A.; et al.: Mathematical Considerations Pertaining to the Accuracy of Position Location and Navigation Systems. AD 629 609, November 1965.

Casselman, C. J.; Denton, R. L.; and Wilson, J. J.: Project FISHBOWL Effects On Omega VLF Transmissions. NELC Report 1207, 20 Dec. 1963.

Casselman, C. J.; Heritage, D. P.; and Tibbals, M. L.: VLF Propagation Measurements for the Radux-Omega Navigation System. Proc. IRE, vol. 47, May 1959, pp. 829-839.

Chilton, C. J.; Conner, J. P.; and Steele, F. K.: A Comparison Between Solar X-Ray Emission and VLF Sudden Phase Anomalies. Proc. IEEE, vol. 53, no. 12, Dec. 1965, pp. 2018-2026.

Clark, J. M.: Aircraft Navigation Using Omega. IEEE Trans. Aerospace and Electronic Systems, vol. AES-5, no. 5, Sept. 1969, pp. 756-761, A69-42539.

Couzens, R.: The 'Beat 2 Receiver' - A Twin Channel Omega Receiver. RAE TR-68225, AD 686 454, Aug. 1968.

_____: The Monitoring of Phase Modulated V.L.F. Signals. A67-22627, IEEE/IEE Air Traffic Control Systems Engineering and Design Conference, London, 13-17 March 1967.

_____: Spatial Modulation in the Omega System, Airborne Trial (July 1968). X70-11684, RAE, Farnborough, England, April 1969.

Crombie, D. D.: Periodic Fading of VLF Signals Received over Long Paths During Sunrise and Sunset. J. Res. Nat. Bur. Std., vol. 68D, no. 1, 27 Jan 1964.

_____: On the Use of VLF Measurements for Obtaining Information on Lower Ionosphere (Especially During Solar Flares). Proc. IEEE, vol. 53, no. 12, Dec. 1965, pp. 2027-2034.

Cunningham, L. L.; and Swartwood, W. M.: Evaluation of the Navy Navigation Satellite System and the Omega Navigation System. AD 657-124, Naval Oceanographic Office, Washington, D.C., August 1967.

Daniel, D. B.: Airborne Omega Navigation Set. A69-21197, 24th Annual Meeting, ION, U.S. Naval Postgraduate School, Monterey, California, 19-21 June 1968.

D-Appolito, J. A.: The Evaluation of Kalman Filter Designs for Multisensor Integrated Navigation Systems. AFAL TR-70-271, The Analytic Sciences Corporation TR 183-1, January 1971.

D'Appolito, J. A.; and Kasper, J. F., Jr.: Predicted Performance of an Integrated Omega/Inertial Navigation System. Proc. 1971 National Aerospace Electronics Conference, Dayton, Ohio, May 1971, pp. 121-128.

David, P.; and Voge, J.: Propagation of Waves. Pergamon Press, 1969.

Davies, Kenneth: Ionospheric Radio Propagation. U. S. Dept. Commerce, Library of Congress Cat. No. 64-60061.

Denbigh, P. N.: Techniques and Errors of Balloon Location by Low-Orbit Meteorological Satellites. A69-38618, Paper Presented at British Interplanetary Society and NATO International Summer School on Earth Resources Survey Satellites, Cambridge, England, 14-25 July 1969.

Dillard, G. M.: Distribution-Free Detection of Communication Signals. NELC TR-1776, Sept. 1971.

Disney, R. A.; and Spaulding, A. D.: Amplitude and Time Statistics of Atmospheric and Man-Made Radio Noise. ESSA TR ERL 150-ITS-98, Feb. 1970.

Eisenberg, R. L.; and Williams, M. F.: The Flight Performance of the NRL Mark 3 Omega Aircraft Navigation Set. AD 861 914L, NRL, Washington, D. C., 29 Oct. 1969.

Eisenberg, R. L.; and Williams, M. F.: Interim Report of Precipitation Effects on Omega Aircraft Receivers. AD 660 377, NRL Memo Report 1810, Aug. 1967.

Enge, F. J.: An Omega Receiver Navigation Set for High Performance Aircraft. A67-22391, Navigation, vol. 13, Winter 1966-67, pp. 343-347.

_____: Application of Omega Position Location Experiment to Mass Transportation. A70-22193, A70-10307, 25th Annual Meeting ION, New York, 24-26 June 1969.

Ferrentino, P. S.: A Two-Dimensional Omega Equation for the 1000-700 mb Layer with Diabatic Heating. M. S. Thesis, AD 488 333, Naval Postgraduate School, May 1966.

Findlay, D. J.: Omega and a Navoceano Test. Status Report. AD 841 337, Naval Oceanographic Office.

Fletcher, L. A.: The Omega Navigation System, An Overview and Status Report. Paper Presented at 1968 Marine Sciences Instrumentation Symposium, Cocoa Beach, Florida, 23 Jan. 1968.

Fox., J. (ed.): Quasi Optics. Polytechnic Press, Polytechnic Inst. Brooklyn, 1964.

Frank, R. L,; and Hudelson, R. L.: Radio Navigation Sensors. A70-26507, Sperry Rand Engineering Review, vol. 22, no. 4, pp. 38-44.

Freiesleben, H.-C.: The Future Development of Long-Range Navigation at Sea. N70-24863, AGARD Advanced Navigational Techniques, Jan. 1970, pp. 23-30.

_____: Introduction--User Problems. A70-13603, Paper Presented at Deutsche Gesellschaft Für Ortung und Navigation, Internationale Navigationstagung, Hamburg, W. Ger., 28-30 Oct. 1969.

Friedman, A.: Cosmic X-Rays - Progress Report. N69-29094, Naval Research Lab., Washington, D. C.

Galejs, J.: Phase Variability of Omega Navigational Transmissions. A69-22595, Electronics Letters, vol. 5, pp. 106-107.

Gallenberger, R. J.: Effects of Ground Conductivity on Phase Velocity of Electromagnetic Waves at Omega Frequencies. NELC TN-1428, 11 Sept. 1968.

_____: Effects of Latitude and Azimuth on Phase Velocity at 10.2 and 13.6 kHz. NELC TN-1512, 15 July 1969.

Gallenberger, R. J.; and Swanson, E. R.: Theoretical Variations in Omega Propagation Parameters. NELC TR 1773, 23 July 1971.

General Precision, Inc.: USC & GS Sea Trials of Hyperbolic Navigation System. Coast and Geodetic Survey Technical Report, 30 Nov. 1964.

Gimber, R. H.; and Rothmuller, I. J.: Signal Phase and Magnetic Index in Trans-Auroral Omega. AD 738 023, NELC TR-1779, June 1971.

Gossard, E. E.; Bickel, J. E.; and Swanson, E. R.: Recommendations by NELC for R&D Programs for the Study of Very Low Frequency Radio Wave Propagation. NELC TN 1363, 26 Feb. 1968.

_____: Technological Forecast in Very Low Frequency Radio Wave Propagation R&D. NELC TD-27, 3 April 1968.

Gossard, E. E.; and Norgard, C. G.: Experimental Research Results on the Accuracy of Differential Omega and of VLF DF Systems. NELC TN-1767, 16 Nov. 1970.

Graves, E. C.; and Bradley, C. L.: OMEGA Error Modeling and Lane Recovery. The Analytical Sciences Corporation TR-136-3, May 1970.

Gressang, R. V.: The Effect of Aircraft Lateral Dynamics on Aircraft Positioning Accuracy when Using LORAN-C. IEEE Trans. Aerospace and Electronic Systems, July 1971, pp. 700-704.

Hall, H. M.: A New Model for Impulsive Phenomena. Stanford University TR 3412-8, August 1966.

Hampton, D. E.: Group Velocity Variations of V.L.F. Signals. AD 480 258L, RAE, Farnborough, England, Dec. 1965.

Handlogten, B.; and Morin, G. R.: Omega Navigation Computer Set. Final Report, Lear Siegler, Inc.
Vol. 1, AD 678 377.
Vol. 2, AD 678 378.

Hanselman. J. C.: Field Strength Recorder for Very Low Frequencies. AD 404 575, NELC Report 1158, 11 Feb. 1963.

Hastings, C. E.: Automatic Real Time OMEGA Accuracy Enhancement. Proc. ION National Marine Meeting, New London, Connecticut, Oct. 1970.

Hastings, C. E.; and Comstock, A. L.: Pinpoint Positioning of Surface Vessels Beyond Line-of-Sight. ION National Marine Navigation Meeting, San Diego, California, Nov. 1969.

Hastings, C. E.; Barker, A. Clifford; and Bradbury, J. T.: Precision Low Cost Marine Radionavigation, a Regional Approach. Symposium Paper RTCM Assembly Meeting, Montreal, Canada, April 1971.

Hill, J. R.: A Method for Rapid Computation of VLF Steep Incidence Reflection. NELC TR-1784, August 1971.

Hilton, G.; Hollenbaugh, R.; Laughlin, C.; and Lavigne, R.: Meteorological Experiment Using the Omega System for Position Location. N66-23735, NASA GSFC, October 1965.

Hilton, G. E.; and Laughlin, C. R.: Omega Location and Satellite Reporting for World-Wide Observation Systems. A66-19508, IEEE 12th Annual East Coast Conference on Aerospace and Navigational Electronics, Baltimore, 27-29 Oct. 1965.

Hilton, G.; Laughlin, C.; and Lavigne, R.: OPLE Experiment. N67-36634, NASA GSFC, June 1967.

Horiuchi, H. S.: Preliminary Experiment Results from the Omega Position Location Equipment--OPLE. A69-19135, International Telemetering Conference, Los Angeles, California, 8-11 Oct. 1968, pp. 631-638.

Horowitz, S.: Numerical Solution of Wave Equations for Long Wavelength Radio Waves. AFCRL-71-0237, April 1971.

Hozumi, H., et al.: Observations of Radio Sources at 9.4 gc/s With Maser and High-Resolution Interferometer. A65-28335, Proc. Res. Inst. Atmospherics, Nagoya University, vol. 12, Jan. 1965, pp. 35-48.

Institute of Navigation: Proc. of the First Omega Symposium. 9-11 Nov. 1971, Washington, D. C.

International Radio Consultative Committee: World Distribution and Characteristics of Atmospheric Radio Noise. Report 322, Documents of the Xth Plenary Assembly, Geneva, 1963.

Jones, S. S. D.: Problems in the Long-Range Navigation of Transport Aircraft. A66-33214, International Federation of Air Line Pilots' Associations Symposium on All Weather Operations, Head-Up Displays, Long-Range Navigational Aids, Rotterdam, The Netherlands, 13-16 Oct. 1965, vol. 2.

_____: VLF Techniques for Navigation. J. Inst. Nav. (Brit.), vol. 23, no. 1, Jan. 1970, p. 23.

Kasper, J. F., Jr.: A Skywave Correction Adjustment Procedure for Improved Omega Accuracy. Proc. ION National Marine Meeting, New London, Connecticut, Oct. 1970.

_____: Application of Differential Omega to Remote Environmental Sensing. A72-44639, ION 28th Annual Meeting, 27-29 June 1972.

_____: Evaluation of OMEGA Configurations for Airways System Operations. Analytic Sciences Corporation, Reading, Massachusetts.

_____: Omega Utilization for Non-Military Subscribers. Analytic Sciences Corporation, Reading, Massachusetts, 31 Dec. 1971.
Vol. I, AD 730 934.
Vol. II, AD 731 980.

Kayton, Myron; and Fried, Walter: Avionics Navigation Systems. John Wiley & Sons, 1969.

Kivett, N. D.; and Wetherington, R. D.: Statistical Data for Omega Propagation. NASA CR-90008, Final Report, 24 Aug. 1967.

Klass, Philip J.: Omega Navaid Aviation Use Studied. Aviation Week & Space Technology, Nov. 29, 1971, pp. 38-42.

Klein, P. I.: Application of the Concept of Referenced Radio Navigation. A68-36812, IEEE Trans. Aerospace & Electronic Systems, vol. AES-4, July 1968, pp. 494-498.

Kugel, C. P.: Omega System Synchronization (U). NELC Report 1529, 10 Jan. 1968.

Laughlin, C. R.: The Relay of Omega Navigation Signals by Satellite to a Central Processing Facility. A7023026, Advanced Navigational Techniques, AGARD Symposium Proc., Milan, Italy, Sept. 12-15, 1967, pp. 62-76.

Laughlin, C. R., et al.: Meteorological Experiment Using the Omega System for Position Location. N66-23735, NASA GSFC, Oct. 1965.

_____: PLACE Experiment Description. N69-19548, NASA GSFC, Nov. 1967.

Lear Siegler, Inc.: Omega Phase Variation Study. AD 689 796, Feb. 1967.

Leslie, F. R.: Omega Short Term Ranging Precision. Pan American Tech. Paper, Nov. 1971.

Levine, Irving: Helicopter Flight Test of Differential Omega. AD 697 128, Army Electronics Command Report ECOM-3188, Sept. 1969.

Levine, S. A.; and Gelb, A.: Geodetic and Geophysical Uncertainties--Fundamental Limitations on Terrestrial Inertial Navigation. A68-37547, AIAA Guidance, Control, and Flight Dynamics Conference, Pasadena, California, 12-14 August 1968.

Lewis, E. A.; and Rassmussen, V. E.: Relative Phase and Amplitude Shifts of VLF Signals Received on Two Paths Almost Parallel with the Sunrise Line. J. Geophys. Res., vol. 67, no. 12, 1962, pp. 4906-4908.

Litchford, G. B.: Application of VLF Navigation and Automatic Calibration of Barometric Altitude Sensing to General Aviation and a National Universal System for the Guidance and Control of Air Traffic. NASA CR-86313, N70-17449, Final Report, Litchford Systems.

_____: Making General Aviation Safer and More Effective Through Universal Electronic Design. Astronautics and Aeronautics, vol. 9, Jan. 1971, pp. 36-41.

Luken, K.; Brogden, J. W.; and Meyers, W. D.: Accuracy Studies of the Differential Omega Technique. N70-41722, AD 709 555, June 29, 1970.

MacFarland, R. H.: The Application of Omega Navigation to General Aviation. NAECON 1971, May 1971.

_____: Experimental Investigation of Simplified Omega Navigation Using a CDI Reference. AD 865 600, Army Electronics Command, Dec. 1969.

_____: Use of a Simple, CDI Presentation for OMEGA Navigation. A70-27920, Army Electronics Command, EASCON 1969 Record.

Markowitz, W. M.: Time and Frequency Measurement, Atomic and Astronomical. A69-31285, Proc. 5th Annual Test Measurement Symposium, Instrument Society of America, 28-31 Oct. 1968, pp. 6271-6276.

Marton (ed.): Advances in Electronics and Electron Physics. V-25, Academic Press, 1968.

McCall, D. C.: Mathematical Programming as an Aid to Engineering Design. NELC TR 1778, August 1971.

McDonald, K. D.; Nickell, R. S.; Calabria, F. M.; and Andrel, R.: An Analysis and Technical Evaluation of Selected Navigation and Communication System Concepts for 1975. NASA CR-77826, Final Report, April 1966.

McGee, Leonard A.; and Christensen, J. V.: Fixed Time-of-Arrival Aircraft Guidance and Navigation Using Kalman Filtering of Radio Aid Data. Ames Research Center Internal Document.

Meyers, W. D.: Lane Counter for the TRACOR 599R OMEGA Receiver. AD 696 529, NRL Memo Report 2036, Sept. 1969.

_____: Measuring Field Intensity of Omega Signals with TRACOR 599R Omega Receiver. NRL Memo Report 2129, April 1970.

MITRE Corp.: Analysis of a Telemetry Range Instrumented Aircraft (TRIA) Application to Reentry Missions. AD 852 339L, Bedford, Massachusetts, March 1969.

Morin, G. Rex: Flight Test Performance of an Airborne Omega Equipment Set. A69-21191, J. Inst. Nav., vol. 16, no. 3, Fall 1969, pp. 308-318.

NASA, Space Applications Programs Office: An Analysis and Technical Evaluation of Selected Navigation and Communication System Concepts for 1975. April 1966.

NELC Omega Navigation System Group: Intercomparison of Nine Rubidium Frequency Standards. NELC TM 695, 22 May 1964.

_____: Technical Evaluation of Omega Navigation System. AD 295 674, NELC-1153, 18 Dec. 1962.

Naval Research Laboratory: Communications Sciences: Problem Notes. N70-28294, Report of NRL Progress, March 1970, pp. 26-27.

_____: Results of Measurement of Omega Reception at French Centers. AD 856 496, 9 May 1969.

Noonkester, V. R.; and Swanson, E. R.: Ionospheric Forecast Requirements of the OMEGA Navigation System. N70-23149, 15th AGARD Symposium, Paper 41, St. Jovite, Quebec, Canada, 2-5 Sept. 1969.

Norgard, C. G.: Special Measurements on Omega Forestport Control Frequency Transmissions. NELC TN-1659, 29 April 1970.

Nortronics: OMEGA Propagation Correction Technique Study. AD 834 288, NELC TD-26, 29 March 1968.

O'Bryant, Richard: OPLE Data Analysis. A70-12180, IEE Resources Roundup, Phoenix, Arizona, April 1969.

Palmer, Winslow: Omega-Inertial Hybrid Receiver. A69-19209, J. Inst. Nav., vol. 15, no. 4, Winter 1968-69, pp. 376-390.

_____: Mean Phase Geometry in the Omega System. Omega-TN-16, October 1969.

Pappert, R. A.: A Numerical Study of VLF Mode Structure and Polarization Below an Anisotropic Ionosphere. Radio Science, vol. 3, no. 3, 1968, pp. 219-233.

Pappert, R. A.; Gossard, E. E.; and Ruthmuller, I. J.: A Numerical Investigation of Classical Approximations Used in VLF Propagation. Radio Science, vol. 2, no. 4, April 1967, pp. 387-400.

Pappert, R. A.; and Shockey, L. R.: A Fortran Program for Wave Propagation. AD 713 168, NELC IR-702, June 1970.

_____: WKB Mode Summing Program for VLF/ELF Antennas of Arbitrary Length. NELC IR-713.

Pappert, R. A.; and Smith, R. R.: Numerical Results for VLF Mode Conversion in the Earth-Ionosphere Waveguide. NELC IR-712, April 1971.

Pappert, R. A.; and Snyder, F. P.: Some Results of a Mode-Conversion Program for VLF. Radio Science, vol. 7, no. 10, Oct. 1972, pp. 913-923.

Phipps, C. R., Jr.: Omega-System Synchronization in the Absolute Mode of Operation. AD 671 997, NELC 1544, 13 March 1968.

Pickard & Burns: VLF Airborne System Noise and Antenna Study and Study of Lane Identification for Omega. Vols. I and II, SRDS Report No. RD-68-17, March 1968.

Pierce, J. A.: Intercontinental Frequency Comparison by Very-Low-Frequency Radio Transmission. Proc. IRE, vol. 45, June 1957, pp. 794-803.

_____: Measurement and Prediction of Group Velocity at Very Low Radio Frequencies. AD 657 949, July 1967.

_____: Omega. IEEE Trans. Aerospace & Electronic Systems, vol. AES-1, 1965, pp. 206-209.

_____: Report on Radux. ATI-48012, Harvard University Report No. TR-17, July 1947.

_____: The Use of Composite Signals at Very Low Radio Frequencies. AD 666 567, Harvard University, February 1968.

_____: Very Low Frequency Propagation. X67-18052, Harvard University, Dec. 1966.

_____: Lane Identification in Omega. AD 746 503, Harvard University, July 1972.

Pierce, J. A.; Palmer, W.; Watt, A. D.; and Woodward, R. H.: Omega, A World-Wide Navigation System. System Specification and Implementation. AD 630 900, Pickard & Burns Report No. 886B, 1966.

Pierce, J. A.; and Woodward, R. H.: The Development of Long-Range Hyperbolic Navigation in the United States. J. Inst. Nav., vol. 18, no. 1, Spring 1971, pp. 51-62.

Powell, C.: Compound Air Navigation Systems. J. Inst. Nav., vol. 16, no. 4, Oct. 1963.

_____: On the Signal Format for the Omega System. A70-23026, Advanced Navigational Techniques, AGARD Symp. Proc., Milan, Italy, 12-15 Sept. 1967, pp. 77-85.

_____: The Use of VLF Transmissions for Navigation. J. Inst. Nav. (Brit.), vol. 15, July 1962, pp. 277-288.

Pozesky, M.: Navy Time Frequency Programs. N69-19864, FAA, Washington, D. C.

Pressey, B. G.; Ashwell, G. E.; and Hargreaves, J.: The Phase Variation of Very-Low-Frequency Waves Propagated over Long Distances. Proc. IEE, vol. 108, part B, no. 38, 1961, pp. 214-221.

RCA: Navigation Traffic Control Satellite Mission Study.
Vol. 1: Summary Final Report. N69-32358, Dec. 1968.
Vol. 2: Candidate Navigation/Traffic Control Satellite Systems Identification, Analysis and Evaluation, Final Report. N69-32359, Dec. 1968.
Vol. 3: Selected Navigation/Traffic Control Satellite System Analysis and Equipment Definition, Final Report. N69-32360, Dec. 1968.
Vol. 4: Critical Technology, Growth and Economic Summaries, Final Report. N69-32361, Dec. 1968.

Rona, P. A.; and Zuccaro, A.: Omega Navigation Performance Off Northwest Africa During Operation No. 267, 23 April-28 May 1968. AD 678 443, Columbia University.

Rothmuller, I. J.: A Linear Regression Analysis Program. NELC TN 1589, 26 Nov. 1969.

_____: Auroral Zone Effects on Omega. NELC TN 1505, 12 June 1969.

_____: The High-Latitude D-Region. NELC TN-1445, 4 November 1968.

Rothmuller, I. J.; Swanson, E. R.; Kugel, C. P.; and Britt, J. E.: Omega Arctic Propagation: Synchronized Monitoring at Wales Alaska 1969-1970. NELC TR 1765, 11 May 1971.

Sage, G. F.: NRL-LSI Mark III Airborne Omega System. A70-22190, A70-10302, 25th Annual Meeting of Institute of Navigation, New York, 24-26 June 1969.

Sailors, D. B.: An Assessment of Omega Signals at NASA Tracking Stations. NELC TN 1777, 4 December 1970.

Scott, R. E.: Study and Evaluation of the OMEGA Navigation System for Trans-oceanic Navigation by Civil Aviation. AD 697 699, Univ. of Mich., Aug. 1969.

Scott, R. E.: VLF Hyperbolic Navigation Error Contours. Paper Presented at 20th Annual Meeting of the Institute of Navigation.

Smith, R. H.; Thornhill, A. F.; and Williams, M. F.: Flight Tests of the Omega Aircraft Receiver. Interim Report No. 8, N64-30739, Naval Research Lab., 3 June 1964.

Smith, R. R.: Numerical Solution of Over-Determined Systems of Equations. NELC TN-1750, 2 October 1970.

Snyder, F. P.; and Pappert, R. A.: A Parametric Study of VLF Modes Below Anisotropic Ionospheres. Radio Science, vol. 4, no. 3, March 1969, pp. 213-226.

Spencer, D. F.: Navigation in Space Electronics. A65-22155, IEEE International Convention, New York, March 22-26, 1965.

Spies and Wait: Mode Calculations for VLF Propagation in the Earth-Ionosphere Waveguide. NBS TN-114, July 17, 1961.

Stanbrough, J. H., Jr.; and Keily, D. P.: Long-Range Relative Navigation by Means of VLF Transmissions. Deep Sea Research, vol. 11, 1964, pp. 249-255.

Stanbrough, J. H., Jr.: A VLF Radio Relative Navigation System. J. Inst. Nav., vol. 11, no. 4, Jan. 1965, pp. 417-428.

Stout, C. C.: The Omega System of Navigation. N70-24865, AGARD Advanced Navigation Techniques, Slough, England, 1970, pp. 47-62.

Stringer, F. S.: A Hybrid System for World-Wide Navigation. J. Inst. Nav. (Brit.), vol. 23, no. 1, Jan. 1970, p. 26.

_____: The Extension of the Long Range Aircraft Navigation System to the Short Range Role. A70-23026, Advanced Navigational Techniques, Proc. AGARD Symposium, Milan, Italy, Sept. 12-15, 1967, pp. 87-90.

_____: Navigation Across the EnRoute/Terminal Area Interface. A67-22655, IEEE/IEE Air Traffic Control Systems Engineering and Design Conference, London, March 13-17, 1967.

Stringer, F. S.; Couzens, R.; Lawson, G. J.; and Rowe, L. E.: Report on the Final Phase of the RAE/FAA VLF Navigation Study, AD 714 385, RAE TR 69262, Nov. 1969.

Swanson, E. R.: A Few Comments on Omega. Proc. from Precise Time and Time Interval (PTTI) Strategic Planning Meeting, vol. 1, 10-11 Dec. 1970, p. 30.

_____: A Statistical Method of Determining Circular Error Probability. AD 427 269, N64-20374, NELC-1188, 24 Oct. 1963.

_____: Accuracy of Omega Navigation System Using 1969 Skywave Corrections. AD 704 504, NELC-1675, Dec. 1969.

Swanson, E. R.: Application of Omega to Aircraft Navigation and Traffic Control. J. Inst. Nav. (Brit.), vol. 24, no. 1, Jan. 1971, pp. 125-128.

_____: Data Supplement to NEL Report 1305, "Omega Lane Resolution." NELC TM 836, 19 August 1965.

_____: Electromagnetic Field Strength Measurements at 10.2 kHz. NELC 1239.

_____: Electromagnetic Field Strength Measurements at 10.2 kilocycles per Second. NELC TM 655, 14 Jan. 1964.

_____: Estimating the Accuracy of Navigation Systems. AD 427 269, NELC-1188, 24 Oct. 1963.

_____: Long Range Synchronization--Recent Omega Operation in the Absolute Mode. Presented at VLF Propagation Discussion Group Meeting AFCRL, Bedford, Massachusetts, October 1966.

_____: Monitoring Requirements for Operational Omega Stations. NELC TM 801, 19 May 1965.

_____: Omega. J. Inst. Nav., vol. 18, no. 2, Summer 1971, pp. 168-175.

_____: Omega as a Research Tool. Presented to USN ELF/VLF Propagation Discussion Group, NELC, 20 July 1965.

_____: Omega Fix Error Program Using a Desk Top Computer. NELC TN-1639, 27 March 1970.

_____: Omega Global VLF Navigation System for Ships and Aircraft. Presented to G-AES Group for Aeronautical and Electronic Systems of the IEEE, San Diego, California, 22 Sept. 1965.

_____: Omega Lane Resolution. AD 472 854, NELC 1305, 5 Aug. 1965.

_____: Omega Multiple Frequency Transmissions. Presented to USN VLF Discussion Group, Washington, 8 June 1966.

_____: Omega Navigation Capability Based on Previous Monitoring and Present Prediction Ability. AD 605 197, NELC 1226, 5 June 1964.

_____: Omega Station Standard Operating Procedure for Synchronization in the Absolute Mode. NELC Unnumbered Document, Feb. 1966.

_____: Present Predictability of Omega 10.2 kc/s Nighttime Signals (U). NELC TM-781, 18 March 1965.

_____: Remarks on the Propagation of 10.2 kHz Electromagnetic Waves: The Effects of Bearing, Total Magnetic Field Strength, Dip Angle of the Magnetic Field and Ground Conductivity. AD 738 022, NELC TN 1375, 29 March 1968.

Swanson, E. R.: Time Dissemination Effects Caused by Instabilities of the Medium. AGARD Conf. Proc. No. 33, Phase and Frequency Instabilities in Electromagnetic Wave Propagation, 1970, pp. 181-198. Also Comments, pp. 759-768.

_____: VLF Phase Prediction. Presented at Symposium on VLF Propagation, Sandefjord, Norway, 27-30 Oct. 1971.

_____: VLF Radio Navigation System. NELC TN-1309 (Rev.), 25 Aug. 1969.

_____: VLF Radio Navigation Systems. Modern Navigation Systems, course notes for Engineering Summer Conference, U. of Mich., July-August 1967, 1968, 1969.
Lecture 1: The Medium.
Lecture 2: Omega.

Swanson, E. R.; and Bradford, W. R.: Diurnal Phase Variation at 10.2 kHz. Presented at Symp. on Long Wave Propagation, Menlo Park, California, 19-21 Jan. 1971.

Swanson, E. R.; and Brown, R. P.: Omega Data Program. AD 738 021, NELC TD-140, October 1971.

Swanson, E. R.; and Davis, W. E.: Data Supplement to NEL Report 1350, "Omega in the Atlantic (1963-1965)" of 10 January 1966. NELC TM-897, 10 Jan. 1966.

_____: Omega in the Atlantic (1963-1965), Inport Measurements from HMS Vidal and HR.MS. Snellius on Oceanographic Survey Navado. AD 631 008, NELC-1350, 10 January 1966.

Swanson, E. R.; and Gallenberger, R. J.: Omega Phase Velocity Dependence on Path Bearing. Presented at Long Wave Propagation Discussion Group Meeting, Boulder, Colorado, Jan. 1970.

Swanson, E. R.; Gimber, R. H.; and Britt, J. E.: Calibrated VLF Phase Measurements. NELC TN-1778, 4 Dec. 1970.

Swanson, E. R.; and Hepperley, E. J.: Composite Omega: Omega Navigation Using a Combination of Information. AD 863 791, NELC 1657, October 1969.

_____: Omega Lane Resolution - Further Measurements in the Absolute Mode. NELC TM-1085, 23 March 1967.

Swanson, E. R.; and Kugel, C. P.: Omega Navigation System Synchronization and Operation 1966-1968. NELC TD-41, 27 August 1968.

_____: Omega Synchronization and Control. AD 732 448, NELC-1757, 19 Mar. 1971.

_____: Omega VLF Timing. Proc. of 25th Annual Frequency Control Symposium, 26-28 April 1971, pp. 159-166.

Swanson, E. R.; and Tibbals, M. L.: Le Système Mondial de Navigation Oméga. Navigation: Revue Technique de Navigation Maritime Aérienne et Spatiale, vol. 13, July 1965, pp. 255-271. In French.

Swanson, E. R.; and Tibbals, M. L.: The Omega Navigation System. J. Inst. Nav., vol. 12, no. 1, Spring 1965, pp. 24-35.

Swartwood, W. M.; and Cunningham, L. L.: Evaluation of the Navy Navigation Satellite System and the Omega Navigation System. AD 657 124, August 1967.

Taylor, W. L.; and Jean, A. G.: VLF Propagation. Proc. of the Mountain States Navy Research and Development Clinic, Raton, New Mexico, Sept. 28-29, 1961, pp. A45-A65.

Tausworthe, Robert: Cycle Slipping in Phase-Locked Loops. IEEE Trans. on Comm. Tech., vol. COM-15, no. 3, June 1967.

Texas Instruments, Inc.: Omega Position Location Equipment Control Center Development and Experiment Data Analysis, U-25-815800-F.
Final Report, NASA CR-103456, 29 Jun. 1966-21 Jan. 1969.
Addendum Final Report, NASA CR-109368, 31 Jan. - 31 Oct. 1969.

Tibbals, M. L.: Omega Navigation System with Global Coverage for Aircraft, Ships and Submarines. A64-21860, AIAA 1st Annual Meeting, Washington, D. C., 29 June - 2 July 1964.

Tibbals, M. L.; and Heritage, D. P.: Accuracy of the Omega Navigation System. AD 422 435, NELC Report 1185, 2 Oct. 1963.

TRW Systems Group: Advanced SST Guidance and Navigation System Requirements Study. Vol. III: Appendices. Final Report, NASA CR-85014, Redondo Beach, California, 30 April 1967.

Turney, H. W., Jr.: Navigation for Surface and Aerospace Vehicles by a Very Low Frequency Radio Network. A69-42834, American Astronautical Society and Operations Research Society of America Joint National Meeting, Denver, Colorado, June 17-20, 1969.

Van Etten, J. P.: Navigation Systems: Fundamentals of Low and Very Low Frequency Hyperbolic Techniques. Electrical Communications, vol. 45, no. 3, 1970, pp. 192-212.

Van Koevering, A. R.: Conception of the "Omega" Airborne Navigational Computers. A69-20778, Navigation (Paris), vol. 17, pp. 11-27. In French.

Wait, J. R.: A New Approach to the Mode Theory for VLF Propagation. J. Res. Nat. Bur. Std., vol. 65D, no. 1, 1961, pp. 37-46.

_____: Calculated Diffraction Effects at VLF from a Localized Ionospheric Depression. NBS Technical Note, 1964.

_____: Diurnal Change of Ionospheric Heights Deduced from Phase Velocity Measurements at VLF. Proc. IRE, vol. 47, 1959, p. 998.

_____: Influence of an Inhomogeneous Ground on the Propagation of VLF Radio Waves in the Earth-Ionosphere Waveguide. J. Res. Nat. Bur. Std. vol. 69D, no. 7, July 1965.

Wait, J. R.: Influence of the Lower Ionosphere on Propagation of VLF Waves at Great Distances. J. Res. Nat. Bur. Std., vol. 67D, no. 4, July-August 1963, pp. 375-381.

_____: Mixed Path Ground Wave Propagation: 1. Short Distances. J. Res. Nat. Bur. Std., vol. 57, no. 1, July 1956.

_____: The Mode Theory of VLF Ionospheric Propagation for Finite Ground Conductivity. Proc. IRE, vol. 45, June 1957, pp. 760-767.

_____: On Phase Changes in VLF Propagation Induced by an Ionospheric Depression of Finite Extent. J. Geophys. Res., vol. 69, no. 3, Feb. 1964.

_____: Terrestrial Propagation of Very Low Frequency Radio Waves, a Theoretical Investigation. J. Res. Nat. Bur. Std. - D. Radio Propagation, vol. 64D, no. 2, March-April 1960, pp. 153-204.

_____: Two-Dimensional Treatment of Mode Theory of Propagation of VLF Radio Waves. Radio Science, vol. 68D, no. 1, 1964, pp. 81-93.

Wait, J. R.; and Spies, K. P.: A Note on Phase Velocity of VLF Radio Waves. J. Geophys. Res., vol. 66, 1961, pp. 992-993.

_____: Characteristics of the Earth-Ionosphere Waveguide for VLF Radio Waves. Nat. Bur. Std. Tech. Note 300, 1964. Also Supplement to this Note, 15 February 1965.

_____: Influence of Finite Ground Conductivity on the Propagation of VLF Waves. J. Res. Nat. Bur. Std., vol. 69D, no. 10, 1965.

Wait and Walters: Reflection of E&M Waves from a Lossy Magnetoplasma. J. Res. Nat. Bur. Std., vol. 68D, Jan-Feb. 1964.

_____: Reflection of VLF Radio Waves from an Inhomogeneous Ionosphere. Part I, Exponentially Varying. J. Res. Nat. Bur. Std., vol. 67, no. 3, May-June 1963, pp. 361-367.

Waldron: Theory of Guided Electromagnetic Waves. Van Nostrand Rinehold, 1970.

Wallenhauer, A.; and Weber, O.: Navigation Via Satellites. A70-11263, Luftfahrttechnik Raumfahrttechnik, vol. 15, pp. 214-220. In German.

Walter, F.: Nonducted VLF Propagation in the Magnetosphere. N70-15525, NASA CR-10761, Stanford University Radioscience Lab.

Watt, A. D.: VLF Radio Engineering. Pergamon Press, Oxford, 1967.

Watt, A. D.; and Croghan, R. D.: Comparison of Observed VLF Attenuation Rates and Excitation Factors with Theory. J. Res. Nat. Bur. Std., vol. 68D, no. 1, January 1964.

Watt, A. D.; and Maxwell, E. L.: Characteristics of Atmospheric Noise from 1 to 100 kHz. Proc. IRE, Feb. 4, 1957.

_____: Measured Statistical Characteristics of VLF Atmospheric Radio Noise. Proc. IRE, Jan. 1957, pp. 55-62.

Watt, A. D.; Maxwell, E. L.; and Whelan, E. H.: Low-Frequency Propagation Paths in Arctic Areas. J. Res. Nat. Bur. Std., vol. 63D, no. 1, July-August 1959, pp. 99-112.

Webb, W. L.: Electrical Structure of the D & E Region. Atmospheric Sciences Laboratory, White Sands, New Mexico, July 1970.

Weekes, K.: The Ground Interference Pattern of Very-Low-Frequency Radio Waves. Proc. IEE, Part III, vol. 97, 1950.

Weinman, R.: Propagation Prediction for the Omega Navigational System. A69-34077, IEEE 1969 NAECON, May 19-21, 1969, pp. 149-154.

Westfall, W. D.: Prediction of VLF Diurnal Phase Changes and Solar Flare Effects. J. Geophys. Res., vol. 66, no. 9, 1961, pp. 2733-2736.

Whale: Effects of Ionospheric Scattering on Very-Long-Distance Radio Communication. Plenium, 1969.

Williams, M. F.: The Application of the Omega Navigation System to Aircraft. A66-12048, Congress on Long Range Navigation Held by Deutsch Gesellschaft Fur Ortung und Navigation, Munich, Germany, 26-31 August 1965.

Wilson, John J.: The Omega Digital Phase Shifter. AD 659 985, NELC 1503, 2 August 1967.

_____: The Omega Digital Phase Shifter, Model 2. AD 847 949, NELC 1595, Nov. 1968.

Wilts, J. R.: On the Amplitude and Phase of Electromagnetic Waves Received by a Submarine. NELC TM-703, 19 June 1964.

Woodward, R. H., et al.: VLF Airborne System Noise and Antenna Study and Study of Lane Identification for Omega. Continental Electronic Manufacturing Co., Waltham, Massachusetts, March 1968.
Vol. 1, AD 675 504.
Vol. 2, N68-34748.

Wright, Julian: Accuracy of OMEGA/VLF Range/Rate Measurements. A69-29857, J. Inst. Nav., vol. 16, no. 1, Spring 1969.

Wright, J. R.: Results of Differential Omega Test and Evaluation Program. A68-36444, Frequency, July 1968. Also in ECOM Proc. of 22nd Annual Symposium on Frequency Control, April 1968.

Zimmerman, William: Optimum Integration of Aircraft Navigation Systems. IEEE Trans. on Aerospace and Electronic Systems, vol. AES-5, no. 5, Sept. 1969, pp. 737-747.

Zuccaro, A.; and Rona, P. A.: Omega Navigation Performance Off Northwest Africa During Operation No. 267, April 23-May 28, 1968. AD 678 443, Hudson Labs. of Columbia University, TR No. 153.

APPENDIX B

THE RELATIONSHIP BETWEEN CENTICYCLES AND PHASE

Given position T of Transmitter and position R of Receiver, then $D = |\vec{T} - \vec{R}|$ is the distance between the transmitter and receiver. Assume v_p = phase velocity of signal. Then time for point of constant phase to "travel" from transmitter to receiver is $t_T = D/v_p$ secs.

For a given frequency f_c a period $1/f_c = T_c$ can be used to define a centicycle, $(.01)T_c$. Then the time t_T can be expressed in terms of centicycles (cec) as

$$t_{T_{cec}} = \frac{D/v_p}{(.01)T_c} = \frac{100\ D}{v_p\ T_c}$$

$$t_{T_{cec}} = \frac{100\ D}{v_p\ T_c} \quad .$$

The "travel" time relates to the phase of the received signal. A cec can be thought of as $2\pi/100$ radians so that for a given path length a given phase measurement can be directly obtained from the time measurement. For a given transmission path it was shown above that the "travel" time is defined in terms of the path length, the phase velocity, and the period of the transmitted signal.

Assume that t_M represents the time measure of a point of zero phase at the receiver recorded in cec. The difference in time $t_M - t_T$ can be related to a phase perturbation ϕ by considering two situations. If $t_M > t_T$ then $\Delta t = (t_M - t_T) \bmod 100$, and

If $\Delta t < 50$ then $\phi = -\Delta t\ (\frac{\pi}{50})$, $-180° \leq \phi < 0$ and a phase lag condition is said to exist.

If $\Delta t > 50$ then $\phi = (100 - \Delta t)\ (\frac{\pi}{50})$, $0 < \Delta\phi \leq 180°$ and a phase lead condition is assumed.

For $t_M < t_T$, $\Delta t = (t_T - t_M) \bmod 100$, and

If $\Delta t > 50$ then $\phi = (\Delta t - 100)\ (\frac{\pi}{50})$, $-180° \leq \phi < 0$ and a phase lag condition exists.

If $\Delta t < 50$ then $\phi = \Delta t\ (\frac{\pi}{50})$, $0 < \phi \leq 180°$ and a phase lead condition is assumed.

For this situation the term "lane width" is the maximum distance over which the phase angle can be determined unambiguously. For this time scheme

PRECEDING PAGE BLANK NOT FILMED

variations of phase on the range [$-180° \leq \phi \leq 180°$] can be determined. Obviously, a phase lead of 200° cannot be differentiated from a phase lag of 160° so that 360° or 1 cycle is the actual lane width.

Table B-1 shows the lane widths $W_\ell(f)$ as calculated, assuming that the phase velocity corresponds to the speed of light c, for frequencies of interest in Omega. The equation

$$W_\ell(f) = \frac{v_p(f)}{f}$$

provides the lane width as a function of phase velocity and frequency, f.

Table B-1. Omega frequencies, frequency differences and associated periods.

Frequency	Velocity of Constant Phase	Lane Width Nautical Miles	Period T(f)
	161783 n.mi./sec		
$1.1\frac{1}{3}$ kHz	c	142 n.mi.	.88 msec
3.4 kHz	c	48 n.mi.	.294 msec
10.2 kHz	c	15.8 n.mi.	98 μsec
$11.3\frac{1}{3}$ kHz	c	14 n.mi.	88 μsec
13.6 kHz	c	11.9 n.mi.	73.5 μsec

It should be noted here that the term "lane width" is more commonly used in terms of phase difference measurements between two stations along the baseline. Commonly "lane width" is the maximum unambiguous range obtained from phase difference measurements and corresponds to one-half wavelength along the baseline between stations. These lane widths $W_\ell'(f)$ would be given as

$$W_{\ell}'(f) = \frac{v_p}{2f} = \frac{W_{\ell}(f)}{2}$$

and are just one-half the distances given in Table B-1.

Off the baseline, the lane width varies in accordance with the hyperbolic geometry.

APPENDIX C

TRANSMISSION TIME FOR 3.4 KHz BEAT SIGNAL

For a waveguide propagation is characterized by a propagation constant γ where E_T is of the form

$$E_T = E\, e^{-\gamma z}$$

where z is the along axis direction or direction of propagation. γ is generally complex and is expressed as $\gamma = \alpha + j\beta$, where α is an attenuation constant and β* is a phase constant at a particular frequency. Phase velocity in a waveguide is the velocity at which a point of constant phase moves so that $v_p = \frac{\omega}{\beta}$ represents the phase velocity. Any information signal can be thought of as traveling at the group velocity of the guide

$$v_g = \frac{\Delta\omega}{\Delta\beta}$$

which describes the phase distortion introduced by the guide at a particular frequency (ref. 29).

Consider the situation with the Omega signal where frequencies 10.2 kHz and 13.6 kHz are transmitted. Each has a phase velocity so that

$$v_{p_{10.2}} = \frac{\omega_{10.2}}{\beta_{10.2}} \quad \text{and} \quad v_{p_{13.6}} = \frac{\omega_{13.6}}{\beta_{13.6}} .$$

Thus $$\beta_{10.2} = \frac{\omega_{10.2}}{v_{p13.6}} \quad \text{and} \quad \beta_{13.6} = \frac{\omega_{13.6}}{v_{p13.6}} .$$

If one were to consider modulating the 10.2 kHz signal with a 3.4 kHz signal, the result would be similar to the situation where one considers propagation of the difference frequency $\Delta f = f_{13.6} - f_{10.2}$ of the actual Omega signal. A modulation signal, or in this case the difference frequency, can be thought of as information which is propagated in the waveguide. The group velocity of a

*β is the phase constant for a guide and usually is expressed in terms of radians per unit length at a given frequency.

PRECEDING PAGE BLANK NOT FILMED

waveguide can be defined as

$$v_g = \frac{\Delta\omega}{\Delta\beta} \qquad \text{(see refs. 30-32).}$$

Then

$$v_{g_{3.4}} = \frac{2\pi(f_{13.6} - f_{10.2})}{\frac{\omega_{13.6}}{v_{p_{13.6}}} - \frac{\omega_{10.2}}{v_{p_{10.2}}}} \quad .$$

Note that D = VT so that

$$\frac{D}{T_{3.4}} = \frac{2\pi(f_{13.6} - f_{10.2})}{2\pi\left(\frac{f_{13.6}T_{13.6}}{D} - \frac{f_{10.2}T_{10.2}}{D}\right)}$$

or

$$T_{3.4} = \frac{f_{13.6}T_{13.6} - f_{10.2}T_{10.2}}{f_{13.6} - f_{10.2}} \quad .$$

Since $f_{13.6} - f_{10.2} = 3.4$ kHz, and

$$\frac{f_{13.6}}{\Delta f} = 4 \quad , \quad \frac{f_{10.2}}{\Delta f} = 3 \quad ,$$

then

$$T_{3.4} = 4T_{13.6} - 3T_{10.2}$$

which is the expression obtained in refs. 11 and 13.

Consider reception of $f_{11\frac{1}{3}}$ and $f_{10.2}$. Using the same reasoning as previously,

$$T_{1.1\frac{1}{3}} = 10\ T_{11\frac{1}{3}} - 9\ T_{10.2} \quad .$$

APPENDIX D

PROGRAM TO COMPARE TRAPEZOIDAL, NAVY AND PIERCE DATA

CALCULATION OF SUNRISE AND SUNSET TIMES

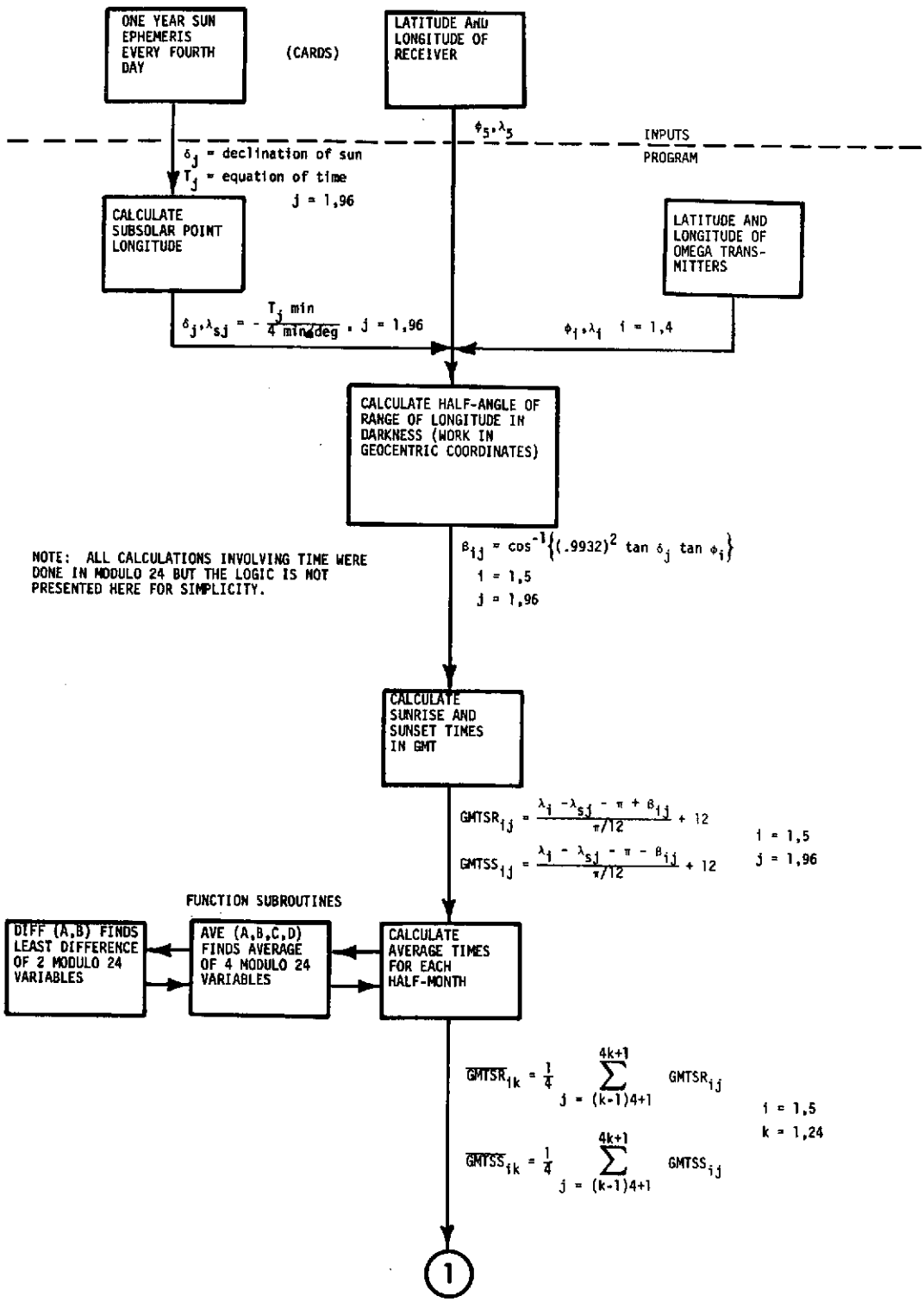

CALCULATION OF TRAPEZOIDAL PHASE PREDICTIONS FOR EACH TRANSMITTER TO RECEIVER PATH

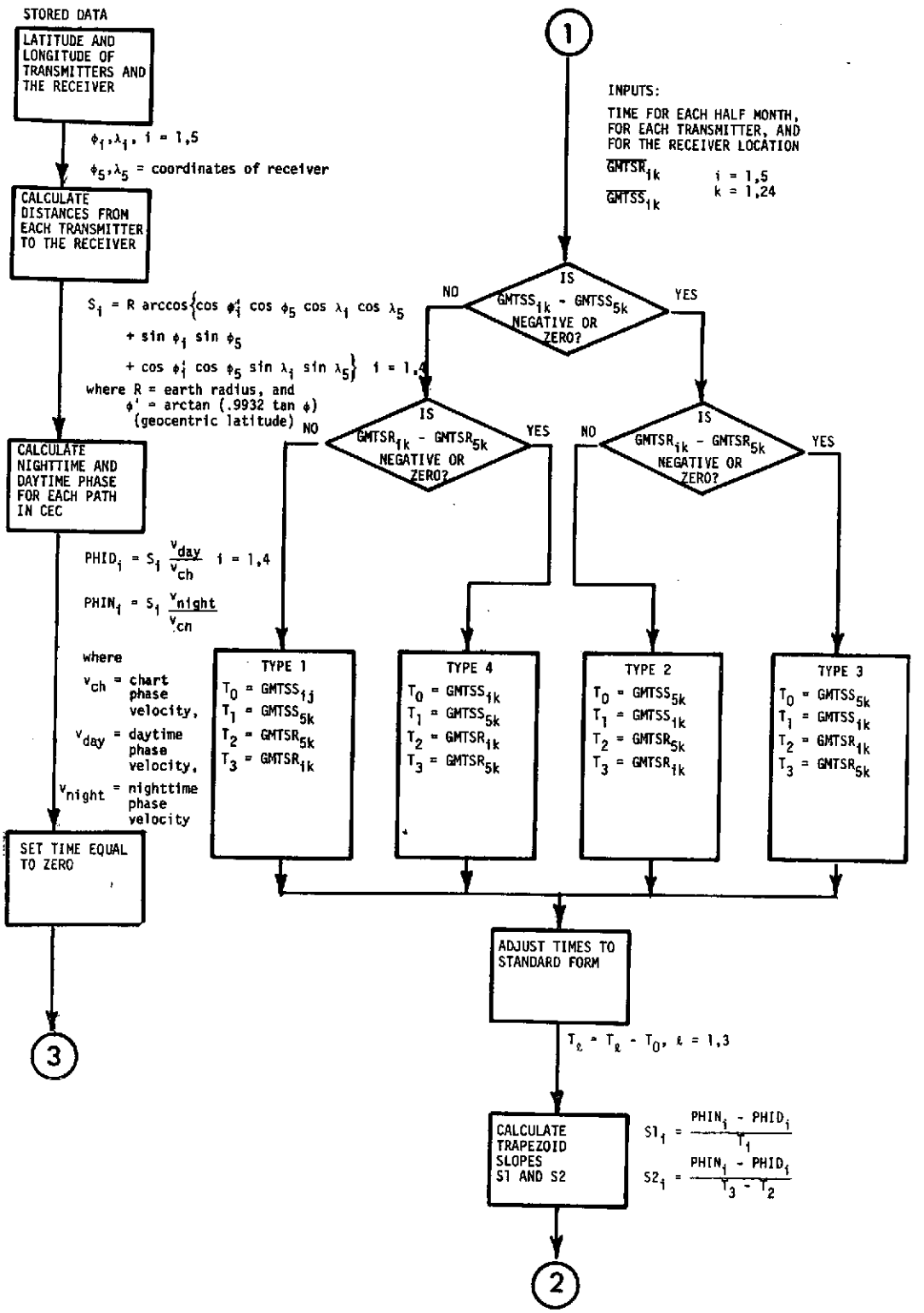

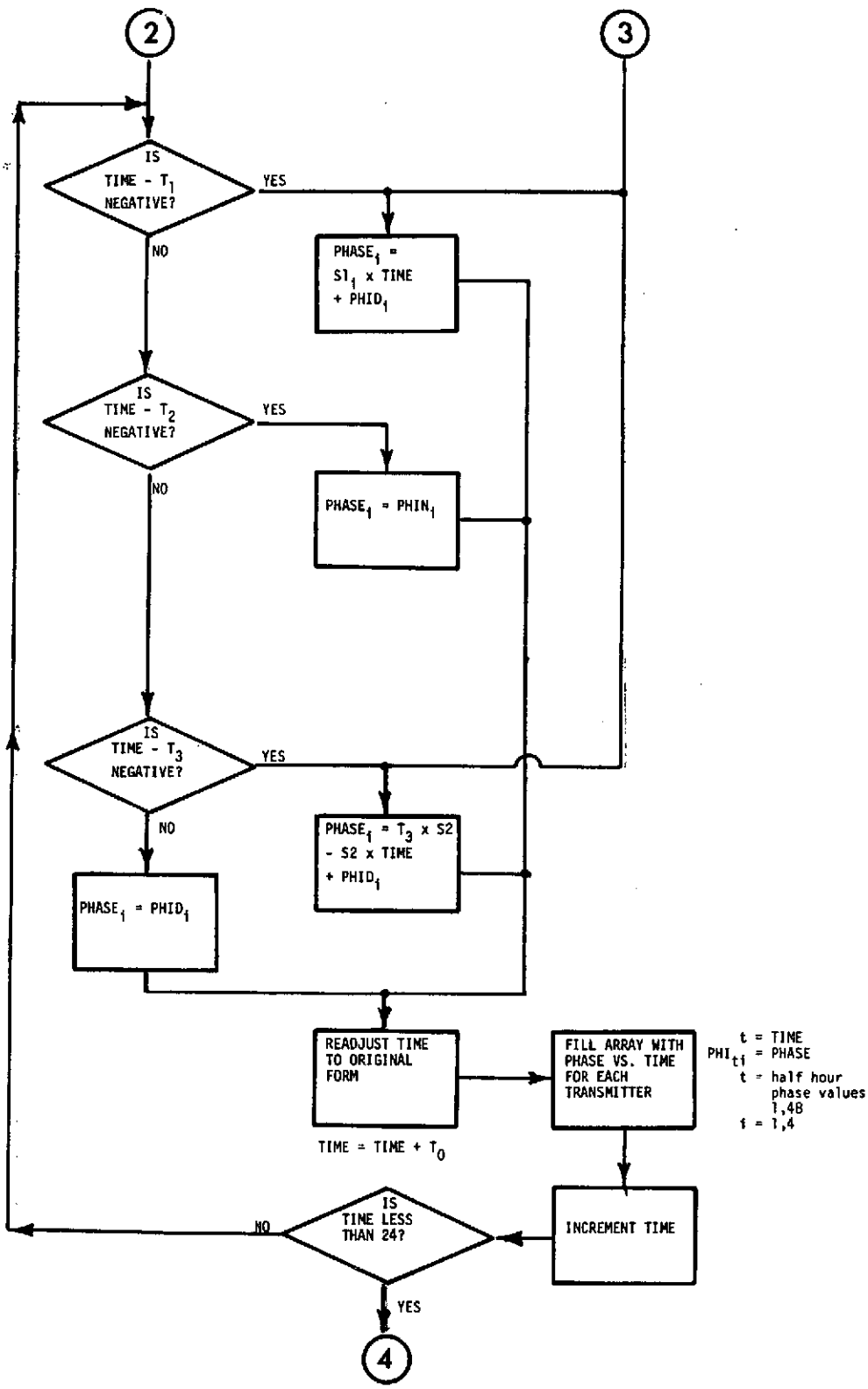
2
3
IS TIME - T_1 NEGATIVE?
YES
NO
$PHASE_1$ = $S1_1$ x TIME + $PHID_1$
IS TIME - T_2 NEGATIVE?
YES
NO
$PHASE_1$ = $PHIN_1$
IS TIME - T_3 NEGATIVE?
YES
NO
$PHASE_1$ = T_3 x S2 - S2 x TIME + $PHID_1$
$PHASE_1$ = $PHID_1$
READJUST TIME TO ORIGINAL FORM
TIME = TIME + T_0
FILL ARRAY WITH PHASE VS. TIME FOR EACH TRANSMITTER
PHI_{ti} t = TIME
= PHASE
t = half hour phase values 1,48
i = 1,4
INCREMENT TIME
IS TIME LESS THAN 24?
NO
YES
4

CALCULATE PHASE DIFFERENCES OF ALL POSSIBLE
COMBINATIONS OF TWO TRANSMITTERS

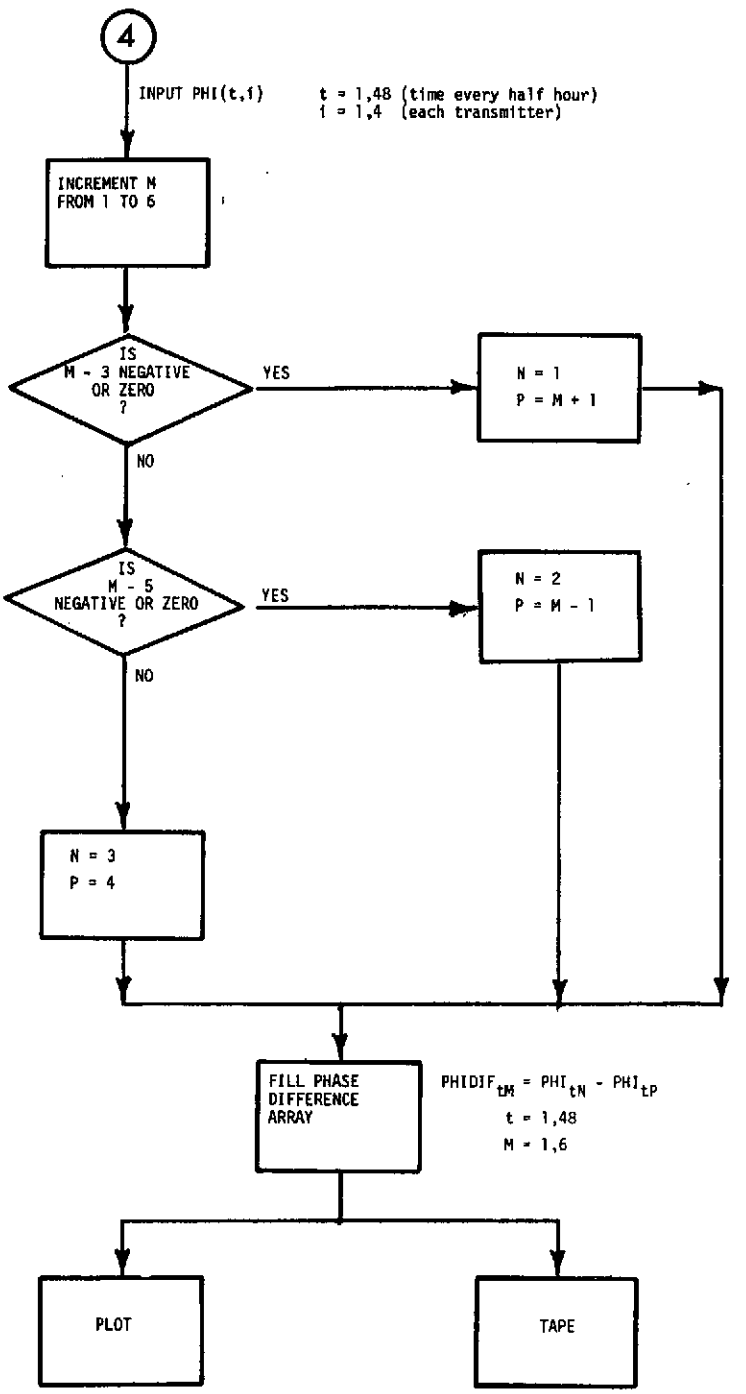

APPENDIX E

PROGRAM TO CALCULATE TRAPEZOIDAL MODEL SKY-WAVE CORRECTIONS FOR A GIVEN POINT ON THE EARTH

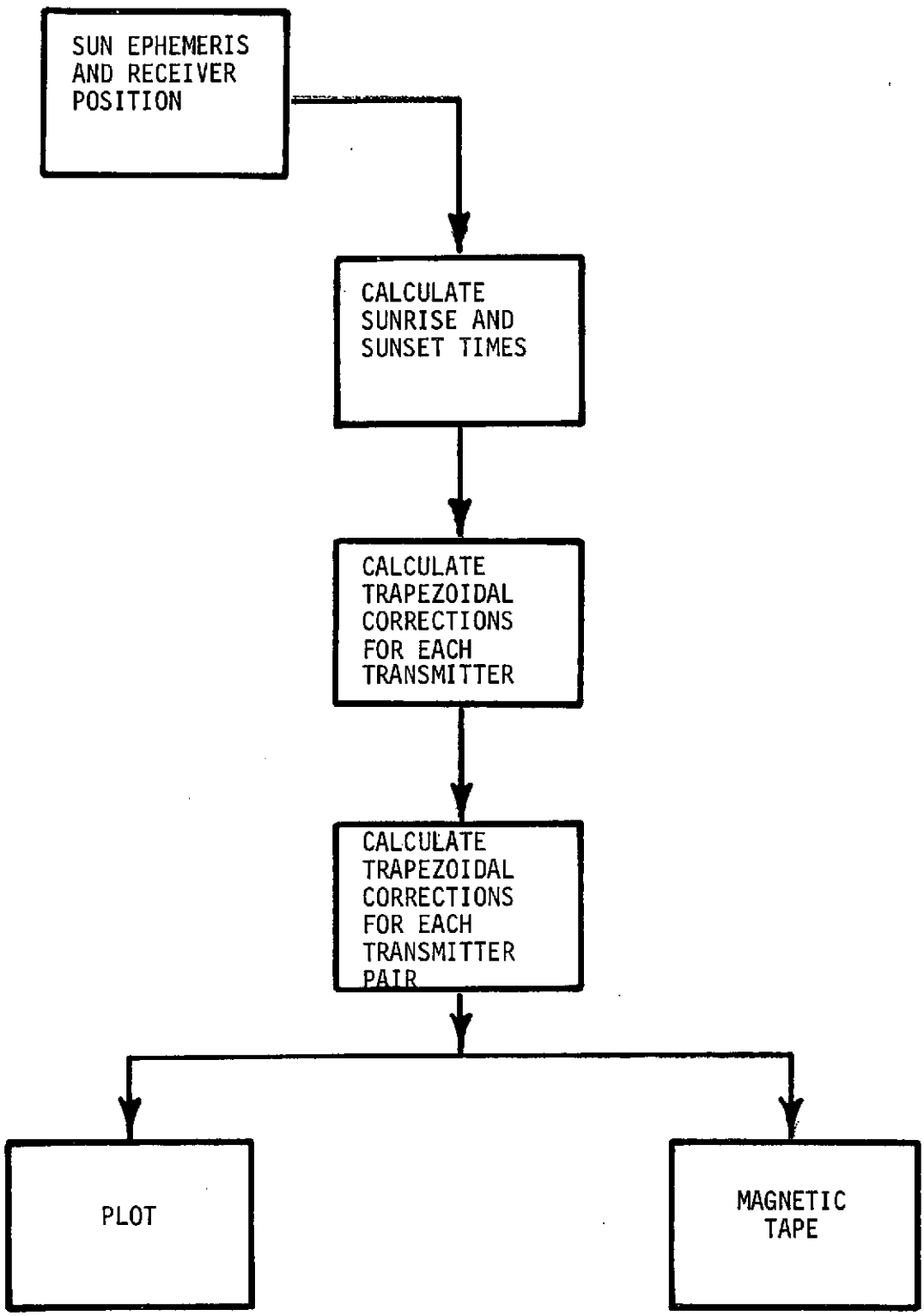

PRECEDING PAGE BLANK NOT FILMED

8.0 REFERENCES

1. Anon.: Omega Table Pair B-C, North America, Area 11. H. O. Pub. No. 224(111), U.S. Naval Oceanographic Office, 1967.

2. Anon.: Omega Skywave Correction Tables for 10.2 kHz, Area 11, North America. U. S. Naval Oceanographic Office, 1970.
   H.O. Pub. No. 224(111-C)A - Norway.
   H.O. Pub. No. 224(111-C)B - Trinidad.
   H.O. Pub. No. 224(111-C)C - Hawaii.
   H.O. Pub. No. 224(111-C)D - New York.

3. Anon.: Air/Surface Omega Navigation Chart, North Atlantic Ocean, Eastern United States. U. S. Naval Oceanographic Office, Edition 2, No. V030-72, November 1965.

4. Barron, D. W.; and Budden, K. G.: The Numerical Solution of Differential Equations Governing Reflection of Long Radio Waves from the Ionosphere III. Proc. Roy. Soc., Ser. A249, No. 1258, 1959, pp. 387-401.

5. Pappert, R. A.; Crossard, E. E.; and Rothmuller, I. J.: A Numerical Investigation of Classical Approximations Used in VLF Propagation. Radio Science, vol. 2, no. 4, April 1967.

6. Wait, J. R.; and Spies, K. P.: Characteristics of the Earth Ionosphere Waveguide for VLF Waves. NBS Tech. Note 300, Dec. 30, 1964.

7. Watt, A. D.: VLF Radio Engineering. Pergamon Press, 1967.

8. Noonkester, V. R.; and Swanson, E. R.: Ionospheric Forecast Requirements of the Omega Navigation System. 15th NATO AGARD Conference Proc., 2-5 September 1969.

9. Swanson, E. R.: VLF Phase Prediction. Symp. on VLF Propagation, Sandefjord, Norway, 27-30 October 1971.

10. Swanson, E. R.: Accuracy of Omega Navigation Using 1969 SWC. NELC 1675, December 1969.

11. Pierce, J. A.: The Use of Composite Signals at Very Low Radio Frequencies. Harvard University Div. of Engineering and Applied Sciences Tech. Report 552, AD 666 567, February 1968.

12. Baltzer, O. J.: Use of Composite Omega in Aircraft Applications. Proc. of the Institute of Navigation First Omega Symposium, November 1971.

13. Pierce, J. A.: Lane Identification in Omega. AD 746 503, Harvard University, July 1972.

14. Anon.: Omega Phase Variation Study. Lear Siegler, Inc., AD 689 796, February 1967.

PRECEDING PAGE BLANK NOT FILMED

15. Josephy, N. H.; and Kasper, J. F.: A Polynomial Approximation Technique for Small-Computer Skywave Correction Implementation. Proc. of the Institute of Navigation First Omega Symposium, November 1971.

16. Parvin, Richard H.: Inertial Navigation. In Principles of Guided Missile Design, G. Merrill, ed., D. Van Nostrand Co., Inc., 1962, p. 158.

17. Anon.: Smithsonian Meteorological Tables. Sixth Ed., 1963, p. 495.

18. Pierce, J. A.: Omega: A World-Wide Navigational System: System Specification and Implementation. Report of Omega Implementation Committee for the U. S. Navy Dept. BuShips, AD 630 900, May 1966.

19. Brogden, J. W.; and Luken, K.: Differential Omega. Naval Research Laboratories Memo. Report 1716, August 1966.

20. Goodman, G. R.: A Proposed Differential Omega System. MSEE Thesis, Naval Postgraduate School, Monterey, California, 1969.

21. Luken, K., et al.: Accuracy Studies of the Differential Omega Techniques. Naval Research Labs., AD 709 555, June 1970.

22. Wright, J. R.: Results of Differential Omega Test and Evaluation Program. Tracor, Inc., 1968.

23. Swartwood, W. M.: An Evaluation of Differential Omega. U. S. Naval Oceanographic Office, Proc. of the Institute of Navigation First Omega Symposium, November 1971.

24. Hastings, C. E.; and Barker, A. C.: Automatic Real Time Omega Accuracy Enhancement. Navigation, Journal of ION, vol. 18, no. 2, Summer 1971.

25. Baltzer, O. J.: DC-6 Flight to Bermuda. Tracor, Inc., September 1968.

26. Nard, G.: Results of Recent Experiments with Differential Omega. Proc. of the Institute of Navigation First Omega Symposium, November 1971.

27. McKaughan, M. E.: Summary of Investigations of a Proposed Differential Omega System. Proc. of the Institute of Navigation First Omega Symposium, November 1971.

28. Poppe, M. C.: LO-CATE III - The Application of Retransmitted Omega to the Tracking of Remote Objects. Proc. of the Institute of Navigation First Omega Symposium, November 1971.

29. Stratton, J. S.: Electromagnetic Theory. McGraw-Hill Book Co., Inc., 1941.

30. Langmuir, R. V.: Electromagnetic Fields and Waves. McGraw-Hill Book Co., Inc., 1961.

31. Ramo, S.; Whinnery, J. R.; and Van Duzer, T.: Fields and Waves in Communication Electronics. John Wiley & Sons, Inc., 1967.

32. Tralli, N.: Classical Electromagnetic Theory. McGraw-Hill Book Co., Inc., 1963.